

**Analysis of trichome differentiation in *Arabidopsis thaliana*:  
From cell fate initiation to cell death**

**Inaugural-Dissertation**

zur

Erlangung des Doktorgrades  
der Mathematisch-Naturwissenschaftlichen Fakultät  
der Universität zu Köln

vorgelegt von

**Daniel Bouyer**

aus Villingen

**2004**

Berichterstatter: Prof. Dr. Martin Hülkamp  
Prof. Dr. Klaus Harter

Prüfungsvorsitzender: Prof. Dr. Siegfried Roth

Tag der mündlichen Prüfung: 11.11.2004

## DANK

schulde ich vielen. Zunächst möchte ich mich bei Martin Hülskamp bedanken für die Betreuung und die Freiheit, die er mir in der Auswahl und der Durchführung meiner Arbeit gegeben hat. Deren Anfänge liegen im Tübinger Institut für Entwicklungsgenetik von Gerd Jürgens; daher auch ihm ein Dankeschön für die Aufnahme in den Kreis der Entwicklungsbiologen (wovon ich während des Studiums immer geträumt habe!).

Einiges in dieser Arbeit wurde von anderen begonnen oder in Zusammenarbeit mit anderen zu Wege gebracht. *STICHEL* wurde von Hilmar Ilgenfritz kloniert, die Analyse und Klonierung von *CPR5* war ein Gemeinschaftsprojekt mit Viktor Kirik, die Herstellung von TTG-Promoter-Konstrukten wurde in unermüdlicher Arbeit von Martina Pesch bewältigt und die Idee der Nicht-Zell-Autonomie von TTG1 wurde von Arp Schnittger schon tatkräftig bearbeitet, bevor ich mich daran zu schaffen machte. Ihnen gilt daher ein dickes Danke!

Susanne Breiding war mir in Köln bei vielen Projekten behilflich und ich hoffe, es waren nicht zu viele! Danken möchte ich auch Herrn Weidner, der alle Verwaltungsangelegenheiten fest im Griff hat und bei dem ich immer gerne Prüfungsbeisitzer war. Uli Herrmann war immer zur Stelle um die Computer am Leben zu erhalten, auch wenn *STICHEL* mal wieder rumzickte. Dass Uschi Claßen eine tolle Arbeit in der Spülküche macht, merkt man natürlich erst, wenn sie nicht da ist, daher an dieser Stelle mal ein großes Dankeschön! Auch allen anderen, die mit ihren Jobs dafür sorgen, dass man im Labor überhaupt arbeiten kann und damit das Labor zum Labor machen, sei hier gedankt.

Die familiäre Atmosphäre hatte ich im Tübinger Labor Arp, Hilmar, Paul, Swen, Ulrike Folkers (UFO), Ulrike Schöbinger und Viktor zu verdanken. Dank Viktor, Susanne, Steffi, Martina, Katja, Britta und Birgit kann man sich auch in Köln ganz wohl fühlen.

Ganz besonders war ich auf die Hilfe bei der Durchsicht meines Manuskripts durch Christina Weinl, Viktor Kirik, Arp Schnittger, Swen Schellmann, Martina Pesch und Steffi Falk angewiesen! Ohne Euch würde ich wahrscheinlich selbst nichts mehr von dem verstehen, was ich da anfänglich so zusammengeschrieben habe ...

Dank einer glücklichen Fügung verschlug es Klaus Harter aus meiner alten Studienstätte Freiburg an das Kölner Nachbarinstitut. Für seine Übernahme des Zweitgutachtens möchte ich ihm danken und hoffe, dass ihm die Zugfahrt durch die Lektüre nicht zu lange wird.

CONTENTS

Zusammenfassung .....	III
Abstract .....	V
Publications .....	VII
Abbreviations and Gene names .....	VIII
Figure index .....	IX
<b>A TRICHOME MOPRHOGENESIS.....</b>	<b>1</b>
A 1. Introduction .....	2
A 1.1. Different steps in the formation of cell shape .....	2
A 1.2. Steps in trichome development .....	2
A 1.3. Endoreplication-dependent trichome morphogenesis .....	3
A 1.4. Endoreplication-independent branch mutants .....	4
A 2. Results .....	6
A 2.1. Analysis of STI .....	6
A 2.1.1. STI belongs to a group of novel genes .....	6
A 2.1.2. <i>STI</i> acts in a dosage-dependent manner .....	10
A 2.1.3. <i>STI</i> is not involved in endoreplication .....	11
A 2.1.4. Localisation of GFP-STI .....	12
A 2.2. Analysis of <i>CPR5</i> .....	13
A 2.2.1. Trichome differentiation in the <i>cpr5</i> mutant .....	13
A 2.2.2. Cell proliferation defect in the <i>cpr5</i> mutant .....	14
A 2.2.3. Cell death in the <i>cpr5</i> mutant .....	16
A 2.2.4. Complementation of the <i>cpr5</i> mutant .....	16
A 3. Discussion .....	17
A 3.1. Analysis of STI .....	17
A 3.1.1. The role of <i>STI</i> in cell morphogenesis .....	17
A 3.1.2. Potential molecular function of STI .....	18
A 3.2. Analysis of <i>CPR5</i> .....	20
<b>B TRICHOME PATTERN FORMATION .....</b>	<b>23</b>
B 1. Introduction .....	24
B 1.1. Trichome initiation in <i>Arabidopsis thaliana</i> .....	24
B 1.2. Elements of the trichome pattern system .....	24
B 1.3. Molecular nature of the trichome patterning genes .....	25
B 1.4. Functions beside trichome patterning .....	26
B 1.5. Special role of TTG1 and interactions between the patterning components .....	26
B 1.6. A model to explain two-dimensional pattern formation .....	27
B 1.7. Application of the activator-inhibitor model to the trichome patterning system .....	28
B 1.8. Intercellular protein movement in plants .....	30
B 1.9. Connection between intra- and intercellular mobility? .....	31
B 1.10. Outlook and aim of the work .....	31
B 2. Results .....	33
B 2.1. <i>TTG1</i> -dependent and -independent trichome development .....	33
B 2.2. Expression analysis of <i>TTG1</i> .....	36
B 2.3. <i>TTG1</i> -YFP localises to the nucleus .....	39
B 2.4. <i>TTG1</i> localisation depends on differentiation status .....	41

B 2.5. Non-cell-autonomous action of <i>TTG1</i> .....	44
B 2.6. TTG1-YFP-fusion is able to move .....	46
B 2.7. TTG1-YFP constructs show pattern defects .....	49
B 2.8. Blocking TTG1 mobility leads to strong pattern defects .....	50
B 2.8.1. Exchanging endogenous TTG1 with an immobile TTG1 .....	50
B 2.8.2. Dependency of <i>TTG<sup>im</sup></i> -phenotype on endogenous <i>TTG1</i> function .....	52
B 2.8.4. Immobilised TTG1 induces ectopic trichome-specific reporters .....	55
B 2.8.5. Dominant negative effect of trichome-specific expression of the immobilised TTG1 .....	56
B 2.8.6. The dominant negative effect of <i>GL2::TTG<sup>im</sup></i> is dependent on TRY/CPC .....	56
B 2.8.7. <i>TTG<sup>im</sup></i> interacts with <i>GL3</i> but not with <i>GL1</i> .....	58
B 3. Discussion .....	59
B 3.1. Non-cell-autonomous action of TTG1 .....	59
B 3.2. Developmental relevance of TTG1 mobility .....	60
B 3.3. Is TTG1 actively transported? .....	62
B 3.4. Intracellular localisation of TTG1 .....	64
B 3.5. Interaction of TTG1 with other patterning genes .....	65
B 3.6. Is the role of TTG1 in agreement with the activator-inhibitor system? .....	67
B 3.7. Another view on the Meinhardt-model .....	69
B 3.8. Outlook .....	73
Material and Methods .....	74
Materials .....	74
Chemicals, antibiotics .....	74
Enzymes and molecularbiological materials .....	74
Cloning vectors .....	74
Bacterial strains .....	75
Plant lines .....	75
Methods .....	75
RNA isolation .....	75
Reverse transcription .....	76
Semiquantitative RT-PCR .....	76
Genomic DNA preparation .....	76
Plasmid DNA preparation from bacteria .....	77
DNA-manipulation .....	77
Cloning of the STI cDNA .....	78
Constructs .....	78
Plant growth conditions .....	81
Crossing of plants .....	81
Plant transformation .....	82
Seed sterilisation .....	82
Heat-shock treatment .....	82
Histochemistry .....	82
Fluoresceine diacetate- & propidium iodid staining .....	83
Microscopy .....	83
DAPI-staining and DNA-measurement .....	83
References .....	85
Erklärung .....	93
Lebenslauf .....	94

## Zusammenfassung

In der folgenden Dissertationsarbeit habe ich mich mit Zelldifferenzierungsprozessen anhand der Blatthaarentwicklung der Modellpflanze *Arabidopsis thaliana* beschäftigt. Der Zelltyp ‚Trichom‘ eignet sich besonders um entwicklungsbiologische Fragestellungen wie beispielsweise die Initiation eines bestimmten Zellschicksals, die Generierung eines geordneten Abstandsmusters oder auch die Prozesse hinsichtlich der Ausbildung einer streng festgelegten dreidimensionalen Zellform zu untersuchen.

In meiner Arbeit habe ich einige dieser Aspekte untersucht. Daher unterteile ich meine Ausführungen in die beiden Abschnitte Morphogenese (Untersuchung der Ausbildung einer bestimmten Zellform) und Trichom-Musterbildung („pattern formation“; Analyse der Prozesse, die für die Zellschicksalsfestlegung der Blatthaare aus anfänglich nicht unterscheidbaren Zellen notwendig sind).

Im Kapitel Morphogenese habe ich mich mit zwei Mutanten beschäftigt, die Störungen der Ausbildung der Zellform aufweisen. In normalen, sogenannten wildtypischen (WT) Blatthaaren wachsen die Zellen aus der Blattoberfläche aus und bilden anschließend ein stereotypisches Verzweigungsmuster. In der *stichel*-Mutante (*sti*) ist die Entstehung der Verzweigungen vollständig gestört, d.h., es entstehen keine Verzweigungen mehr. Es konnte in der Arbeit gezeigt werden, dass das *STI*-Gen diesen Prozess in einer Dosis-abhängigen Art reguliert. Eine Reduzierung der *STI*-Aktivität führt demnach zu einer Reduktion der Verzweigungen und eine Erhöhung zu einer vermehrten Verzweigung. Daneben legte die Klonierung des *STI*-Gens durch Hilmar Ilgenfritz eine Verbindung der Morphogenese mit bestimmten Zell-Zyklus-Prozessen nahe. Frühere Untersuchungen ergaben, dass Trichom-Zellen einen bestimmten Typ von Zellzyklus durchlaufen. Der DNA-Gehalt wird dabei wie bei einer normalen Zellteilung verdoppelt, die Zelle teilt sich jedoch nicht. Dieser Prozess wird als Endoreduplikation oder auch Endoreplikation bezeichnet. Tatsächlich kodiert *STI* für ein Protein, das Ähnlichkeiten mit einer DNA-Polymerase-Untereinheit besitzt, also mit einem Enzym, das maßgeblich an der Synthese von DNA während des Zellzyklus beteiligt ist. Allerdings konnte weder eine Verminderung des DNA-Gehalts in *sti*-Mutanten noch eine Erhöhung in Pflanzen, die *STI* vermehrt produzieren, beobachtet werden. Die weitere Analyse zeigte jedoch, dass *STI* zu einer phylogenetisch separierten Gruppe von Proteinen gehört, die bislang nur in Pflanzen gefunden wurde und wahrscheinlich nicht in direktem Zusammenhang mit den DNA-Polymerase-Untereinheiten steht.

Diese Vermutung wurde weiter untermauert durch die Beobachtung, dass das STI-Protein nicht im Kern, also dem Ort der DNA-Synthese, sondern an den zukünftigen Verzweigungspunkten der Trichome gefunden wurde. STI scheint also direkt an der Ausbildung der Verzweigungen beteiligt zu sein.

Die zweite Morphogenese-Mutante (*cpr5*), die von mir in dieser Arbeit untersucht wurde, ähnelt *sti* insofern, als auch hier eine starke Reduktion der Trichom-Verzweigung zu beobachten ist. Darüber hinaus konnte ich zeigen, dass es hierbei, im Gegensatz zu *sti*, zu einer Reduktion des DNA-Gehalts in den Trichomen der *cpr5*-Mutante kommt. Die weitere Analyse ergab, dass es in *cpr5* zu einem Absterben der Trichome kommt, was auch in anderen Teilen der Pflanze beobachtet wurde. Daneben weist *cpr5* ein vermindertes Wachstum auf und scheint in mehreren Prozessen gestört zu sein. Gemeinsam mit Viktor Kirik wurde das *CPR5*-Gen kloniert und es zeigte sich, dass es für ein Protein unbekannter Funktion kodiert. Die Proteinstruktur lässt keine genaueren Vermutungen über die molekulare Funktion von CPR5 zu.

Im zweiten Teil dieser Arbeit konzentriere ich mich auf die Prozesse der Ausbildung des regelmäßigen Abstandsmusters der Trichome zueinander. Dabei war vor allem eine Komponente dieses Musterbildungssystems, das *TTG1*-Gen, noch nicht genauer charakterisiert. Ich konnte die Aktivität des *TTG1*-Gens in zellulärer und zeitlicher Auflösung anhand von Promoter-GUS-Analysen aufzeigen und die Lokalisation des TTG1-Proteins innerhalb der Zelle klären. Dabei zeigte sich, dass *TTG1* überall in der Zone der Trichom-Musterbildung exprimiert wird und dass das Protein anfänglich überwiegend in den Kernen und mit zunehmender Entwicklung des Blattes überwiegend im Cytoplasma der Zellen zu finden ist. Allerdings behalten die Trichome die Lokalisation von TTG1 in den Kernen über ihre gesamte Entwicklung hinweg bei. Daneben konnte ich zeigen, dass TTG1 nicht-zellautonom wirkt und das Protein zwischen Zellen mobil ist. Diese Mobilität scheint auch für das Zustandekommen eines regelmäßigen Musters wichtig zu sein. Dies wird offensichtlich wenn die Mobilität des Proteins gestört oder gar verhindert wird, wobei es zu schwerwiegenden Störungen des Musters kommt.

**Abstract**

In the following PhD thesis I studied cell differentiation processes of leaf hairs, trichomes, in *Arabidopsis thaliana*. This cell type is very well suited for the analyses of the initiation of a certain cell fate, the generation of a regular spacing pattern or the processes that are required for the formation of a three-dimensional cell form.

In my thesis I have investigated several of these aspects. Therefore this work is subdivided into the sections trichome morphogenesis (analysis of the formation of a certain cell form) and trichome pattern formation (analysis of the processes that are important for the commitment and the generation of a spacing pattern of a certain cell type that is derived from initially equal cells). In the chapter morphogenesis I studied two mutants that show defects in the generation of the trichome-cell form. A typical trichome in *Arabidopsis* grows out of the leaf surface and forms three branches in a highly stereotypical manner. In the *stichel* (*sti*) mutant the development of these branches is completely abolished.

Previous genetic analysis and my studies suggest that *STI* acts in this process in a dosage-dependent manner. A reduction of *STI* activity leads to a reduction in branch number and a elevated *STI* activity leads to an increase in branch number. The cloning of the gene suggested a connection between morphogenesis and a certain kind of the cell cycle, called endoreduplication or endoreplication. This process leads to DNA-synthesis as observed in the usual cell cycle, however without division, which results in a higher DNA content in the cell. In fact *STI* encodes for a protein with sequence similarities to a DNA-Polymerase subunit, an enzyme that is involved in DNA-synthesis during the cell cycle. However neither *sti* mutants nor plants that ectopically express *STI* show changes in the DNA content.

The further analysis showed that *STI* belongs to a group of proteins that is separated from the conventional DNA-polymerase subunits. This assumption was supported by the observation that the *STI* protein is not found in the nucleus, the place of DNA-synthesis, but at the future branch initiation point in trichomes. Therefore *STI* seems to play a direct role in the formation of the trichome branches.

The second morphogenesis mutant (*cpr5*) that was subject of my work, resembles *sti* with respect to the reduction of trichome branches. However in contrast to *sti*, the DNA-content is reduced in the *cpr5* mutant. Moreover, during further development the trichomes in *cpr5* die, a process that

is also observed in other parts of the mutant plant. Beside this, *cpr5* is also impaired in the proliferation and growth and seems to be defective in several aspects. Together with Viktor Kirik the *CPR5* gene was cloned and shown to encode a novel protein with unknown function.

In the second part of my thesis I examined the processes that control the formation of a regular trichome spacing pattern on the leaf surface. An important component of this patterning system, TTG1, was investigated in more detail. I could reveal the temporal and spatial activity of the gene in promoter-GUS analyses and the localisation of the protein in the cell. This revealed that *TTG1* is expressed throughout the entire trichome-patterning zone and that the protein changes its localisation from predominantly nuclear in the early leaf-development to more cytoplasmatic during further development of the epidermal cells. However trichomes keep the nuclear localisation throughout their development. Moreover it was shown that *TTG1* acts non-cell-autonomous and that the TTG1-protein is able to move between cells. This transport seems to be important for the generation of the spacing pattern, which is reflected by the patterning defects if the protein-mobility is impaired or even completely blocked. In the latter case the pattern is strongly impaired. These observations are summarised into a model to explain the early patterning events during trichome differentiation.

**Publications:**

***CPR5* is involved in cell proliferation and cell death control and encodes a novel transmembrane protein.**

Kirik V, Bouyer D, Schöbinger U, Bechtold N, Herzog M, Bonneville JM, Hülskamp M  
*Curr Biol* 2001, **11**: 1891–1895

Shared first authorship; I generated the rescue construct and did most of the mutant analysis, including trichome phenotype analysis, trichome DNA content measurements and cell-death analysis.

**Ectopic D-type cyclin expression induces not only DNA replication but also cell division in *Arabidopsis* trichomes.**

Schnittger A, Schöbinger U, Bouyer D, Weinl C, Stierhof YD, Hülskamp M  
*Proc Natl Acad Sci U S A*. 2001, **99**: 6410-6415

For this work I did some of the endoreplication measurements and trichome morphogenesis analysis.

**The *Arabidopsis* *STICHEL* gene is a regulator of trichome branch number and encodes a novel protein.**

Ilgenfritz H, Bouyer D, Schnittger A, Mathur J, Kirik V, Schwab B, Chua NH, Jürgens G, Hülskamp M

*Plant Physiol* 2003, **131**: 643-655

Shared first authorship; I generated the *STI* cDNA together with Hilmar Ilgenfritz and created all transformation constructs and transgenic plants. The analysis of the overexpression phenotype of *35S::STI* was performed and the alignments with the *STI*-homologues. Birger Marin helped me in the generation of the phylogenetic tree.

**Misexpression of the cyclin-dependent kinase inhibitor ICK1/KRP1 in single-celled *Arabidopsis* trichomes reduces endoreduplication and cell size and induces cell death.**

Schnittger A, Weinl C, Bouyer D, Schöbinger U, Hülskamp M

*Plant Cell* **15**, 303-315

In this work I designed and generated the ICK deletion constructs and produced the corresponding transgenic plants. Furthermore I did most of the phenotypical characterisation and the endoreplication analysis of the trichomes in these plants.

**Cell polarity in *Arabidopsis* trichomes.**

Bouyer D, Kirik V, Hülskamp M

*Semin Cell Dev Biol* 2001, **12**: 353-356

**Branching of single cells in *Arabidopsis*.**

Bouyer D, Hülskamp M

In: Davies JA (Editor): *Branching Morphogenesis* 2003

## Abbreviations and Gene names

°C	degree Celsius	<i>Ler</i>	Landsberg <i>erecta</i>
μ	micro	KRP	kip related protein (=ICK)
35S	35S promoter from Cauliflower Mosaic virus	MP	movement protein
AN	ANGUSTIFOLIA	mRNA	messenger RNA
AN11	ANTHOCYANINLESS11	MT	microtubules
ATP	Adenosine triphosphate	n	number
bp	base pair	NLS	nuclear localisation signal/sequence
bHLH	basic helix-loop-helix	NOK	NOEK
C	DNA-content of a haploid genome	PCR	polymerase chain reaction
CaMV	Cauliflower Mosaic virus	p	promoter
CDK	cyclin dependent kinase	PD	plasmodesmata
cDNA	complementary DNA	RFC	replication factor C
CDS	coding sequence	RNA	ribonucleic acid
CLSM	confocal laser scanning microscopy	rpm	rounds per minute
CPC	CAPRICE	RT-PCR	reverse transcription PCR
Col	Columbia	SD	standard deviation
CPR5	constitutive pathogen response5	SEL	size exclusion limit
cv.	cultivar/ecotype	SIM	SIAMESE
D	Dalton	SPK	SPIKE
DAPI	4',6-Diamidino-2-phenylindole	STI	STICHEL
DIG	Digoxygenin	T-DNA	transferred DNA
DNA	Desoxyribonucleic acid	TIS	trichome initiation site
e.g.	<i>exempli gratia</i> [Lat.] for example	TRY	TRIPTYCHON
ER	endoplasmatic reticulum	TTG1	TRANSPARENT TESTA GLABRA1
ERH3	ELONGATED ROOT HAIR3	TON	TONEAU
<i>et al.</i>	<i>et alterni</i> [Lat.] and others	UTR	untranslated region
ETC1/2	ENHANCER OF TRY CPC1/2	WT	wild type
FDA	fluorescein diacetate	YFP	yellow fluorescent protein
Fig.	Figure	ZWI	ZWICHEL
FRA	FRAGILE FIBRE	WS-O	Wassilewskaja
FRC	FURCA		
FS	FASS		
GA	gibberelic acid		
GFP	green fluorescent protein		
GL1	GLABRA1		
GL2	GLABRA2		
GL3	GLABRA3		
GUS	glucuronidase		
ICK	inhibitor of CDK		
k	kilo		
KAK2	KAKTUS2		
kb	kilo bp		
kD	kilo Dalton		

All gene- and mutant names are written in italics. WT-genes are written in capital letters. Proteins are written in non-italic letters.

## Figure index

<b>Fig. 1:</b> Steps in trichome development.....	3
<b>Fig. 2:</b> Sequence alignment of STI with prokaryotic DNA polymerase III $\gamma$ -subunits and the small subunits of eukaryotic and archaeobacterial replication factor Cs.....	7
<b>Fig. 3:</b> Sequence comparison between STI with its closest homologues.....	8
<b>Fig. 4:</b> Phylogenetic tree of the STI, the DNA polymerase III $\gamma$ -subunit, and the RFC small subunit family.....	9
<b>Fig. 5:</b> Trichome-phenotypes of <i>sti</i> and <i>35S::STI</i> .....	10
<b>Fig. 6:</b> Analysis of expression levels in <i>35S::STI</i> lines by semiquantitative RT-PCR.....	11
<b>Fig. 7:</b> Confocal laser scanning micrographs of GFP-STI.....	12
<b>Fig. 8:</b> Endoreplication in <i>cpr5</i> .....	13
<b>Fig. 9:</b> Cell proliferation in <i>cpr5</i> .....	14
<b>Fig. 10:</b> Trichome and lesion phenotype in <i>cpr5</i> mutants.....	15
<b>Fig. 11:</b> Trichome differentiation and mathematical modelling.....	28
<b>Fig. 12:</b> Trichome patterning model.....	29
<b>Fig. 13:</b> Mutant analysis of negative regulators in combination with <i>ttg1</i> and <i>gll</i> .....	35
<b>Fig. 14:</b> Expression analysis of <i>TTG1</i> .....	37
<b>Fig. 15:</b> Analysis of TTG1-YFP localisation.....	40
<b>Fig. 16:</b> TTG1-YFP localisation is dynamic.....	42
<b>Fig. 17:</b> Non-cell-autonomous action of <i>TTG1</i> .....	45
<b>Fig. 18:</b> TTG1-YFP fusion moves between cells.....	47
<b>Fig. 19:</b> Trichome phenotype of immobilised TTG1 ( <i>TTG1<sup>im</sup></i> ).....	51
<b>Fig. 20:</b> Effect of <i>pTTG1::TTG1<sup>im</sup></i> in different <i>ttg1</i> and other mutant backgrounds.....	53
<b>Fig. 21:</b> Dominant negative effect of <i>pGL2::TTG1<sup>im</sup></i> .....	57
<b>Fig. 22:</b> Model to explain the early steps in pattern formation.....	71



# Trichome Morphogenesis

## A 1. INTRODUCTION

### A 1.1. Different steps in the formation of cell shape

Formally, cell shape can be considered to be established in three steps (Hülkamp *et al.* 1998). In a first step, spatial information, e.g. cell polarity, is established by intracellular mechanisms or provided by outer cues. In a second step, this information is used to reorganize the cell, e.g. change the cytoskeletal arrangement. Finally, actual growth takes place, which includes the incorporation of membrane and cell wall material at defined areas of the cell periphery.

Although some of the biochemistry of the last two steps of the cytoskeletal function and cell wall synthesis is known, the mechanisms underlying the spatial control of cell morphogenesis are largely elusive. Single-cell model systems such as pollen tubes, root hairs, and leaf hairs (trichomes) that are accessible to genetic approaches provide the means to study spatial control mechanisms (Aeschbacher *et al.* 1994, Marks 1997, Oppenheimer 1998, Hülkamp *et al.* 1999, Kost *et al.* 1999, Wilhelmi and Preuss 1999). Among these model cell types, trichomes in *Arabidopsis* are particularly well suited because they consistently develop a complex three-dimensional form, thus providing excellent criteria to isolate mutants affecting discrete aspects of morphogenesis (Oppenheimer 1998, Hülkamp *et al.* 1999).

### A 1.2. Steps in trichome development

Leaf trichomes in *Arabidopsis* are large single cells that originate from the epidermis and are up to 500  $\mu\text{m}$  tall. After trichome fate commitment the cells stop dividing but continue DNA synthesis (endoreduplication; Hülkamp *et al.* 1994). Fig. 1 shows the development of a trichome. The incipient trichome extends out of the leaf surface and undergoes two successive branching events (Hülkamp *et al.* 1994). The orientation of the first branching is co-aligned with the proximal-distal leaf axis. The primary branch, which points toward the leaf tip (main stem), undergoes a second branching in a plane perpendicular to the primary branching plane (Folkers *et al.* 1997). Subsequently, the trichome extensively elongates concomitant with an increase in vacuolization. The mature trichome has, on average, a DNA content of 32 C, suggesting that trichomes proceed through four endore-duplication cycles (Hülkamp *et al.* 1994). Trichome

branching requires the coordinated action of at least 18 genes (Marks 1997, Oppenheimer 1998, Hülkamp *et al.* 1999).

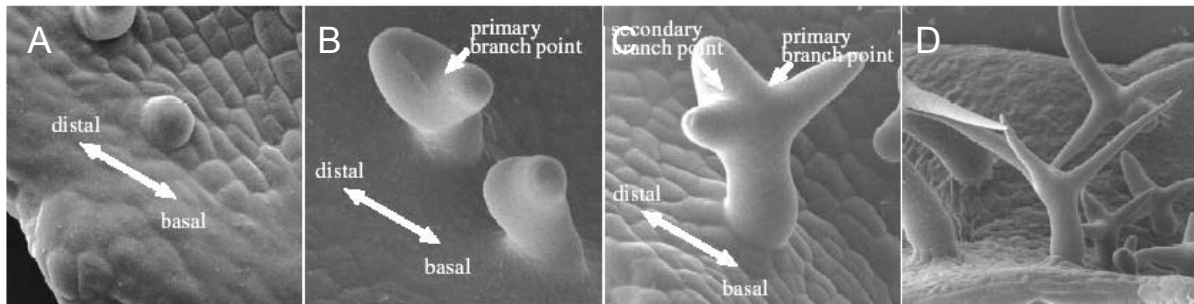


**Figure 1: Steps in trichome development.** Scanning electron micrographs of developing wild-type trichomes. **(A)** Incipient unbranched trichome. **(B)** Trichome with primary branch point. Note orientation of the branches with respect to the basal-distal leaf axis. **(C)** Trichome with primary and secondary branch. **(D)** Mature trichome. [Figure modified from Schwab *et al.* 2000].

### A 1.3. Endoreplication-dependent trichome morphogenesis

One group of genes appears to affect primarily the number of endoreduplication cycles and probably, as a consequence, also branch number (Hülkamp *et al.* 1994, Perazza *et al.* 1999, Kirik *et al.* 2001, Schnittger *et al.* 2003). The *gl3* mutant is reduced in branching and shows a reduction of endoreplication cycles in the trichome from approximately 32C to 16C, whereas trichome-specific overexpression lead to enhanced branching and a DNA-content of approximately 128C (Hülkamp *et al.* 1994, Kirik *et al.* 2004c). Beside trichome morphogenesis and endoreplication, *GL3* is also involved in trichome-pattern formation and encodes for a bHLH transcription factor (Payne *et al.* 2000). Moreover the *try* mutant that has been isolated as a patterning mutant, also shows trichomes with up to five branch points and has a DNA content of approximately 64C on average (Hülkamp *et al.* 1994). *TRY* encodes for a MYB-like transcription factor (Schellmann *et al.* 2002). Another group of mutants, the so-called *kaktus* group, show overbranching that is coupled with enhanced DNA content (Perazza *et al.* 1998). Those studies revealed a link between gibberelic acid (GA) signalling and trichome morphogenesis, because the *spindly* mutant that shows a GA-oversensing phenotype also results in trichomes with enhanced branching (Perazza *et al.* 1998). The *KAK2* gene has been cloned and shown to be an E3-ubiquitin ligase, thereby indicating that the control of protein degradation processes is crucial for the correct trichome morphogenesis (Downes *et al.* 2003, El Refi *et al.*

2003).

Direct interfering with the cell-cycle machinery in *Arabidopsis* trichomes has been shown to result in altered morphogenesis (Schnittger *et al.* 2001a, Schnittger *et al.* 2001b, Schnittger *et al.* 2003). The trichome specific expression of an inhibitor of the cell cycle dependent kinase (CDK), the KRP1 (Kip related protein1)/ICK1 (Inhibitor of Cyclin dependent kinase1) gene results in less branched trichomes and a strong reduction in DNA content (Schnittger *et al.* 2003). Surprisingly those cells eventually collapsed and died, which gave a hint to the connection of cell-cycle regulation and cell death control (Schnittger *et al.* 2003). The study of the *cpr5* mutant, that shows reduced endoreduplication and trichome-branching, revealed a similar relationship (Kirik *et al.* 2001), and will be part of this work.

The sequence analysis of the *STI* gene, which was cloned by Hilmar Ilgenfritz, revealed a homology with prokaryotic DNA-replication factor C and DNA-polymerase  $\gamma$ -subunits. This suggested that DNA replication might be regulated by *STI* (Ilgenfritz *et al.* 2003). However the further analysis, which is given in this work, revealed no such relationship with *STI*.

#### **A 1.4. Endoreplication-independent branch mutants**

A second group of branching mutants affects branch number without affecting endoreduplication (Folkers *et al.* 1997, Luo and Oppenheimer 1999, Qiu *et al.* 2002). The genetic analysis of branching mutants suggests several redundant pathways control branch formation (Luo and Oppenheimer 1999). To date, five branching genes have been cloned and all appear to be involved in the regulation of the microtubule cytoskeleton at different levels. The *ZWI* (*ZWICHEL*) gene encodes a kinesin motor protein with a calmodulin-binding domain, indicating that microtubule-based transport is important for branch formation (Oppenheimer *et al.* 1997). That the spatial organization of microtubules is important for trichome branching is suggested by the finding that in *an* (*angustifolia*) mutants, reduced trichome branching is correlated with the failure to establish a higher microtubule density at the tip of the developing trichome (Folkers *et al.* 2002). The underlying biochemical mechanism, however, remains unclear because AN encodes a novel protein with sequence similarity to C-terminal binding protein/BrefeldinA ribosylated substrates that are known to be involved in transcriptional regulation or in vesicle

budding but not in microtubule function (Folkers *et al.* 2002, Kim *et al.* 2002). The *FRA2* (*FRAGILE FIBER2*)/*ERH3* (*ECTOPIC ROOT HAIR3*) gene appears to be involved in the regulation microtubule assembly and disassembly. In *fra2/erh3* mutants trichomes are underbranched; also, other cell types show morphogenesis defects (Burk *et al.* 2001, Webb *et al.* 2002). *FRA2/ERH3* encodes for a katanin-p60 protein, suggesting that it functions as a microtubule-severing protein (Burk *et al.* 2001, Webb *et al.* 2002). In *fs* (*fass*)/*ton2* (*toneau2*) mutants, shape changes of various cell types have been correlated with distortions of the microtubule cytoskeleton (Traas *et al.* 1995, McClinton and Sung 1997). Therefore, it is likely that the unbranched trichome phenotype in *fs* mutants (Torres-Ruiz and Jürgens 1994) is also linked to the microtubule phenotype. *TON2* encodes a novel protein phosphatase 2A regulatory subunit, suggesting that microtubule organization in plants is controlled by the phosphorylation and dephosphorylation of proteins (Camilleri *et al.* 2002). Mutation in the *SPIKE1* gene results in underbranched trichomes along with morphogenesis defects in various cell types. Microtubule organization is misregulated in *spk1* mutants and the recent cloning of *SPK1* revealed that it encodes an adapter protein involved in the integration of extracellular signals with the cytoskeletal organization (Qiu *et al.* 2002). These observations are supported by drug inhibitor studies that revealed distinct roles of actin and tubulin during trichome cell morphogenesis (Mathur *et al.* 1999, Szymanski *et al.* 1999, Mathur and Chua 2000). Although the inhibition of the actin cytoskeleton causes irregularities in the directionality of cell expansion, experiments with drugs disturbing the microtubule cytoskeleton result in reduced trichome branching.

To further elucidate the molecular mechanisms underlying branch formation, I have studied the *STI* (*STICHEL*) gene. *sti* mutants exhibit the strongest branch phenotype: All trichomes are unbranched. Positional cloning revealed that *STI* encodes a novel protein containing a domain with sequence similarity to eubacterial DNA-polymerase III  $\gamma$ -subunits (Ilgenfritz *et al.* 2003).

The *cpr5* mutant is similar to the *sti* mutant because it also shows a trichome-branch defect. However the further analysis revealed a link to cell-proliferation and cell-death control in a more pleiotropic manner and therefore the analysis of *cpr5* will be separated from the analysis of *sti*.

## A 2. RESULTS

### A 2.1. Analysis of STI

#### A 2.1.1. STI belongs to a group of novel genes

The sequence analysis of *STI* revealed that it encodes for a protein of 1,218 amino acid residues with a predicted molecular mass of 135.3 kD. Sequence comparison with other known proteins and motifs identified three putative functional domains. A large domain between amino acids 454 and 799 shows sequence similarity to eubacterial DNA polymerase III  $\gamma$ -subunits (Fig. 2A, Ilgenfritz *et al.* 2002). The prokaryotic DNA Polymerase  $\gamma$  III -subunit is the main component of the  $\gamma$ -complex, which is important for the formation of the replication initiation complex with the dimeric  $\beta$ -subunit. In principle, the DNA polymerase III is able to perform DNA replication without the  $\gamma$ -subunit, but the processivity is lower by several orders of magnitude. Upon ATP binding, the  $\gamma$ -complex loads the  $\beta$ -subunit onto a primer DNA template. Dissociation of the  $\gamma$ -complex from the  $\beta$ -subunit to allow the polymerase to bind the  $\beta$ -subunit requires ATP hydrolysis (Bertram *et al.*, 1998). The similarity is 49% to 55% (identity 29%– 35%) within the homology region. Similarity to the family of 36- to 40-kD ATP-binding subunits of replication factor C (RFC, also known as activator 1), the archaeobacterial and eukaryotic functional counterparts of the bacterial  $\gamma$  subunit (Chen *et al.*, 1992a, 1992b), is less pronounced (42%–44% similarity, 23%–27% identity). Fig. 2B shows the alignment of STI with this group of proteins, including the putative RFC from Arabidopsis. The latter is that member of a class of four putative RFCs in Arabidopsis that shows highest sequence similarity with the eukaryotic RFCs (Fig. 2B). Figure 4 illustrates that STI and four STI homologues from Arabidopsis represent a phylogenetically separate branch, thereby defining a new, potentially plant-specific, subfamily among the  $\gamma$ -subunit homologues. The five proteins of this subfamily are markedly larger than the relatively small RFC proteins and the prokaryotic DNAPol III  $\gamma$  subunits and show sequence similarity outside the RFC/ $\gamma$  subunit domain (Fig. 3).



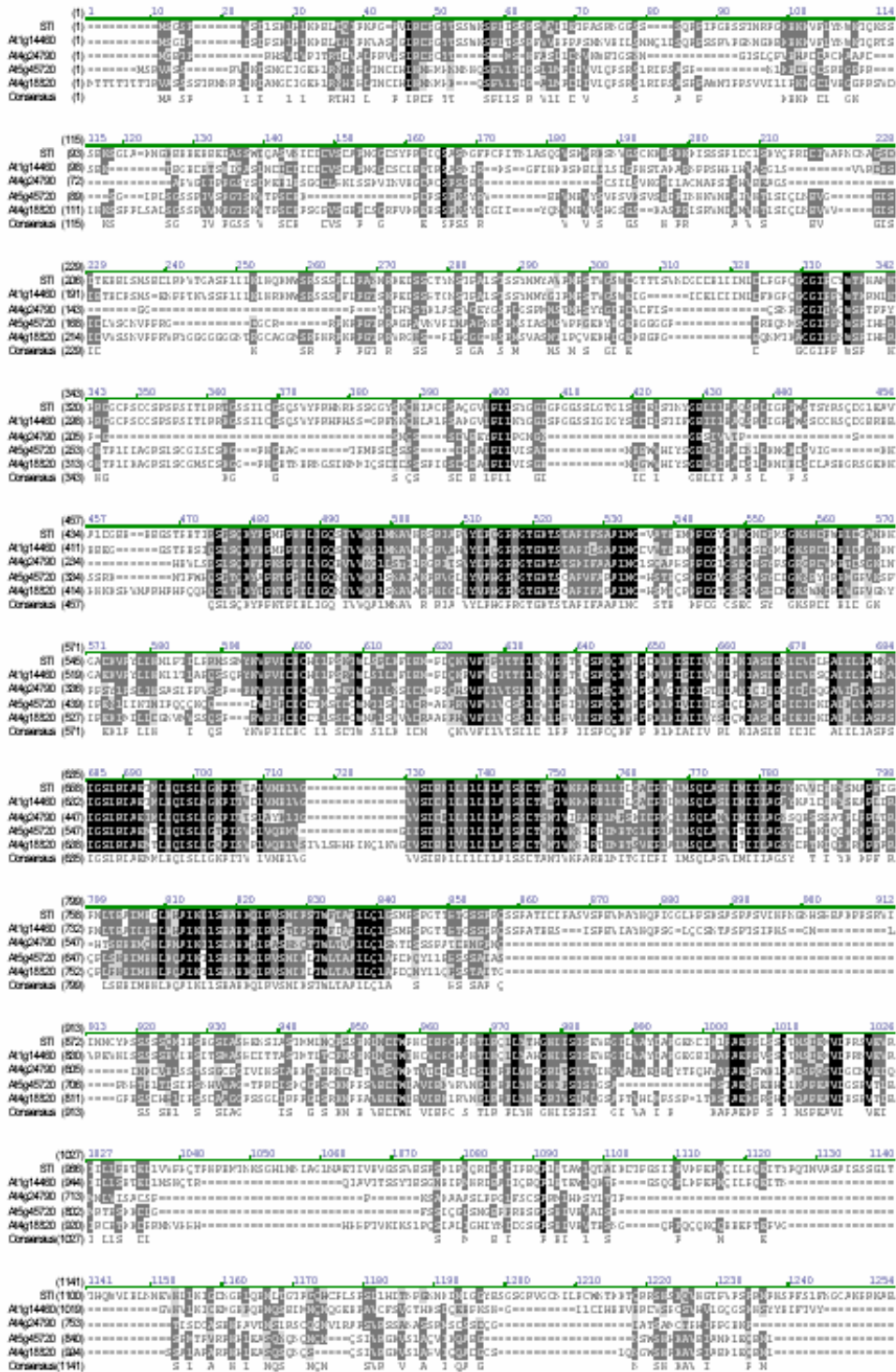


**Figure 3: Sequence comparison between STI with its closest homologs.** STI is a member of a class of five homologs that share sequence similarity outside the DNA polymerase III  $\gamma$ -subunit/RFC domain. Black-shaded amino acids are identical, dark grey-shaded amino acids are conserved, and light grey indicates weak similarity. [Figure from Ilgenfritz *et al.* 2003]

Two regions, one between amino acids 273 and 304 and a second between amino acids 425 and 449, show similarity to PEST domains known to mediate rapid protein degradation. According to the score calculated based on the PEST hypothesis by Rodgers *et al.* (1986), the two PEST domains found in STI have a very high score of 9.24 and 9.58. Three nuclear localization signals (NLSs) suggest that STI is targeted to the nucleus with a probability of 87%. One NLS is located in the N-terminal part, and the two others are located tandemly at the very C terminus.

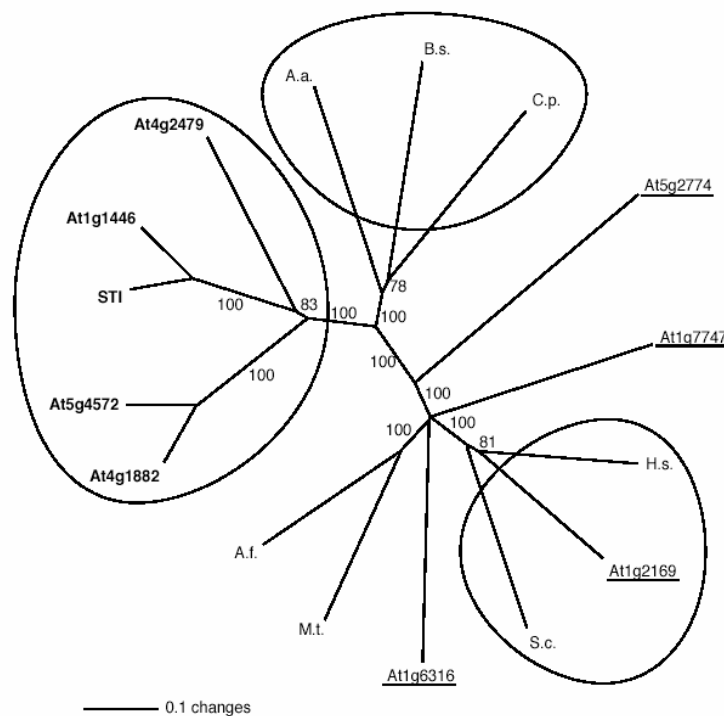


**Figure 4: Phylogenetic tree of the STI, the DNA polymerase III  $\gamma$ -subunit, and the RFC small subunit family.** The phylogenetic tree of STI, the DNA polymerase III  $\gamma$  subunit and the RFC small subunit family were calculated using only the core homology region corresponding to amino acids 449 to 799 in STI. The phylogenetic distance is shown as an unrooted dendrogram. The scale bar indicates 10% changes of amino acids. The bootstrap values are indicated for each branch. The five closest related STI homologs are bold and the four putative RFC-like proteins in Arabidopsis are underlined. The five closest STI homologs fall in a class that is separate from both, the prokaryotic DNA polymerase III  $\gamma$ -subunits and the eukaryotic RFC small subunits (the three groups are marked by circles). Note that only one of the Arabidopsis RFCs, At1g2169, is in the same group as the known eukaryotic RFC small subunits. A.a. *A. aeolius* (aq 1855); B.s., *B. subtilis* (Bsu0019); C.p., *C. pneumoniae* (CPn0040); A.f., *A. fulgidus* (AF20608); M.t., *M. thermo-autotrophicum* (MTH241); S.c., yeast (YSCRFC2); H.s., human. [Figure adopted from Ilgenfritz *et al.* 2003]

### A 2.1.2. *STI* acts in a dosage-dependent manner

Previous experiments using different *sti* alleles and the genetic interactions of representative strong and weak alleles with other mutants affecting branching and/or endoreduplication revealed that *STI* acts in a dose-dependant manner (Fig. 5, Ilgenfritz *et al.* 2003). This analysis showed that strong *sti* alleles invariably exhibit almost only unbranched trichomes, two weaker alleles have an increased frequency of two-branched trichomes (Ilgenfritz *et al.* 2003). The *sti-40* allele has been shown to contain a mutation in the splice-donor site, thereby leading most likely to premature STOP if the transcript is spliced in the wrong way, however stronger alleles have more C-terminally mutations leading to premature STOP codons (Ilgenfritz *et al.* 2003). The mutation in the weak *sti-47* allele leads to the most N-terminal premature STOP of all mutant alleles. This effect was explained by a reinitiation of translation at the next ATG bearing a minimal Kozak sequence (Ilgenfritz *et al.* 2003). In addition double and triple mutant combinations of strong and weak *sti* alleles suggest that *STI* acts in a dose-dependent manner (Folkers *et al.* 1997, Ilgenfritz *et al.* 2003).

Therefore the question was if an ectopic expression of *STI* would have an effect on branching. Therefore the cDNA of *STI* was fused to the 35S Cauliflower Mosaic virus promoter and this construct was introduced into the *sti* mutant. Sixty-seven transgenic lines were studied for the rescue of the mutant phenotype. Seventeen lines showed a weak rescue, and 34 showed complete rescue with up to three branches. In addition, we found in 11 lines trichomes with more than two branch points, occasionally up to six branch points (Fig. 5D). Semiquantitative RT-PCR analysis of the 35S:*STI* specific expression levels did not reveal clear differences in the RNA levels between lines exhibiting weaker or stronger rescue (Table 1; Fig. 6). Thus, in summary, the overexpression of *STI* does not only rescue the *sti* phenotype, but also leads to extra branch formation.

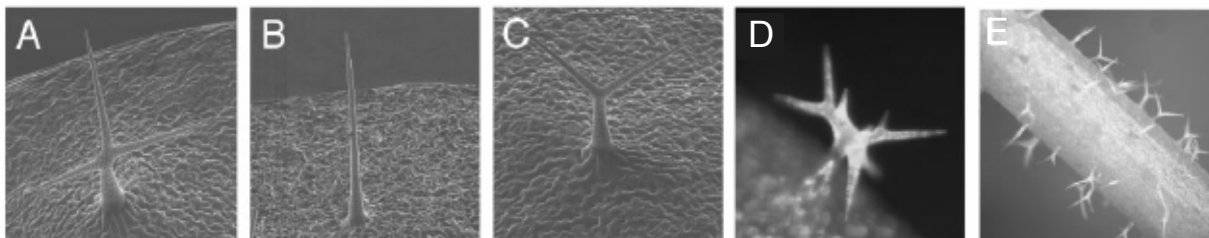


**Figure 5: Trichome-phenotypes of *sti* and 35S::*STI*.** (A) – (C) scanning electron micrographs of trichomes, (A) WT three-branched trichome, (B) *sti-146* mutant unbranched trichome, (C) *sti-40* mutant two-branched trichome, (D) 35S::*STI* leaf trichome with six branch points, (E) 35S::*STI* stem trichomes with branches. [Figure adopted from Ilgenfritz *et al.* 2003].

Line	% Branch points				Number of trichomes
	0	1	2	3	
<i>Ler</i>	-	3	97	-	622
<i>sti-146</i>	97	3	-	-	468
<i>35S::STI #12</i>	2	58	40	-	422
<i>35S::STI #67</i>	1	38	61	-	370
<i>35S::STI #60</i>	-	4	92	4	379
<i>35S::STI #8</i>	-	1	61	38	360
<i>35S::STI #7</i>	-	-	58	42	219
<i>35S::GFP-STI #24</i>	9	28	45	18	1016

**Table 1: Effect of 35S::STI on trichome branching.** Trichomes were counted on the third and fourth leaf of 10 or more plants.

Also, in 35S:*STI* lines, stem trichomes that are normally unbranched exhibited up to two branch points (Fig. 5E), suggesting that organ-specific differences in trichome branching are controlled by *STI*.

### A 2.1.3. *STI* is not involved in endoreplication

Previous analysis of the DNA content in *sti* trichomes revealed no effect in endoreplication (Ilgenfritz *et al.* 2003).

Because of the homology of *STI* to DNA-polymerase III  $\gamma$  subunits, the possible role of *STI* in endoreplication was further analysed by measuring the DNA-content of the 35S:*STI* lines that showed an overbranched phenotype (Table 1). This was studied in two independent lines. In both lines, trichomes had a DNA content indistinguishable from wild type ( $38 \pm 15$  C, n = 149;  $37 \pm 16$  C, n = 60; WT:  $38 \pm 17$  C, n = 49).

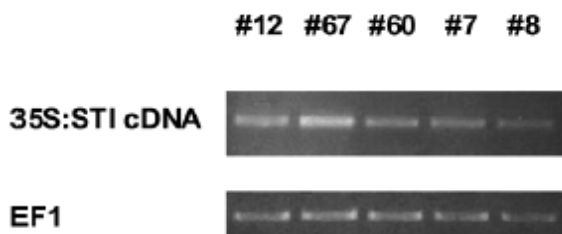


**Figure 6: Analysis of expression levels in 35S:*STI* lines by semiquantitative RT-PCR.** The numbers of the lines correspond to those in Table 1. The elongation factor1 EF1 was used as a control. [Figure adopted from Ilgenfritz *et al.* 2003].

#### A 2.1.4. Localisation of GFP-STI

The homology to the DNAPoIII  $\gamma$  /RFC subunit and the existence of three nuclear localisation signals (NLS) point towards a nuclear function of *STI*. However the nuclear DNA content was neither impaired in the mutant nor in the 35S::*STI* lines. Therefore it was important to reveal the intracellular localisation of *STI*.

The *STI*-CDS was fused N-terminally to a *GFP* and expressed under the CaMV 35S promoter in *sti-146* plants. Rescued lines (see table 1) were selected and further analysed for GFP-fluorescence using confocal laser scanning microscope (CLSM).

Interestingly fluorescence could not be detected in nuclei, but quite specific in young trichomes that started to branch (Fig. 7A). This fluorescence was visible at the just initiated side branch and ceased during the outgrowth of the branch (Fig. 7A). Single optical sections of the trichome branch sites show a speckled fluorescence of the GFP-signal (Fig. 7B). Ulrich Herrmann could confirm this localisation with an epifluorescence microscope, however the signal is barely visible (Ulrich Herrmann unpublished observation). Although *STI* is expressed in all organs of the plant, it was not possible to detect a specific fluorescence in other cells beside trichomes (data not shown).

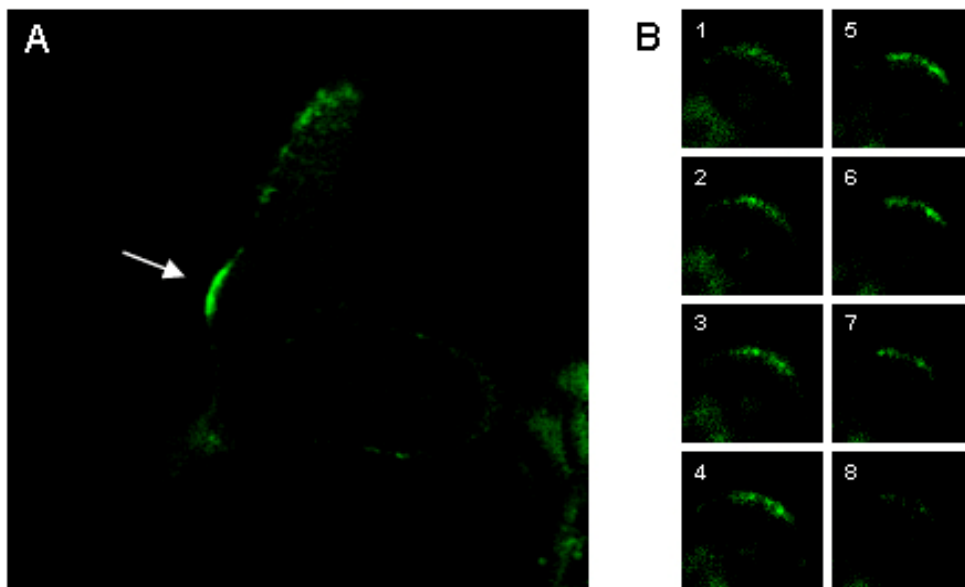


**Figure 7: Confocal laser scanning micrographs of GFP-STI.**

(A) Above-view on a young trichome. GFP-signal appears at trichome branch initiation (arrow)  
(B) Series through a branch point showing speckle-like structures.

## A 2.2. Analysis of *CPR5*

### A 2.2.1. Trichome differentiation in the *cpr5* mutant

In a screen of T-DNA mutagenised plants for trichome mutants, Viktor Kirik found two recessive mutants exhibiting reduced trichome branching, the *ctz8* mutant and the *5758-1* mutant (Fig. 10B) (Kirik *et al.* 2001). Both mutants exhibited the same phenotypes and resulted from a T-DNA insertion in the *CPR5* gene (accession number AY033229). The *ctz8* mutant and the *5758-1* mutant were renamed *cpr5-T1* and *cpr5-T2*, respectively.

In the *cpr5-T1* mutant, the number of trichome branches is drastically reduced (58% unbranched, 38% two branches, 3% three branches,  $n = 661$ ) compared to the corresponding wild-type WS (0% unbranched, 10% two branches, 90% three branches,  $n = 1029$ ) (Fig. 10b). Because trichome cells appeared to be reduced in size, I determined whether the ploidy level is also reduced (Fig. 8). The comparison of the relative fluorescence of DAPI-stained nuclei in *cpr5-T1* trichomes with that of wild-type (32C) and the *glabra3* (16C) mutant revealed that the DNA content in *cpr5-T1* trichomes corresponds to approximately 8C, suggesting that endoreduplication cycles stop after the second cycle is completed (Fig. 8). It was also found that the cell size and the nuclear size of epidermal pavement cells was greatly reduced (Figure 9B), such that, in 3-week-old plants, cell size and nuclear size of 98% of all cells in *cpr5* mutants corresponded to about 50% of the smallest cells in wild-type. This suggests that endoreduplication levels are also reduced in epidermal cells.

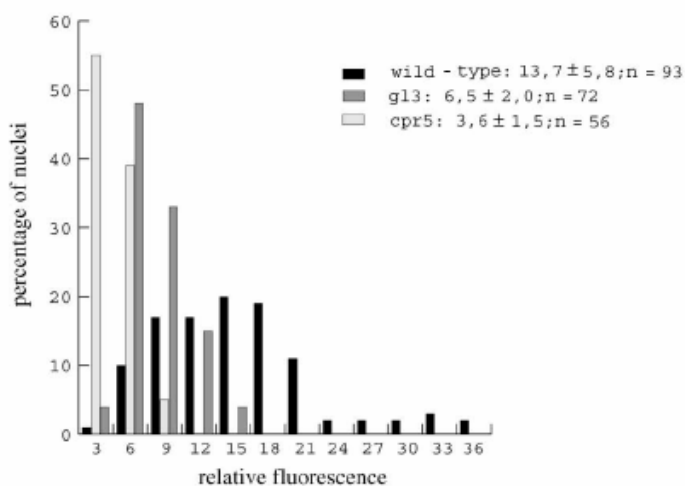


**Figure 8: Endoreplication in *cpr5*.**

Relative fluorescence of trichome nuclei is blotted against the percentage of nuclei that were grouped into classes of three fluorescence units. The distribution of nuclei in *cpr5-T1*, *gl3*, and wild-type is shown in the diagram, and the mean values and standard deviations are shown at the side.

[Figure from Kirik *et al.* 2001]

### A 2.2.2. Cell proliferation defect in the *cpr5* mutant

As *cpr5* mutant plants are much smaller than wild-type plants (Fig. 10A), it was tested whether cell divisions are generally affected. The number of pavement cells on rosette leaves of 3-week-old plants along the length and the width axis was compared. Along the length axis, *cpr5* mutant leaves had approximately 70% fewer cells than wild-type (wild-type:  $471 \pm 65$ ; *cpr5*:  $149 \pm 35$ ,  $n = 20$ ). Along the width axis, the cell number was reduced by about 60% (wild-type:  $269 \pm 23$ ; *cpr5*:  $109 \pm 35$ ,  $n = 20$ ). In order to determine whether these phenotypes are caused by growth retardation or by a premature growth arrest, the leaf elongation between *cpr5* mutants and wild-type was compared (Fig. 9A). Initial growth rates were indistinguishable. After 5 days, *cpr5* mutant leaves stopped growing, while wild-type leaves continued to grow.

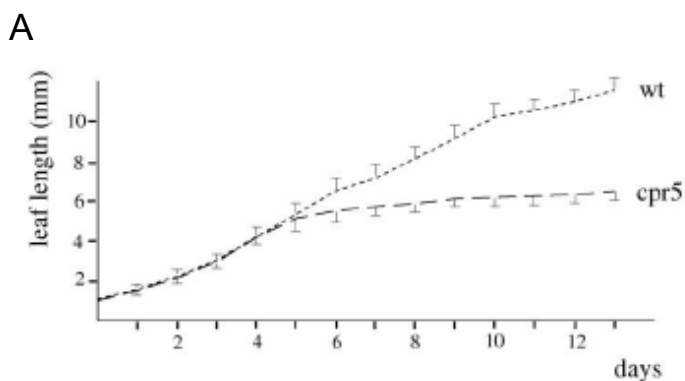
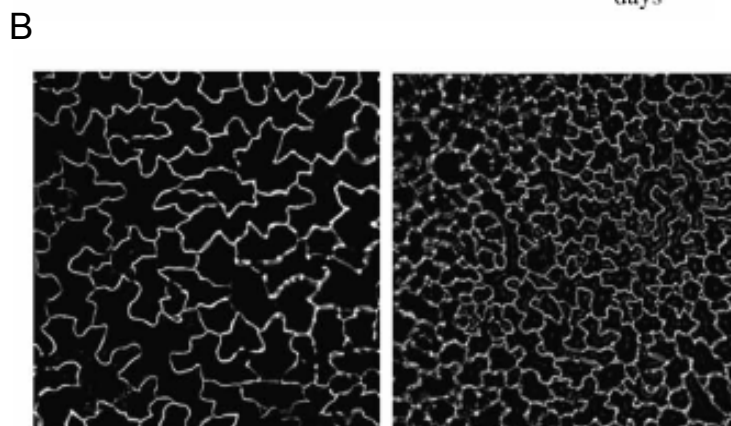


**Figure 9: Cell proliferation in *cpr5*.**

**(A)** Leaf length measurements of leaf number 5 at daily intervals. The standard deviation is shown for wild-type toward the top and for the *cpr5* mutant toward the bottom.

**(B)** Comparison of wild-type (left) and *cpr5* mutant (right) pavement cells at the same magnification.

[Figure adopted from Kirik *et al.* 2001]



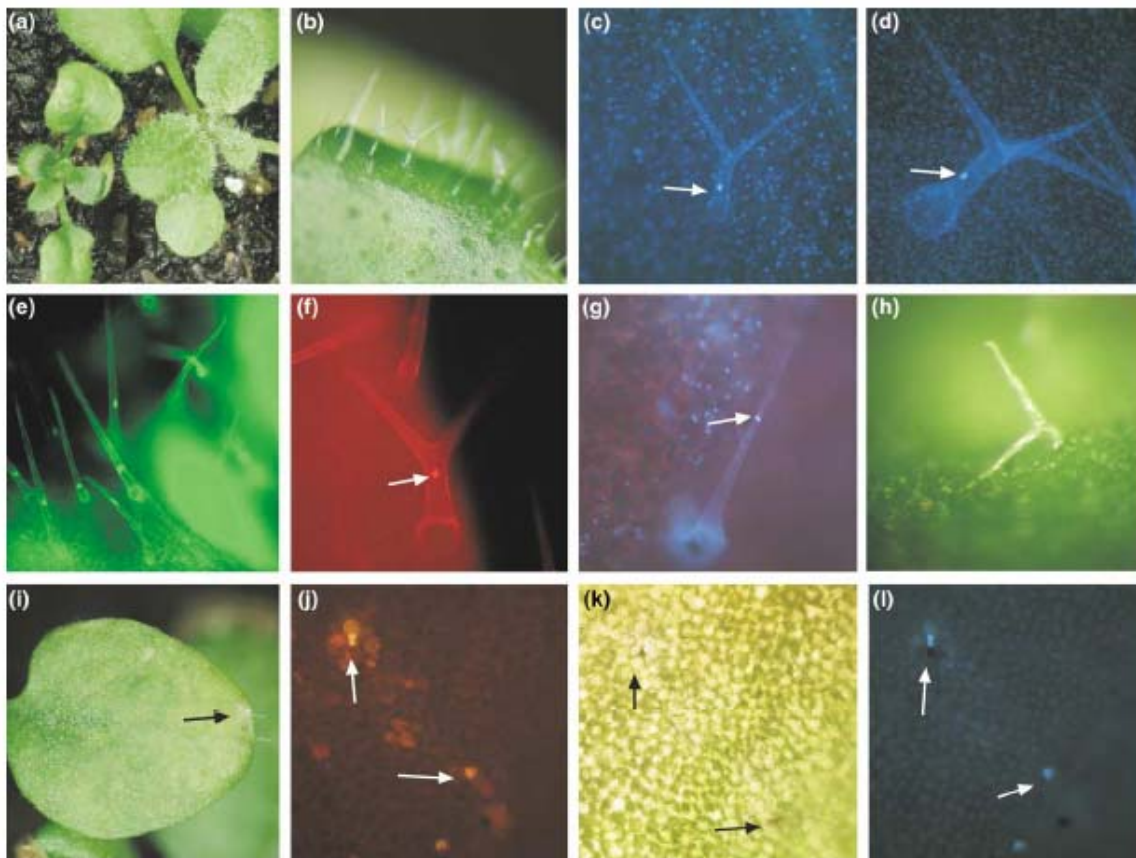


**Figure 10: Trichome and lesion phenotype in *cpr5* mutants.**

(a) A mature wild-type (right) and *cpr5* mutant plant (left).

(b) *cpr5* mutant trichomes on rosette leaves.

(c) DAPI-stained *cpr5* mutant trichome; the nucleus is marked with an arrow.

(d) DAPI-stained mature wild-type trichome cell; the nucleus is marked with an arrow.

(e) Mature FDA-stained *cpr5* mutant trichomes; note that the cytoplasmic region around the nucleus and the thin lining of the cytoplasm is stained, indicating that the cell is alive.

(f) Propidium iodide-stained *cpr5* mutant cell; staining indicates that membranes are not intact anymore and that the cell is dead. Note that the nucleus still has a normal morphology (arrow).

(g) DAPI-stained *cpr5* mutant trichome cell, the nucleus is drastically reduced in size and is condensed (arrow).

(h) Collapsed trichome cell.

(i) Lesions on rosette leaves of *cpr5* mutants (arrow).

(j) Propidium iodide-stained leaf tissue; note that single cells have started to die (arrow).

(k) Light micrograph of the same leaf area as in (j); note the single brownish dead cells (arrow).

(l) Same leaf area as in (j) and (k), using the UV filter set. Note that autofluorescent cells are different from the brown cells shown in (k) (arrow).

[Figure adopted from Kirik *et al.* 2001].

### A 2.2.3. Cell death in the *cpr5* mutant

During the course of experiments, I noticed that *cpr5-T1* mutant trichomes on mature leaves eventually died and collapsed (Fig. 10h). Fluorescein diacetate (FDA), which labels only living cells, was found to stain mature *cpr5-T1* mutant trichomes (Fig. 10e), indicating that these trichomes had completed their normal differentiation program before cell death occurred. On 4-week-old plants, trichomes began to die, as indicated by propidium iodide staining (Fig. 10f). Initially, the nucleus appeared to be normal. However, eventually trichomes were found containing extremely small and condensed nuclei, indicating that the nucleus disintegrated (Fig. 10g). On 6- to 7-week-old plants, all trichome cells were collapsed, leaving the cell wall remnants behind (Fig. 10h).

Cell death was also observed in other cell types. On 6- to 7-week-old plants, single cells (Fig. 10k) or small leaf areas (Fig. 11i) were found to form lesions containing brownish cells (Figure 10i & 10k). In propidium iodide-stained leaves, single cells or cell groups were stained, indicating that cell death had occurred. Frequently, cells displaying a high autofluorescence were found (Fig. 10j, 10l), which is indicative of the production of high amounts of phenolic compounds and often correlates with cell death.

### A 2.2.4. Complementation of the *cpr5* mutant

The *cpr5-T1* and *cpr5-T2* mutants were isolated from screens of two different *Arabidopsis* T-DNA insertion mutant populations by Viktor Kirik. The genomic DNA sequences flanking the T-DNA insertions mapped to the P1 clone MXK3 on chromosome V (Kirik *et al.* 2001). According to the annotated sequence information, both T-DNA insertions are located in the first intron of the *CPR5* gene and most likely result in a complete loss of gene function (Kirik *et al.* 2001). In order to prove the correct identity of the gene, I used a 6340-bp BamHI fragment containing 3.407 bp 5' and 500 bp 3' of the annotated gene for rescue. A total of 16 transgenic lines were recovered, which all showed complete rescue of the *cpr5-T1* mutant phenotype.

Sequence analysis revealed that the *CPR5* gene encodes a novel putative transmembrane protein containing five putative transmembrane helices at the C terminus. *CPR5* is predicted to be a Type IIIa membrane protein, with the N terminus being cytoplasmatic (PSORT). In addition, a bipartite NLS is found at the N terminus at position 40–56 (PSORT) (Kirik *et al.* 2001).

### A 3. DISCUSSION

Although the genetic and cell biological analysis of trichome branching provides a well-defined framework for the formal logic of the system, little is known about the underlying molecular mechanisms. The molecular analysis of several branching mutants revealed links to the control of the microtubule function at different regulation levels, including the microtubule-based transport processes (Oppenheimer *et al.* 1997), the regulation of microtubule assembly and disassembly (Burk *et al.* 2001, Webb *et al.* 2002), and the control of microtubule organization (Traas *et al.* 1995, Camilleri *et al.* 2002, Folkers *et al.* 2002, Kim *et al.* 2002, Qiu *et al.* 2002). Although these findings provide an excellent entry point into the understanding of the final steps of cell morphogenesis, earlier steps such as the control of branch initiation and its spatial control remain misunderstood.

The trichome phenotype of the *sti* and the *cpr5* mutants are both similar in the reduction of branches. The elucidation of the protein structure of STI suggested a function of the gene in the context of DNA replication that is also affected in the *cpr5* mutant. However further analysis of the *35S::STI* and the *sti* mutant lines revealed no direct function of *STI* in this context. In addition the localisation of GFP-STI does not hint towards a nuclear function of STI although the protein contains three nuclear localisation signals.

On the other side the *cpr5* mutant was shown to be pleiotropic and has initially been identified as a mutant showing constitutive pathogen response (and was named accordingly). Therefore both mutants do not provide evidence for acting at a common pathway regulating trichome morphogenesis and will therefore be discussed separately.

#### A 3.1. Analysis of STI

##### A 3.1.1. The role of *STI* in cell morphogenesis

Three lines of evidence suggest that *STI* regulates branching in a dosage-dependent manner. First, mutations in the *STI* gene do not simply eliminate its function, but depending on the severity of

the defect, intermediate phenotypic defects are also observed. This suggests that less STI activity results in fewer branches. Second, conversely, lines overexpressing *STI* can trigger extra branch formation. A third line of evidence supporting a regulatory role of STI in branch formation comes from the genetic analysis of double mutants. In a previous study, the finding that *sti* mutants can be rescued in double mutants with *nok* but not with *try* has led to the assumption that STI and NOK might specifically counteract each other (Folkers *et al.* 1997). However, the findings that weak *sti* alleles can also be rescued by *try* and that the additional removal of *TRY* in a *sti nok* background results in an even better rescue suggests that mutations in the *sti* gene can be bypassed in several ways (Ilgenfritz *et al.* 2003). This suggests that STI is not required to make branches, but involved in the regulation of their number.

The cell biological analysis of *sti* mutants revealed no deviation from wild type at the subcellular level (Ilgenfritz *et al.* 2003). One criterion to monitor cell differentiation is the timing and extent of cell vacuolization. Reduced vacuolization was found to be associated with severe growth abnormalities of root hairs in *rhd3* mutants (Galway *et al.* 1997). Vacuolization in *sti* mutant trichomes, however, was normal (Birgit Schwab & Martin Hülskamp, unpublished result). A second important aspect is the organization and function of the actin and microtubule cytoskeleton. The general organization of both cytoskeletal elements was normal, suggesting that STI is not involved in the control of the microtubule or actin organization (Ilgenfritz *et al.* 2003).

### **A 3.1.2. Potential molecular function of STI**

The sequence similarities of STI to other proteins provide few clues about its molecular function. The presence of NLS domains and a DNA-polymerase III  $\gamma$ -subunit/RFC domain suggest that STI might be involved in the regulation of DNA replication. This, however, seems to be unlikely because the ploidy level in trichomes is normal in *sti* mutants and in lines overexpressing STI, indicating that replication is not affected in both situations. Consistent with this interpretation is the finding that *STI* belongs to a group of five genes that is clearly distinct from the putative Arabidopsis RFC genes. These five genes also show sequence similarity outside the DNAPolymerase III  $\gamma$ -subunit/RFC domain, suggesting that they may have adopted a new plant-specific role.

The analysis of the GFP-STI fusion leads towards such a potential role of STI during trichome

branch formation. The finding that the fusion localised exactly at the site of future branch formation suggests that STI has a quite direct role in the early initiation of this process. The fluorescence is detected even before any visible branch has formed. From the observed GFP-fluorescence it cannot be concluded to which cellular structure the protein is localised. Three main possibilities are conceivable, the cytoplasm, the plasma membrane or the cell wall. Cytoplasmic versus an anchored localisation could be determined with plasmolysis experiments. The speckled appearance of the GFP-signal suggests that STI localises to specific spots at the future branch point.

With one exception STI has been shown to be epistatic to all other branching mutant thereby confirming its importance for cell-morphogenesis (Folkers *et al.* 1998). Another important issue in this context would be the analysis of STI-localisation in different mutant backgrounds. One aspect is of special interest. The fact that unicellular trichomes can be multicellularised by a single mutation, *siamese (sia)*, or by ectopically expression of cyclin B1;2 and cyclin D3;1 (Larkin *et al.* 2000, Schnittger *et al.* 2002a & 2002b), suggests that unicellularity of trichomes may be an evolutionary new invention. This is additionally supported by the observation of multicellular trichomes in evolutionary older plant-species, like *verbascum* (Uphof, 1962). The example *verbascum* shows in addition that new branches of a trichome are established as new cells, thereby linking the initiation of branching with the decision of cell division (Uphof, 1962). Recent studies with another trichome-branch gene, *ZWI*, which encodes for a Kinesin like Calmodulin binding protein (KCBP), revealed a role of *ZWI* in cytokinesis (Bowser & Reddy 1997, Smirnova *et al.* 1998, Vos *et al.* 2000). Moreover *ZWI* and *ANGUSTIFOLIA (AN)* interact genetically and in yeast two-hybrid assays and *AN* contains a potential cyclin-dependent kinase (CDK)-specific phosphorylation site (Folkers *et al.* 1997, Folkers *et al.* 2002). The CDK $\alpha$  in *Arabidopsis* has been shown to colocalise with microtubule (MT) structures during cell division and in turn *an* mutants show MT organisation defects (Weingartner *et al.* 2001, Folkers *et al.* 2002, Kim *et al.* 2002). Therefore it is conceivable that the mechanism leading to the positioning of a new branch is derived from the positioning of the phragmoplast/cell-plate during the cell-cycle. How would STI localise therefore in a multicellularised trichome?

The fact that *sti-sia* double-mutants still produce multicellular but unbranched trichomes show that STI cannot be solely responsible for the positioning of the future cell plate in this multicellularised trichomes. However, there may be redundant genes acting. The *Arabidopsis*

genome contains four additional members of the *STI*-family, one showing very high homology to the STI protein, therefore it is conceivable that the members of the *STI* gene family play a role in positioning the site of cellular growth changes, either in such a process like branching or polar outgrowth and/or in a possibly related cell-division process (Ilgenfritz *et al.* 2003).

### A 3.2. Analysis of CPR5

The finding that the *CPR5* gene is involved in several processes including cell death, cell cycle, and pathogen response raises the question of what the primary cellular function of CPR5 is. Initially, the *cpr5* mutant was identified as an important component in the plant pathogen response pathway (Bowling 1997). *cpr5* belongs to a class of mutants that show several plant pathogen response reactions in the absence of a pathogen attack (Bowling 1997, Dietrich *et al.* 1994, Greenberg *et al.* 1994, Rate *et al.* 1999, Shah *et al.* 1999). In *Arabidopsis*, most of these spontaneous lesion mutants express features characteristic for systemic-acquired resistance (SAR) and are more resistant to pathogens. SAR is frequently associated with the HR and leads to an enhanced immunity in secondary plant tissues by systemic signaling (Ryals *et al.* 1996). Features characteristic of SAR that are also expressed in the spontaneous lesion mutants include an enhancement of salicylic acid (SA) levels and the expression of PR genes (pathogenesis-related genes). In some of these mutants' lesion formation, PR gene expression and resistance can be suppressed by overexpressing the bacterial salicylate hydroxylase gene, which leads to a reduction of endogenous SA levels (Shah *et al.* 1999, Weymann *et al.* 1999). This indicates that, in these mutants, SA mediates all other responses. In other mutants, including *cpr5*, the reduction of SA compromises the expression of PR genes and the pathogen resistance, but not lesion formation (Bowling *et al.* 1997, Hunt *et al.* 1997). Therefore, the constitutive exopathogen response phenotypes are considered secondary (Bowling *et al.* 1997). Whether *CPR5* controls SA accumulation and cell death by different pathways or whether SA accumulation in *cpr5* mutants is a consequence of cell death is unclear. Our finding that *cpr5* mutants are severely affected in the ploidy levels of trichomes and exhibit a marked reduction in cell number indicates that *CPR5* is also involved in the control of cell proliferation. Our finding that FDA stains mature *cpr5* mutant trichome cells indicates that the endoreduplication defects precede the initiation of cell death. Thus, as judged by the relative timing of events, the primary defect of *cpr5* mutants is a

defect in the proper control of cell proliferation. It is, however, unlikely that this cell cycle defect as such leads to the observed cell death, since trichome mutants such as the *gl3* mutant that display a reduced ploidy level without showing a cell death phenotype (Hülkamp *et al.* 1994) are known. Similarly, a large fraction of pavement cells also remains diploid in the wildtype without undergoing cell death (Melaragno *et al.* 1993).

However the recent finding that the ectopic expression of the inhibitor of cyclin dependent kinase 1 (ICK1) in *Arabidopsis* trichomes also leads to growth arrest and cell death raises the question how far cell cycle control is also involved in cell death control (Schnittger *et al.* 2003). Viktor Kirik and myself addressed this question with respect to trichome development in *cpr5* in more detail. Neither the ectopic expression of a mitotically active cyclin, which can induce multicellular trichomes (Schnittger *et al.* 2001a) nor the ectopic expression of *GL3*, which leads to enhanced endoreplication in the WT (Kirik *et al.* 2004c) can complement the *cpr5* mutant. The same was also found in double mutant combinations of *cpr5* with *try*, a mutant that shows enhanced endoreplication in trichomes (Hülkamp *et al.* 1994) or with *siamese (sia)*, a mutant that produces multicellular trichomes (Walker *et al.* 2000). However the trichomes in the *cpr5 try* double mutant shows a weak rescue of branching, but not of cell size (Viktor Kirik & Daniel Bouyer, unpublished observation). In addition the ectopic trichome-specific expression of *GL3* in *cpr5*, leads to swollen but still very small trichomes, in contrast to the very large trichomes in WT plants that overexpress *GL3* (Viktor Kirik, unpublished observation). This indicates that *CPR5* might be a limiting factor for cell growth and endoreplication.

The sequence analysis of the *CPR5* amino acid sequence reveals several domains, leading to contradictory predictions on the intracellular localization of *CPR5*. On the one hand, *CPR5* is predicted to be a Type IIIa membrane protein with five transmembrane helices at the C-terminus and a cytoplasmatic N-terminus. On the other side, a well-conserved bipartite NLS sequence in the cytoplasmatic region predicts a nuclear localization. An exciting possibility that would explain this apparent contradiction is that *CPR5* might function similarly to membrane-bound transcription factors that are kept in a dormant state in the cytosole by membrane anchors and are released by proteolytic cleavage, enabling the transcription factors to enter the nucleus (Brown *et al.* 2000, Hope *et al.* 2001).

To test the possibility that *CPR5* might be cleaved, I expressed the N- and C-terminal parts separately to see if the N-terminus, that contains the NLS, is able to rescue *cpr5*. However none

of the transgenic plants generated revealed any obvious phenotype. Therefore I think it is quite unlikely that a cleavage mechanism exists for CPR5 function.

Furthermore I tested if *CPR5* might be an active repressor of cell death. Trichome specific expression of *CPR5* did not show any phenotype and could not rescue the cell death phenotype in the *ICK1* misexpression lines. On the other side the ectopic expression of repressors of plant apoptosis, the BAX-inhibitor (Kawai-Yamada *et al.* 2003) and p35 (Lincoln *et al.* 2002) was not able to complement the *cpr5* mediated cell death phenotype (Viktor Kirik, unpublished observation). This indicates that the cell-death phenotype in *cpr5* is not a caspase-induced apoptosis event, or a BAX-induced cell-death event. Both processes have been shown to be forms of programmed cell death (PCD) (Lincoln *et al.* 2002, Kawai-Yamada *et al.* 2003). So, none of the further experiments revealed a possible molecular function of *CPR5* and its elucidation is still awaited.

**B**

# Trichome Pattern Formation

## B 1. INTRODUCTION

### B 1.1. Trichome initiation in *Arabidopsis thaliana*

The development of trichomes, the leaf hairs of *Arabidopsis thaliana* is an excellent model system to study pattern formation (Hülkamp *et al.* 1994, Marks 1997, Hülkamp *et al.* 1999, Szymanski *et al.* 2000, Larkin *et al.* 2003). How are cells recruited from initially equivalent cells to differentiate and arranged in a well-ordered manner? Trichomes on rosette leaves form such a simple two-dimensional spacing pattern and are initiated with regular distance to each other. This pattern is established very early during leaf development when the leaf is around 100 $\mu$ m in length, where it starts at the distal tip and proceeds basipetally (Fig. 11A and Hülkamp *et al.* 1994, Larkin *et al.* 1996). The resulting pattern is tightly controlled because the distance between the developing trichomes is at least three to four cells and trichomes adjacent to one another (clusters) are much less frequent as would be expected by a random distribution (Hülkamp *et al.* 1994, Larkin *et al.* 1996).

An inducible positive regulator of trichome development has been used to show that trichome development is restricted to a certain stage during leaf development and coincides with mitotically active regions of the leaf (Lloyd *et al.* 1994). Clonal analysis of trichome development suggested that cell lineage is not involved, because trichomes do not derive from systematic cell division patterns (Larkin *et al.* 1996). It is likely that during the pattern formation process inhibitory interactions between the trichome precursors take place and that trichome patterning does not rely on underlying prepatterns but is rather based on a *de novo* mechanism (Larkin *et al.* 1996, Schnittger *et al.* 1998, Schnittger *et al.* 1999).

### B 1.2. Elements of the trichome pattern system

In genetic screens several mutants have been identified that show defects in trichome initiation and pattern formation. Activators like *GLABRA1* (*GL1*), *GLABRA3* (*GL3*), *ENHANCER\_OF\_GL3-1* (*EGL3*) and *TRANSPARENT\_TESTA\_GLABRA1* (*TTG1*) are necessary for the production of trichomes, the respective mutants have fewer or no trichomes (Oppenheimer

*et al.* 1991, Hülkamp *et al.* 1994, Zhang *et al.* 2003, Koorneef 1981). Mutations in *TTG2* result in reduction and aberrant development of trichomes (Johnson *et al.* 2002).

Mutations in negative regulators of trichome initiation like *caprice* (*cpc*) or *triptychon* (*try*) result in increased trichome number or formation of trichome clusters, respectively (Wada *et al.* 1997, Hülkamp *et al.* 1994, Schellmann *et al.* 2002).

Several of these factors involved in trichome initiation and pattern formation also play a role in trichome morphogenesis. Instead of having three branches, the *try* mutant trichomes exhibit up to six branches and results in bigger trichomes (Hülkamp *et al.* 1994, Schellmann *et al.* 2002). In contrast the *gl3* mutant exhibits reduced branching and cell size, which is also observed in weak *ttg1* alleles and in the *ttg2* mutant (Hülkamp *et al.* 1994, Payne *et al.* 2000, Larkin *et al.* 1994, Larkin *et al.* 1999, Schnittger *et al.* 1999, Johnson *et al.* 2002).

### **B 1.3. Molecular nature of the trichome patterning genes**

*GL1* encodes for an R2R3-type MYB transcription factor, *GL3* and *EGL3*, which are partially redundant, are members of the basic helix-loop-helix (bHLH) transcription factor family (Oppenheimer *et al.* 1991, Payne *et al.* 2000, Zhang *et al.* 2003). The *TTG1* protein contains four or five WD-40 domains, which are thought to mediate protein-protein interactions (Walker *et al.* 1999, Larkin *et al.* 2003).

*TRY* and *CPC* are members of a subfamily of at least four partially redundant small MYB-like transcription factor like genes, containing only one MYB-R3 domain, lacking a transcriptional activator-domain and have therefore been assumed to function as transcriptional repressors (Wada *et al.* 1997, Schellmann *et al.* 2002, Kirik *et al.* 2004a, Kirik *et al.* 2004b). Redundancy among these genes has recently been demonstrated because the double mutant *try cpc* result in the formation of large clusters of up to 30 trichomes and triple mutants of *try cpc* together with the other members of this subfamily, the *enhancer\_of\_try\_cpc1* (*etc1*) and *etc2* result in even more enhanced ectopic trichome formation, although the *etc1* and the *etc2* mutant are completely masked as single mutants (Kirik *et al.* 2004a, Kirik *et al.* 2004b).

#### **B 1.4. Functions besides trichome patterning**

Besides trichome formation most of the above listed genes also act, or have homologues counterparts, in *Arabidopsis* epidermal root and hypocotyl pattern formation (Lee & Schiefelbein 2001, Schiefelbein 2003, Larkin *et al.* 2003, Berger *et al.* 1998, Zhang *et al.* 2003). It is assumed that in both, the root and the shoot (leaf) a competition for either non-hair cell fate or the trichome cell fate takes place (Schiefelbein 2003). However in contrast to the leaf, in the root positional cues are important for guiding the patterning mechanism, because root-hair cell files arise over the intercellular space between the underlying cortex cells. The mechanism(s), which guide this process, are unknown.

In addition, because the same set of molecular components, like an R2R3 MYB (*TRANSPARENT\_TESTA2*, *TT2*), *GL3/EGL3* (plus the *TT8* bHLH gene) and *TTG1* are involved in the regulation of anthocyanin/thannin biosynthesis, the underlying mechanism might be similar (Nesi *et al.* 2001, Zhang *et al.* 2003, Koorneef 1981).

#### **B 1.5. Special role of TTG1 and interactions between the patterning components**

During trichome development *TTG1* seems to have a dual role in activation and inhibition of trichome formation. Strong alleles are nearly completely glabrous whereas weak *ttg1* alleles develop trichomes in clusters (Larkin *et al.* 1994, Walker *et al.* 1999, Larkin *et al.* 1999). A strong argument for the role of *TTG1* in the negative regulation comes from the analysis of transheterozygotes of different *ttg1* alleles with *try*, in which a strong enhancement of nest formation has been shown in transheterozygotes, that is not observed in homologous *try-g11* or *try-g13* combinations (Larkin *et al.* 1999, Schnittger *et al.* 1999).

*ttg1* mutants can be, at least partially, rescued for example by ectopically expressing *GL3* together with *GL1* or *EGL3*, or by over expressing *GL1* in the absence of *TRY*. Therefore it has been assumed that *TTG1* acts upstream or together with these genes and has a more modulating role (Payne *et al.* 2000, Schnittger *et al.* 1999, Zhang *et al.* 2003).

Genetic and biochemical analysis have shown that these gene-products in fact interact and are thought to form either an activator, or an inhibitor complex (Schnittger *et al.* 1999, Larkin *et al.*

1999, Payne *et al.* 2000, Schellmann *et al.* 2000). Esch *et al.* could show that GL1 and TRY compete for the binding to the same domain of GL3 in a yeast-three-hybrid interaction assay whereas TTG1 is binding to a different site of GL3 (Payne *et al.* 2000, Esch *et al.* 2003). Although a direct biochemical interaction of GL1 or TRY with TTG1 does not seem to take place, double mutant analyses have shown genetic interaction (Larkin *et al.* 1999, Schnittger *et al.* 1999, Schellmann *et al.* 2002). Figure 12 shows a model that summarises these interactions for trichome patterning. How do these genes interact to create a pattern? First I want to introduce a theoretical assumption to explain two-dimensional pattern formation and its application to trichome development.

### **B 1.6. A model to explain two-dimensional pattern formation**

Meinhardt and Gierer have proposed a model to explain biological pattern formation, based on the reaction diffusion mechanism studied by Turing in the 50s (Meinhardt & Gierer 1974, for review see Koch & Meinhardt 1994, Meinhardt & Gierer 2000). In Turing's experiments the interaction of two substrates with different diffusion rates can generate spatial concentration patterns starting from near-uniform distributions (Turing 1952).

In the mathematical model of Meinhardt and Gierer, thereafter called activator-inhibitor model, a stable pattern is established by local self-enhancement and long-range lateral inhibition. The term self-enhancement means that a slight increase of the activator leads to a further increase of this activator. However this is not sufficient to create a regular pattern because it would lead to an overall activation of every small fluctuation. The inhibitor in this system complements the self-enhancement of the activator. This is established due the fast diffusion of the inhibitor, which prevents the activation of the surrounding tissue and at the same time does not disturb the incipient local increase of the activator.

A Computer simulation of this process is shown in figure 11B demonstrate that minute local increases lead to strong self-enhancement of the activator, which in turn are followed by increasing concentrations of the inhibitor. The activator gets more and more restricted to certain peaks, which are followed by the inhibitor, however the inhibitor concentration is increasing throughout the entire tissue thereby stabilising the pattern (Fig. 11B).

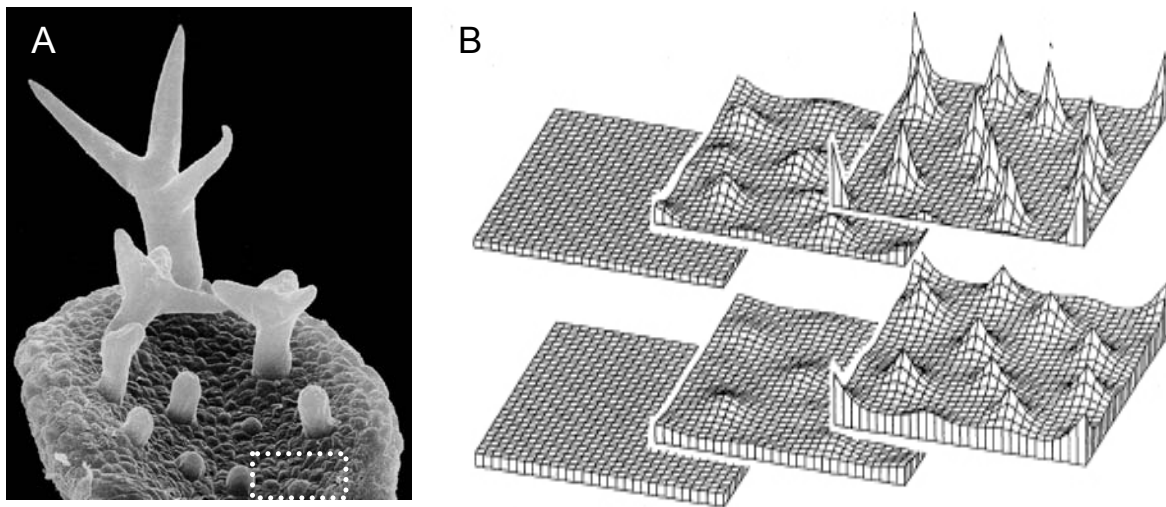


**Figure 11: Trichome differentiation and mathematical modelling.**

(A) Micrograph of a young leaf with developing trichomes at different developmental stages. Trichome pattern is established at the very early stages and thereafter trichomes are further separated by cell division of pavement cells (micrograph from Schnittger *et al.* 1999).

(B) Computer simulation using the equations of the activator-inhibitor model for the concentration of the activator (above) and the inhibitor (below). (Figure from Koch & Meinhardt 1994).

### B 1.7. Application of the activator-inhibitor model to the trichome patterning system

Do the activators in the trichome patterning system act in an autocatalytic feedback loop and do the inhibitors complement this by lateral inhibition? First the relationships between the postulated activators and inhibitors in the trichome patterning system have to be clarified, e.g. is the inhibitor activated by the activator, and does the inhibitor inhibit the function of the activator?

The overexpression of *GLI* does result in enhanced trichome production and strongly increased cluster frequency in the *try* mutant only, suggesting that *TRY* prevents cluster formation by inhibiting *GLI* as would be expected by the model (Schnittger *et al.* 1998, Szymanski *et al.* 1998a, Schnittger *et al.* 1999). The enhanced cluster formation was also found for the *GL3* homologous gene *R* from maize in *try* mutant background and is additionally enhanced if both activators, *R* and *GLI*, are ectopically expressed in the absence of *TRY* (Schnittger *et al.* 1999). Therefore *TRY* is supposed to mediate lateral inhibition by suppressing *GLI* and *GL3* function. In addition the analysis of trichome clusters in the *try* mutant background has shown that these

clusters are not of clonal origin, suggesting that *TRY* mediates intercellular signalling (Schnittger *et al.* 1999). However the non-cell-autonomous action of *TRY* has not been shown.

The activator-inhibitor model predicts that the negative regulator follows the expression pattern of the activator. In fact the activators and inhibitors show the same dynamic expression pattern with initial ubiquitous distribution throughout the patterning zone of the leaf and the following restriction to the trichomes (Larkin *et al.* 1993, Schellmann *et al.* 2002, Zhang *et al.* 2003). However it is not clear if the activators induce the expression of the negative regulators as predicted by the activator-inhibitor model. However there is some evidence that the activity of *TRY* depends on the dosage of the positive regulator *TTG1* (Schnittger *et al.* 1999, Larkin *et al.* 1999).

The activator-inhibitor model explains the generation of a regular pattern by a competition mechanism between activator and inhibitor. A competition between the positive regulator GL1 and the negative regulator TRY to bind to the GL3 protein was recently demonstrated by a yeast three-hybrid interaction assay (Esch *et al.* 2003).

The activator-inhibitor model involves cell-cell communication. But instead of signal peptides and respective receptors that have been shown to mediate lateral inhibition in animals (for review see Simpson 1997), all known factors in the trichome patterning system encode for transcription factors and one WD40 domain repeat protein (see above). Instead intercellular communication in plants is established due to symplastic connection, which allows the cells to exchange signalling molecules.

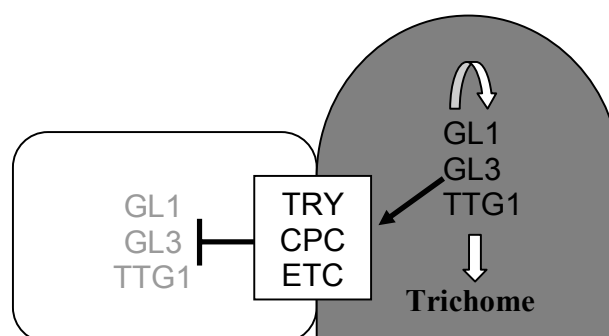


**Figure 12: Trichome patterning model.** This figure shows a simplified model to explain the competition mechanism between leaf epidermal cells. Interactions between the trichome patterning genes are shown. GL1, GL3 and TTG1 form an activating complex and will autocatalyze their own activity and activate the inhibitors TRY CPC and ETC(1/2), which due to their mobility move into neighbouring cells to inhibit the activating complex. (Figure modified from Schellmann *et al.* 2002).

### **B 1.8. Intercellular protein movement in plants**

Movement of transcription factors is a quite common phenomenon in plants and is most likely enabled by plasmodesmata (PD) (Kim *et al.* 2002, Lucas *et al.* 1995, Perbal *et al.* 1996, Sessions *et al.* 2000, Wu *et al.* 2002, Wu *et al.* 2003, Zambryski 2004). PDs symplastically connect plant cells, thereby building microchannels that allow the exchange of nutrients and specific signalling molecules (for recent reviews see Ghoshroy & Citovsky 1997, Heinlein 2002, Jackson 2000, Wu *et al.* 2002). Those processes are tightly regulated by the size exclusion limit (SEL) of the PD (Wu *et al.* 2002). The SEL varies between different tissues and different developmental stages and can be altered by specific factors, such as viral movement proteins (MPs) or endogenous proteins like the NtNCAPP in tobacco (Lee *et al.* 2003) and specific transcription factors, like the maize KNOTTED1 homeobox-transcription factor (KN1) (Lucas *et al.* 1995).

There exists a certain degree of directionality of movement that has been shown by the movement of KN1 from subepidermal tissue into the epidermis, but not from the epidermis into the mesophyll in leaves of *Arabidopsis* (Kim *et al.* 2003). However when expressed in the epidermis of the shoot apical meristem, the Green\_fluorescent\_protein (GFP)-KN1 fusion could be detected also in subepidermal tissue, showing that protein transport is developmentally regulated (Kim *et al.* 2003).

First insights into the biological significance of intercellular transcription factor movement came from studies of the radial patterning of the *Arabidopsis* root. The GRAS-family transcription factor SHORTROOT (SHR) is expressed in the vascular cylinder of the root, although the protein can be detected in both the vascular cylinder and the surrounding endodermis, a tissue which is missing in the *shr* mutant (Nakajima *et al.* 2001). It has been shown that the movement of SHR is necessary for the specification of the root endodermis thereby providing positional information; interestingly SHR moves only from the stele into the endodermis and not any further. Moreover in the endodermis SHR is strictly nuclear localised, whereas in the stele the protein can be detected in both the nucleus and the cytoplasm (Nakajima *et al.* 2001).

### **B 1.9. Connection between intra- and intercellular mobility?**

The correlation between intracellular localisation and the capability of the proteins to move between cells does not follow strict rules (Crawford & Zambryski 2000, Wu *et al.* 2003, Kim *et al.* 2002). The addition of a nuclear localisation signal (NLS) to GFP leads to a slight reduction of the passive transport of the protein, whereas the targeting to the ER completely abolishes mobility (Crawford & Zambryski 2000). However the loss of the nuclear localisation in KN1-protein leads to a loss in the movement ability, whereas mutated forms of the non-autonomous transcription factor LEAFY (LFY) that lead to exclusively nuclear localisation instead of the normal nuclear and cytoplasmic distribution, in turn lead to a decrease in mobility (Kim *et al.* 2002, Wu *et al.* 2003).

This rose the question of how specific protein mobility in plants really is, meaning that movement is rather the default state and in turn non-cell-autonomy is actively achieved (Wu *et al.* 2003). A problem in the studies of Wu *et al.* (2003) is that the used deletion and mutated forms of LFY have not been shown to be functional in plants, thereby raising the question of the significance of the gained insights into protein movement in plants. In addition the biological relevance of LFY-movement is still not clear, because it is expressed throughout the domain of its action.

### **B 1.10. Outlook and aim of the work**

Several aspects of trichome patterning are still elusive. How is the intercellular communication established and how do the genes act together to establish pattern formation? Especially the role of *TTG1* is still elusive because it has a double function in trichome patterning, e.g. positive and negative regulation. However the need for *TTG1* during trichome development can be bypassed. The aspect of intercellular communication in trichome-development is obvious, but so far none of the factors involved in this process have been tested for a non-cell-autonomous function.

In the following I studied the role of *TTG1* during trichome development. First, *TTG1* is the only member of the trichome patterning system whose expression pattern and cellular localisation was still not resolved. Therefore I did expression analysis and studied the intracellular targeting of TTG1. Moreover *TTG1* was shown to act non-cell-autonomous and there is evidence that the

TTG1 protein is able to move between cells. In several experiments I tried to test the relevance of the TTG1 mobility. Finally it was shown that TTG1 interacts with GL3 and the negative regulators *in planta*

The results are summarized in a new model to explain the very early steps of trichome pattern formation.

.

## B 2. RESULTS

### B 2.1. *TTG1*-dependent and -independent trichome development

Genetic studies of the relationship between the trichome regulators have implicated that both, the positive and the negative regulation of trichome-development are *TTG1*-dependent (Hülkamp *et al.* 1994, Larkin *et al.* 1994, Schnittger *et al.* 1999, Larkin *et al.* 1999). Previous experiments using ectopic expression of *GL1* and *GL3/EGL3* have shown that *TTG1* is not required for trichome formation (Schnittger *et al.* 1999, Payne *et al.* 2000, Zhang *et al.* 2003). The recent identification of redundant members of the negative regulator-class required a more detailed analysis of the *TTG*- independent trichome development (Schellmann *et al.* 2002, Kirik *et al.* 2004a & 2004b). Therefore triple and quadruple mutants were generated to test the genetic dependencies between the positive (*GL1*, *TTG1*) and the negative (*TRY*, *CPC*, *ETC1*, *ETC2*) regulators. Does the reduction of the inhibitor lead to trichome formation in the absence of *TTG1* or *GL1* without ectopically expression of the activators?

In the following experiments I used the *ttg1-13* mutant where the *TTG1* activity is completely abolished due to a complete deletion of the gene, which leads to a complete loss of trichomes (Fig. 13I, Walker *et al.* 1999). The *try cpc* double mutant shows formation of clusters with up to 30 trichomes (Fig. 13A and Schellmann *et al.* 2002). In fact the triple-mutant *ttg1-13 try cpc* is able to promote initiation and also outgrowth of trichomes (Fig. 13B, C). However complete differentiation and branching was not observed (Fig. 13C). This shows that the reduction in the inhibitor activity is sufficient to circumvent the need for *TTG1* to produce trichomes. However trichome production, although very limited, has also been observed if *ttg1-13* is backcrossed several times into the Col background (Larkin *et al.* 1999). The *ttg1-13 try cpc* triple mutant is a mixture of RLD, *Ler* and WS-O backgrounds and I could observe differences among the descendants of the crossings according to their trichome-development, which suggests that this process is quite sensitive to ecotype-specific modifiers (Larkin *et al.* 1996).

To test for a dose-dependent effect of the negative regulators, the quadruple mutants *ttg1-13 try cpc etc1* and *ttg1-13 try cpc etc2* were generated. Although the *etc1* and *etc2* mutant phenotypes are completely masked as single mutants, the combination with *try-cpc* revealed a redundancy in lateral inhibition with the mutation of *etc1* resulting in increased trichome cluster size (Fig. 13D, K), or tissue specific trichome formation on the stele of the leaves in the case of *etc2* (see Fig.

13F, Kirik *et al.* 2004a & 2004b). The reduction of *TRY*, *CPC* and either *ETC1* or *ETC2* can in fact more effectively compensate for the loss of *TTG1* (Fig. 13E, J, L). In the *ttg1 try cpc etc1* quadruple mutant background several trichomes are initiated that grow out and are able to build up to three branches, but appear glassy (Fig. 13L & Q). In the case of *ttg1 try cpc etc2* trichome development also takes place, but they are less branched (Fig. 13J). The reduction of the negative regulators does not lead to a complete rescue of *ttg1*. However a dose-dependent partial compensation can be observed. The phenotype of the quadruple mutant trichomes rather implicates that *TTG1* is required for correct trichome development.

This is in contrast to the *try cpc gl1-1* triple and *try cpc etc2 gl1-1* quadruple mutant that produces large clusters at the margins of the leaves, even on the first two leaves that never show trichome formation in the *gl1-1* mutant (Fig. 13M, G, N). However the very recent elucidation of redundancy of *GLI* with the *MYB23* gene limits the significance of these results (Kirik *et al.* 2004c). Therefore it is likely that the phenotype seen in the *try cpc etc2 gl1-1* quadruple mutant is due to the presence of *MYB23*.

In the triple and quadruple mutant combination of *gl1-1* with *try cpc* and *try cpc etc2* trichomes are formed on the hypocotyl and the cotyledons, thereby showing the same phenotype as the respective mutants containing the entire *GLI*, which shows that *GLI* is not required for trichome development in these organs *GLI* (Schellmann *et al.* 2002, Kirik *et al.* 2004a, Kirik *et al.* 2004b, Martina Pesch unpublished data). One explanation for this could be, that these tissues express *WEREWOLF* (*WER*), which is functional equivalent to *GLI* (Lee & Schiefelbein 2000, Lee & Schiefelbein 2001). A possible role of *MYB23* in the formation of ectopic trichomes on hypocotyls and cotyledons has to be elucidated. However I never observed trichome development on hypocotyls or cotyledons of the *TTG1* gene is absent (data not shown).

However the differences between the trichome phenotypes of *ttg1* and *gl1* in the negative mutant backgrounds are evident: The quadruple mutants of *ttg1* with *try cpc etc1* or *try cpc etc2* leads to a synthetic trichome phenotype, whereas *gl1* in combination with the *try cpc* or *try cpc etc2* shows the trichome morphology and cluster phenotype of the negative regulator mutants (compare Fig. 13O with 13P). This means that *try/cpc/etc2* are epistatic over *gl1*, trichome development is independent of *GLI*. However the redundancy of *GLI* with *MYB23* makes it difficult to conclude a clear hierarchical relationship between those genes.

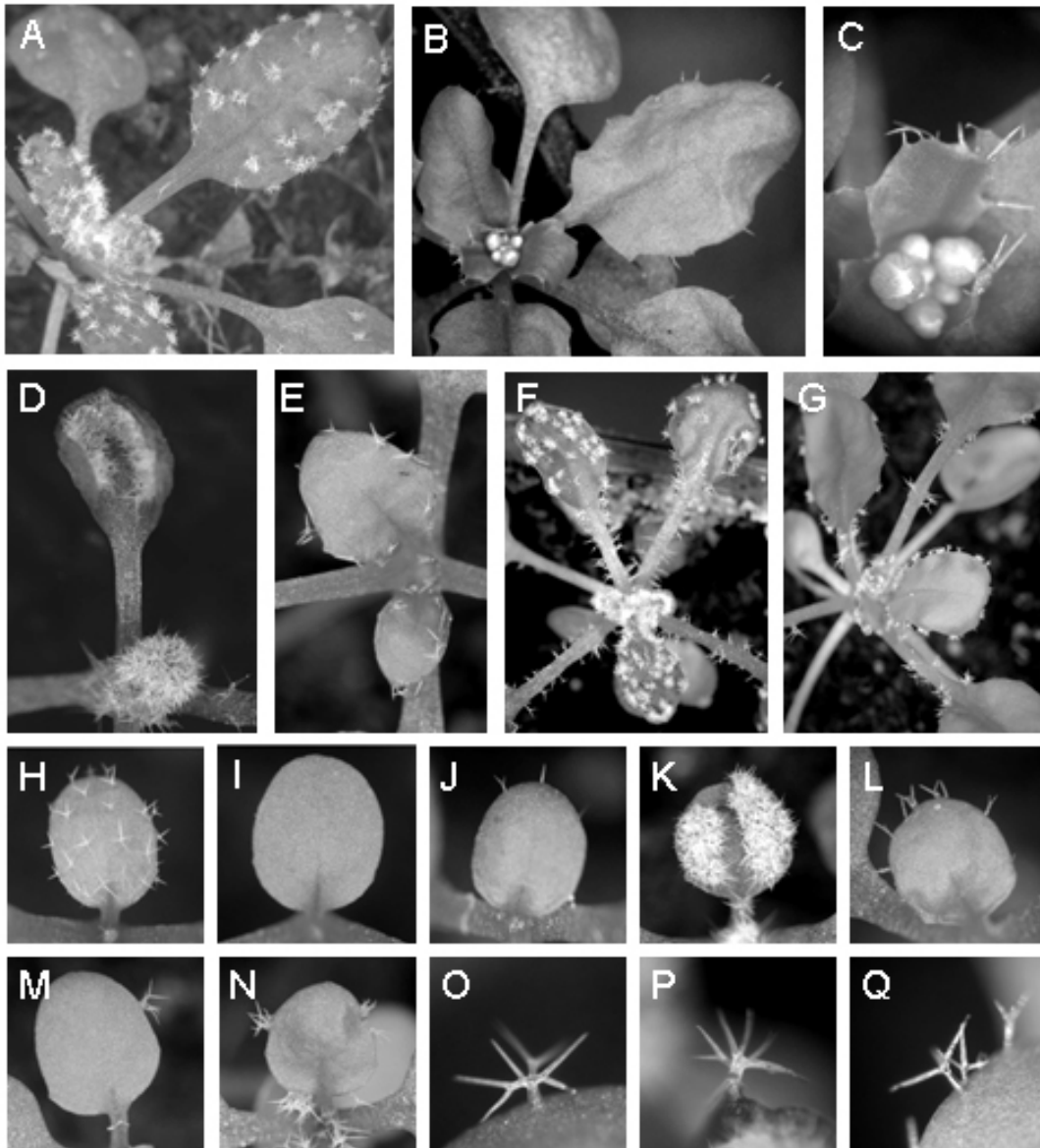


**Figure 13: Mutant analysis of negative regulators in combination with *ttg1* and *gl1*.**

(A) *try cpc* double mutant showing formation of large trichome clusters; (B) the *try cpc ttg1-13* triple mutant is able to promote trichome formation at the leaf edges; (C) detail of the *try cpc ttg1-13* triple mutant showing unbranched trichomes; (D) *try cpc etc1* triple mutant showing dramatic trichome clustering; (E) the *try cpc etc1 ttg1-13* quadruple mutant shows enhanced trichome formation compared with the *try cpc ttg1-13* triple mutant (B). (F) The *try cpc etc2* mutant leads to trichome formation at the stalks of the leaves. (G) In the *try cpc etc2 gl1-1* quadruple mutant trichome cluster formation takes place at the leaf margin and stalk. (H) – (N) first leaf stage of (H) RLD WT, (I) *ttg1-13* mutant, (J) *try cpc etc2 ttg1-13* quadruple mutant showing trichome formation and a two-branched trichome, (K) *try cpc etc1* triple mutant, (L) *try cpc etc1 ttg1-13* quadruple mutant showing enhanced trichome formation compared with *try cpc etc2 ttg1-13*, (M) *try cpc gl1-1* triple mutant showing a single trichome cluster, (N) *try cpc etc2 gl1-1* quadruple mutant showing several trichome clusters at the leaf edge, (O) single overbranched trichome of a *try cpc etc2 gl1-1* quadruple mutant, which looks similar to (P) *try cpc etc2* single overbranched trichome. In contrast, (Q) *try cpc etc1 ttg1-13* quadruple mutant trichomes shows only up to three branches and appear glassy.

On the other hand the *ttg1* dependent phenotypes suggest that *TTG1* and the negative regulators act at the same level. In contrast to *GLI*, trichome development on hypocotyls and cotyledons is dependent on *TTG1*.

### B 2.2. Expression analysis of *TTG1*

RT-PCR analysis has shown that the *TTG1*-gene is expressed in all tissues of the plant (Walker *et al.* 1999). However to analyse the role of *TTG1* in patterning it is important to obtain a cellular and temporal resolution of the *TTG1* expression. Therefore a 2,2 kb fragment 5' of the open reading frame (ORF) –start, including the 5' UTR of *TTG1*, was fused in front of the  $\beta$ -*Glucuronidase* (*GUS*) gene. This promoter fragment, thereafter termed pTTG1, can rescue trichome formation seed coat colouring phenotype of the *ttg1-13* null allele completely when fused to the *TTG1*-coding sequence (CDS) (see table 2), whereas a Cauliflower Mosaic virus 35S-promoter (35S)-driven *TTG1* construct did not result in complete rescue of the *ttg1-13* phenotype, which suggests that the used *TTG1* promoter fragment reflects the expression in the WT-situation (see table 2). *In situ* hybridisation of *TTG1*-mRNA has been performed previously and did not reveal any detectable signal (data not shown).

*Ler* plants carrying the reporter construct were assayed for GUS-activity. GUS staining could be detected in leaf primordia and young leaves (Fig. 14A & B). Developing trichomes showed also GUS-staining (Fig. 14B & D). During maturation/proliferation of the leaf the expression starts to cease at the tip and progresses during further development to the base (Fig. 14A). Trichomes keep higher GUS-activity for a short time while neighbouring tissues show only weak staining. This staining ceases before trichomes are fully mature (Fig. 14A, B). This expression pattern reflects the role of *TTG1* in trichome-initiation and -pattern formation. But the expression of *TTG1* is less trichome-specific than the expression of all other trichome patterning genes analysed so far.

Roots showed GUS activity only in the differentiation zone of the root tip in primary roots (Fig. 14F) and in newly initiated lateral roots (Fig. 14G). In contrast to other root-patterning genes like *WER*, *CPC* and *GL2*, *TTG1* is not exclusively expressed in files of atrichoblast-precursor cells (Fig. 14F).

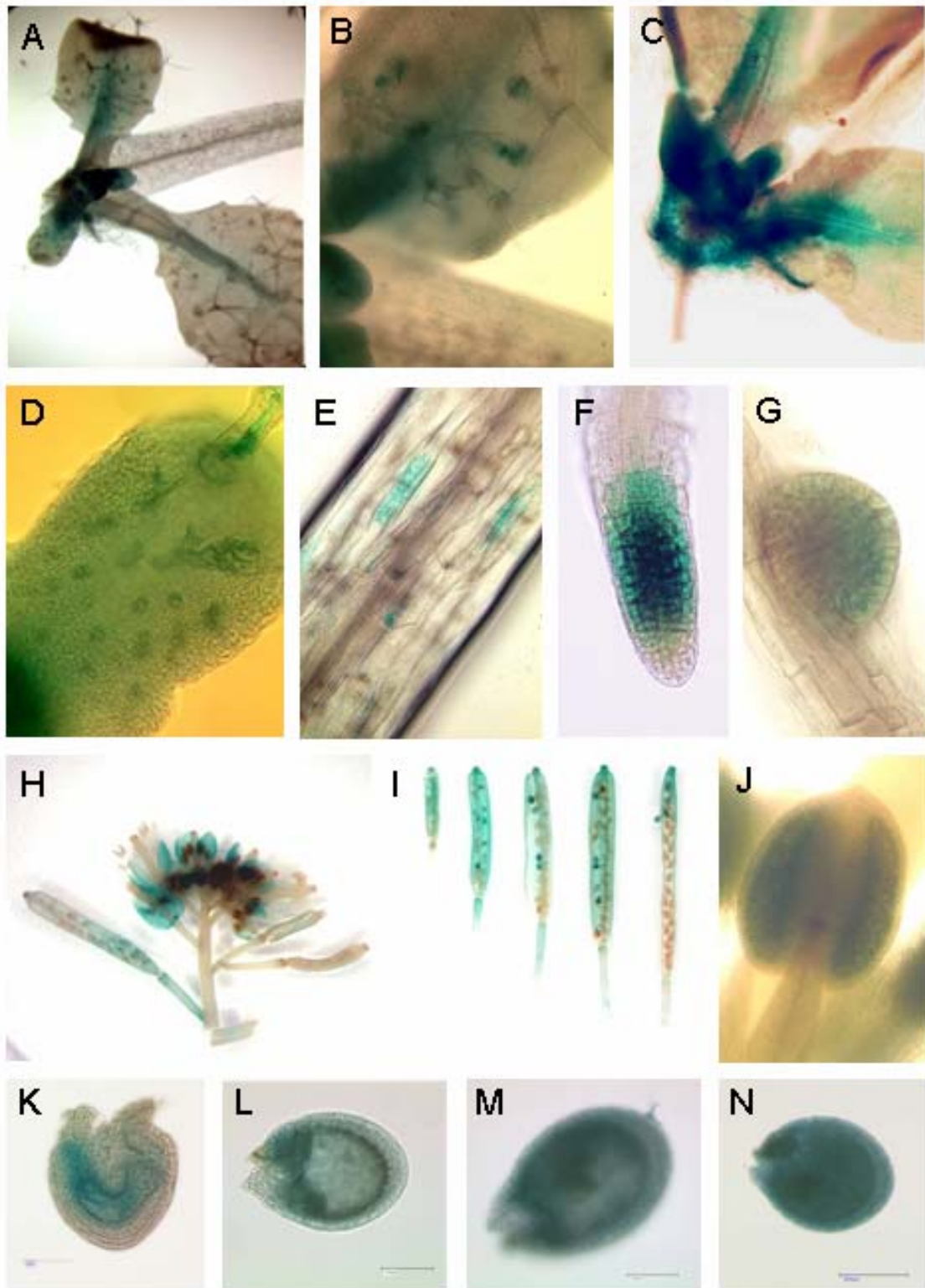


**Figure 14: Expression analysis of *TTG1*.** A description is given on the next page.

Staining of the hypocotyl resulted in a rather patchy pattern. These stained cells always appeared to be neighbouring stomata guard cells. Those cells were always much smaller and looked like newly divided compared to the other epidermal hypocotyl-cells, judged by the arrangement of the cell walls (Fig. 14E). Cotyledons also showed weak GUS staining that ceases at the time point when the first true leaves grow out (data not shown).

*pTTG1::GUS* expression was also detected in flowers (Fig. 14H). Weak staining was found in anthers although no corresponding mutant phenotype has been observed for *ttg1* (Fig. 14J). Quite strong staining could be observed in siliques, especially in the developing seeds (Fig. 14I). GUS expression resulted in a rather irregular staining of the siliques with randomly distributed blue-stained seeds (Fig. 14I). During seed maturation expression disappears (Fig. 14I). Throughout early ovule development GUS activity is detected in tissues that correspond to the female gametophyte (Fig. 14K), where the two integuments will form the future seed coat, a tissue that is affected in seed coat anthocyanin/thannin- and mucilage production in *ttg1* mutants (Koorneef 1981). *pTTG1::GUS* expression domain spreads throughout seed development and is later distributed over the whole seed coat (Fig. 14L – M). Fig. 14L & M show GUS-staining of seeds that correspond to the embryonic globular and early heart stage, respectively.

*pTTG1::GUS* expression does not depend on *TTG1* activity, because *ttg1*-mutants showed the same GUS-staining pattern as WT-plants (Fig 14C). Proper GUS staining of *pTTG1::GUS* takes about 24h, whereas a 35S::GUS construct showed saturated colouring after approximately 12h (Fig. 17G), suggesting that *TTG1* is expressed at a relatively low level.

---

← **Figure 14 Expression analyses of *pTTG1::GUS*.**

**(A):** Rosette showing leaves of different stages with stronger staining in young leaves and at the base of older leaves.

**(B)** detail of (A) showing the base of a young leaf with adult trichomes showing GUS-staining.

**(C)** Rosette of a *ttg1-13* mutant showing similar expression pattern as WT (A).

**(D)** Very young leaf with different stages of trichome development, *pTTG1::GUS* is ubiquitously expressed at this early stage.

**(E)** Upper part of a hypocotyl showing GUS staining around stomata.

**(F)** Root tip with strong staining at the differentiation zone and

**(G)** staining of newly initiated side root.

**(H)** Flower showing staining of sepals and siliques.

**(I)** Siliques shown at advancing stages from left to right, bearing stained and unstained seeds.

**(J)** Anther showing weak signal.

**(K) – (N)** seed at different developmental stages, (K) before visible embryogenesis and stained gametophyte, scale bar = 50µm, (L) seed at the globular embryo stage, scale bar = 100µm. (M) Seed at heart-shaped embryo stage, scale bar = 100µm. (N) fully developed seed before dissication with strong staining, scale bar = 200µm.

### B 2.3. TTG1-YFP localises to the nucleus

*GL1*, *GL3*, *TRY* and *CPC* encode for transcription-factor-like genes and have been shown to interact with each other in yeast two-hybrid analyses and to localise to the nucleus *in planta* (Katja Wester, unpublished and Szymanski *et al.* 1998a, Payne *et al.* 2000, Esch *et al.* 2003).

*TTG1* does not encode for a transcription-factor and shows no clear nuclear localisation signal (NLS) but also interacts with other trichome-patterning genes in yeast two-hybrid analyses (Walker *et al.* 1999, Payne *et al.* 2000). In order to test the cellular localisation of TTG1 I made a C-terminal translational fusion of TTG1 with the yellow fluorescent protein (YFP) under the control of the *TTG1* promoter. This construct is able to produce the number of trichomes comparable with the corresponding WT when transformed into the *ttg1-13* mutant (see table 2).

Analyses of these plants using an epifluorescence microscope revealed a weak fluorescence in nuclei of outgrown trichomes (Fig. 15A & 15C). Because of autofluorescence of the leaf chlorophyll, localisation at the base of young leaves or of pavement cells could not be visualised with the epifluorescence microscope (Fig. 15C).

For a better visualisation a confocal laser scanning microscopy (CLSM) was used. YFP-specific signal could be detected in the nucleus of all epidermal cells of young leaves and leaf primordia (Fig. 15D & E). A weak fluorescence was also detected in the cytoplasm (for detail see Fig. 16E). Developing trichomes showed slightly stronger fluorescence in comparison to pavement cells, similar to the GUS-expression pattern (Fig. 15D – F).

---

#### Figure 15: Localisation of TTG1-YFP. →

- (A): Epifluorescence micrograph of a rosette showing YFP signal in the trichome nuclei.
- (B): Nomarsky optical view of a young leaf showing different stages of trichome development.
- (C): Same leaf as in (B) showing YFP-fluorescence in the nuclei of developing trichomes.
- (D): CLSM with overlapping red (Chlorophyll) and green (YFP-emission signal); the YFP signal is strong in leaf primordia and young leaves and shows a nuclear and cytoplasmic fluorescence.
- (E): YFP-signal of a very young leaf with initial stages of trichome development at the leaf tip, trichomes show slight increase in fluorescence, but the signal is detectable in all cells.
- (F): YFP-signal of a leaf with differentiated trichomes that show enhanced nuclear fluorescence, inlay shows the same leaf as surface structure micrograph. (G) – (I) Transverse section through the leaf blade including trichomes.
- (G): YFP-specific signal showing fluorescence in epidermal and subepidermal tissue.
- (H): Fluorescence from chlorophyll in the subepidermis.
- (I): Overlay of (G) and (H)
- (J): YFP-signal in the root
- (K): YFP-signal of a silique bearing a developing seed with enhanced fluorescence
- (L): YFP-signal of the seed coat
- (M): Untransformed seed with the same settings as in (L)

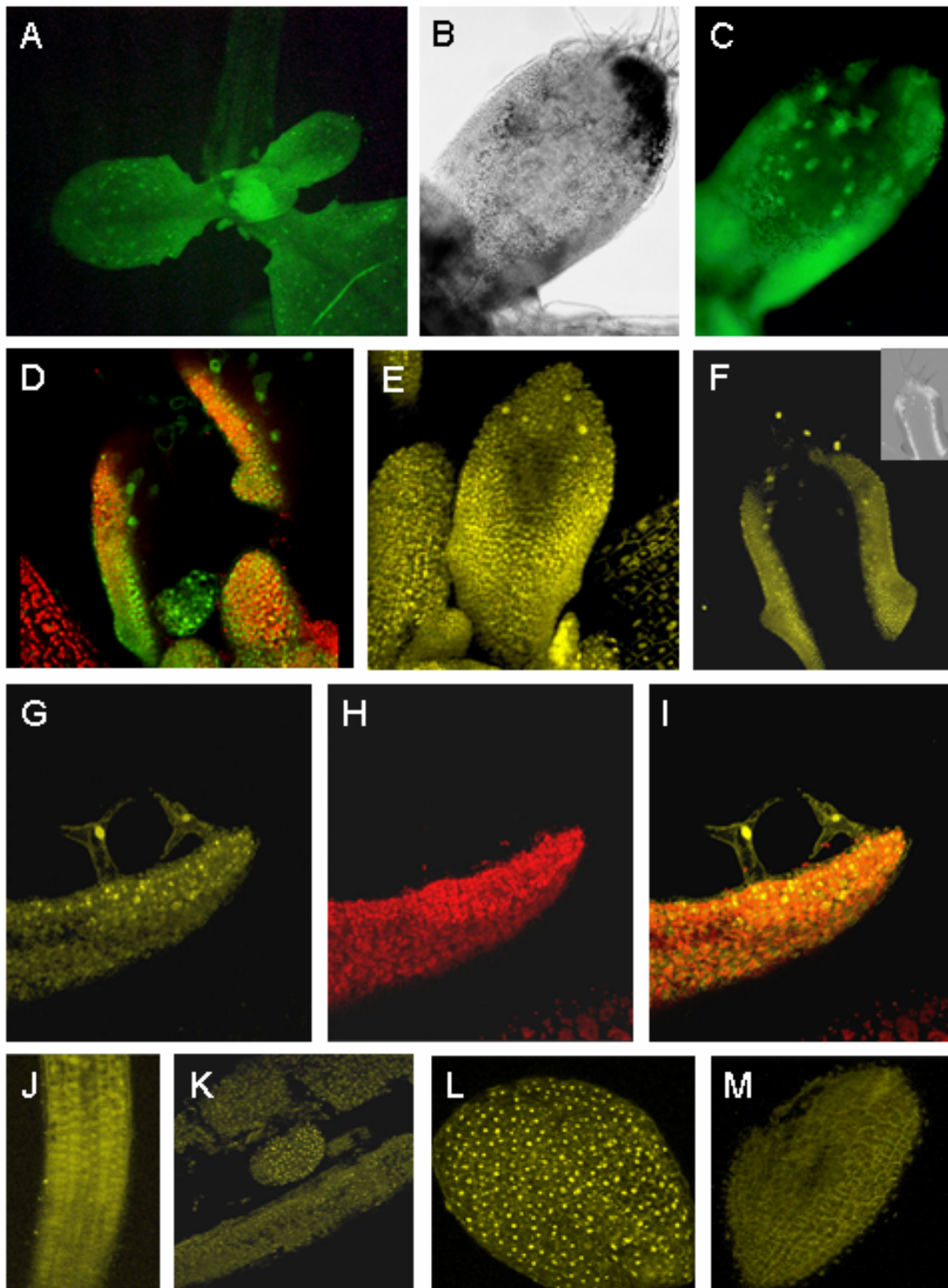


**Figure 15: Analysis of TTG1-YFP localisation.** description is given on the previous page.

In cross sections of leaves the YFP signal was also detected in the nuclei of subepidermal cells (Fig. 15 G – H).

Fluorescence that corresponds with the histochemical analysis of *pTTG1::GUS* was also observed in root tip cells and cells of the seed coat (Fig. 15 J, K & L). However the fluorescence in the root was at detection limits, which is in contrast to the strong GUS-expression in this tissue (Fig. 15 J, compare with Fig. 14 E).

An additionally used 35S::GFP-TTG1-fusion that also leads to trichome-formation in the *ttg1-13* mutant showed the same localisation as the TTG1-YFP-fusion, confirming the results obtained with the C-terminal fusion (Fig. 16 R).

#### **B 2.4. TTG1 localisation depends on differentiation status**

Analysis of the cellular localisation of the *TTG1* ortholog AN11 from petunia revealed a cytoplasmic targeting of the protein in cell fractionation experiments (de Vetten *et al.* 1997). This is in contrast to my results that suggest that TTG1 is mainly nuclear localised. Therefore I asked whether TTG1-YFP is restricted predominantly to the nucleus or if the intracellular localisation changes during development. Therefore the localisation of a 35S-driven TTG1-YFP was compared with a 35S::NLS-TTG1-YFP fusion. A GFP-GUS fused to the NLS has previously been shown to result in exclusively nuclear targeting of the fusion protein (Chytilova *et al.* 1999). To retain possible post-transcriptional regulation beside localisation I used the TTG1 protein instead of an “unrelated” NLS-marker. Moreover I wanted to test the functionality of the nuclear localisation of TTG1 by localising it exclusively to the nucleus.

While the 35S::TTG1-YFP is quite similar to 35S::NLS-TTG1-YFP in young epidermal tissue and throughout the development of the trichome, fluorescence in the cells of older tissue appeared quite different between both fusion proteins (compare Fig. 16D – F with 16G – I and 16J – L with 16M – O). Whereas the NLS-TTG1-YFP fusion still shows strong nuclear fluorescence, TTG1-YFP was hardly detectable in the nuclei of the pavement cells and appeared to be rather cytoplasmic (Fig. 16 J - L). An untransformed leaf of the same stage with the same CLSM settings did not show YFP-specific fluorescence (data not shown).

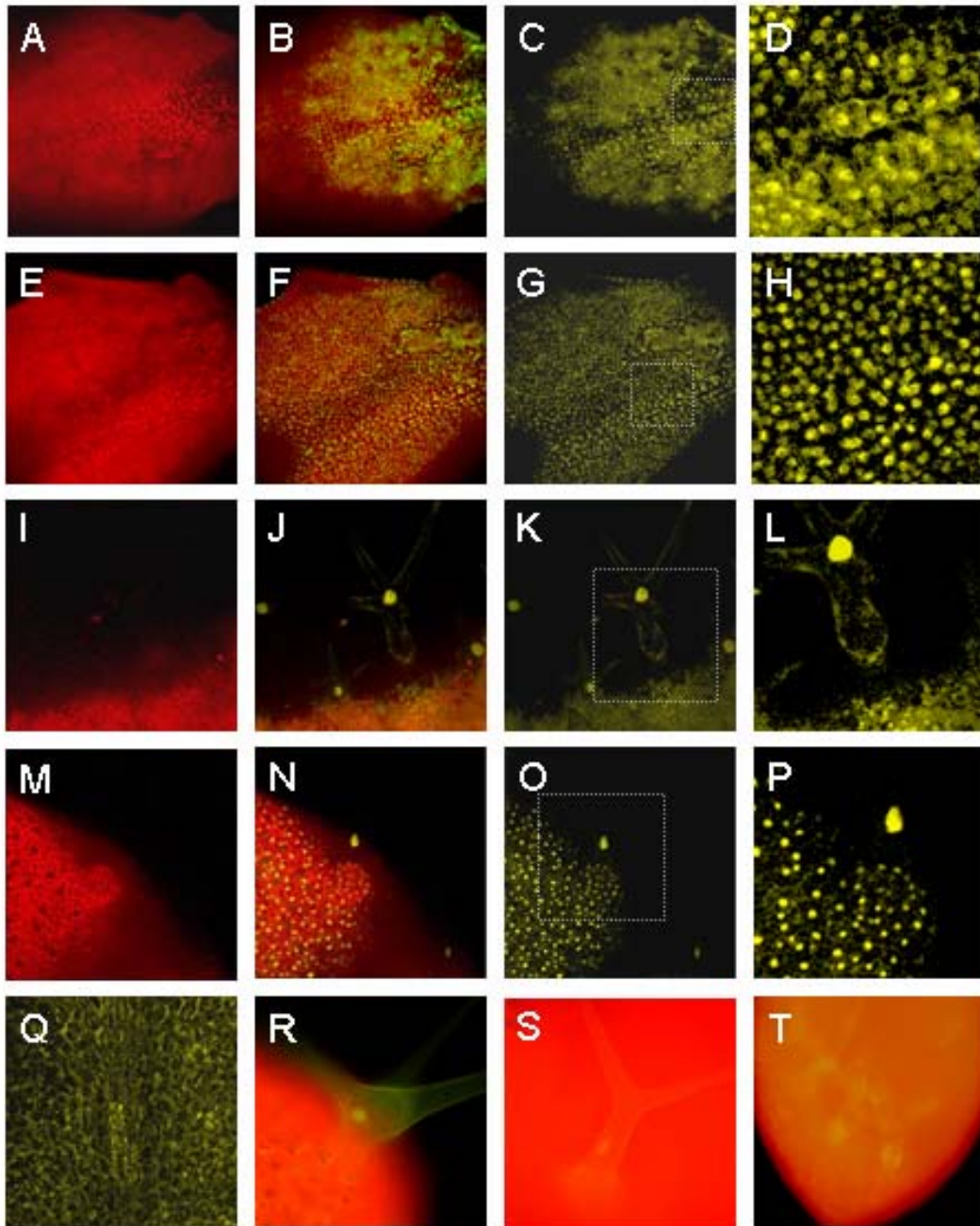


**Figure 16: TTG1-YFP localisation is dynamic.** description is given on the next page.

The NLS-TTG1-YFP fusion leads to trichome development in the *ttg1-13* mutant background; however in contrast to 35S::TTG1-YFP the rescue was not as efficient (data not shown). However the fusion of *TTG1* to the *NLS* without the addition of YFP leads to a reasonable good complementation of *ttg1-13* (see table 2).

A recent publication has implicated that the nuclear localisation of *PFWD*, a *TTG1*-homologue from *Perilla frutescens*, is enhanced if *MYC-RP*, a bHLH gene similar to *GL3*, is transiently co-expressed in onion epidermal cells, using particle gun experiments (Sompornpailin *et al.* 2002). Therefore I tested if a reduction of *GL3* activity would lead to an impaired nuclear localisation of *TTG1-YFP*. In fact *gl3* mutants transformed with 35S::*TTG1-YFP* did not show a clear nuclear YFP-specific fluorescence in trichome-cells compared with *Ler* plants transformed with the same construct using an epifluorescence microscope (Fig. 16S). The fluorescence seemed to be rather uniformly distributed between nucleus and cytoplasm in the *gl3* mutant background (Fig. 16S & T). In addition the presence of the *EGL3* gene may still lead to some nuclear localisation of TTG1-YFP.

---

← **Figure 16 Comparison between 35S::TTG1-YFP and 35S::NLS-TTG1-YFP.**

**(A) – (D):** TTG1-YFP in a young leaf, (A) chlorophyll-specific fluorescence, (B) chlorophyll- and YFP-specific fluorescence, (C) YFP-specific fluorescence, (D) Magnification of (C) showing nuclear and cytoplasmic signal.

**(E) – (H):** NLS-TTG1-YFP in a young leaf, (E) chlorophyll-specific fluorescence, (F) merge of chlorophyll and YFP-channel, (G) YFP-specific fluorescence, (H) Magnification of (G) showing exclusively nuclear signal.

**(I) – (L):** TTG1-YFP in older leaf segment with a single trichome, (I) chlorophyll specific fluorescence, (J) merge of chlorophyll and YFP-signal, (K) YFP-specific signal, (L) Magnification of (K) showing nuclear and cytoplasmic localisation in trichome and cytoplasmic localisation in pavement cells.

**(M) – (P):** NLS-TTG-YFP in older leaf with single trichome, (M) chlorophyll-specific fluorescence, (N) merge of chlorophyll and YFP signal, (O) YFP-specific signal, (P) magnification of (P) showing exclusively nuclear signal.

**(Q):** TTG1-YFP in the centre of an older leaf, the fluorescence is only particular and weak in the nucleus.

**(R):** GFP-TTG1 epifluorescence microscopy of a single trichome with nuclear GFP-fluorescence.

**(S):** TTG1-YFP epifluorescence microscopy of a single trichome in a *gl3* mutant background, with only weak nuclear localisation.

**(T):** TTG-YFP in young *gl3* mutant leaf showing several trichomes with impaired nuclear localisation of the YFP signal.

### B 2.5. Non-cell-autonomous action of *TTG1*

A model to explain two-dimensional pattern-formation is the activator-inhibitor-model applied for biological systems, by Meinhardt and Gierer (Meinhardt & Gierer 1974). According to this model the creation of a stable pattern needs two components, an activator that activates his own activity and an inhibitor that is activated by the activator, which itself is inhibited by the inhibitor, thereby building an interdependent feedback loop. Apart from the feedback loop of the two components the main criteria to establish a stable pattern is the different behaviour of the activator and the inhibitor according to their mobility. In the Meinhardt-model the activator acts in a more immobile manner whereas the inhibitor is mobile. Applied to the trichome-pattern this model predicts that an activator acts in a cell-autonomous manner and an inhibitor in a non-cell-autonomous way.

*TTG1* has a role in lateral inhibition and may therefore act in a non-cell-autonomous manner. To test the cell-autonomy of *TTG1* clonal analysis of *TTG1* was performed using the *Cre-LoxP* recombination system in a *ttg1-13* background. The *LoxP*-flanked cassette contains a *GUS*-reporter gene under the control of the CaMV 35S promoter and *35S::TTG* and results in complete *GUS* staining of the seedling (Fig. 17G) and rescue of the *ttg1-13* mutant (see table 1). The corresponding *Cre*-recombinase is under the control of a heat-shock inducible promoter (HS) that has previously shown to be functional in *Arabidopsis* (Sieburth *et al.* 1998). Those lines were crossed to *ttg1-13* mutants to obtain the *HS::CRE* plant in *ttg1* background. From both, *TTG-LOX* and *HS-CRE* lines, homozygous lines were crossed and their descendants used for heat-shock treatment.

First it was examined which stage of leaf development is sensitive to the loss of *TTG1*. Therefore a saturating heat treatment was given that lead to a complete excision of the *LoxP*-flanked cassette resulting in *GUS*-free plants (Fig. 17 A). Those plants were analysed for the presence of trichomes. The first two leaf-pairs still had some trichomes and only the following leaves were glabrous (Fig. 17B & C).

The existence of trichomes on the first two leaved indicates that *TTG1* is not needed later in trichome-development but rather at very early stages, which is in agreement with previous results that showed that trichome formation is restricted to the young parts of the leaf (Lloyd *et al.* 1994). Thus for the following analysis only leaves starting with number three were used.

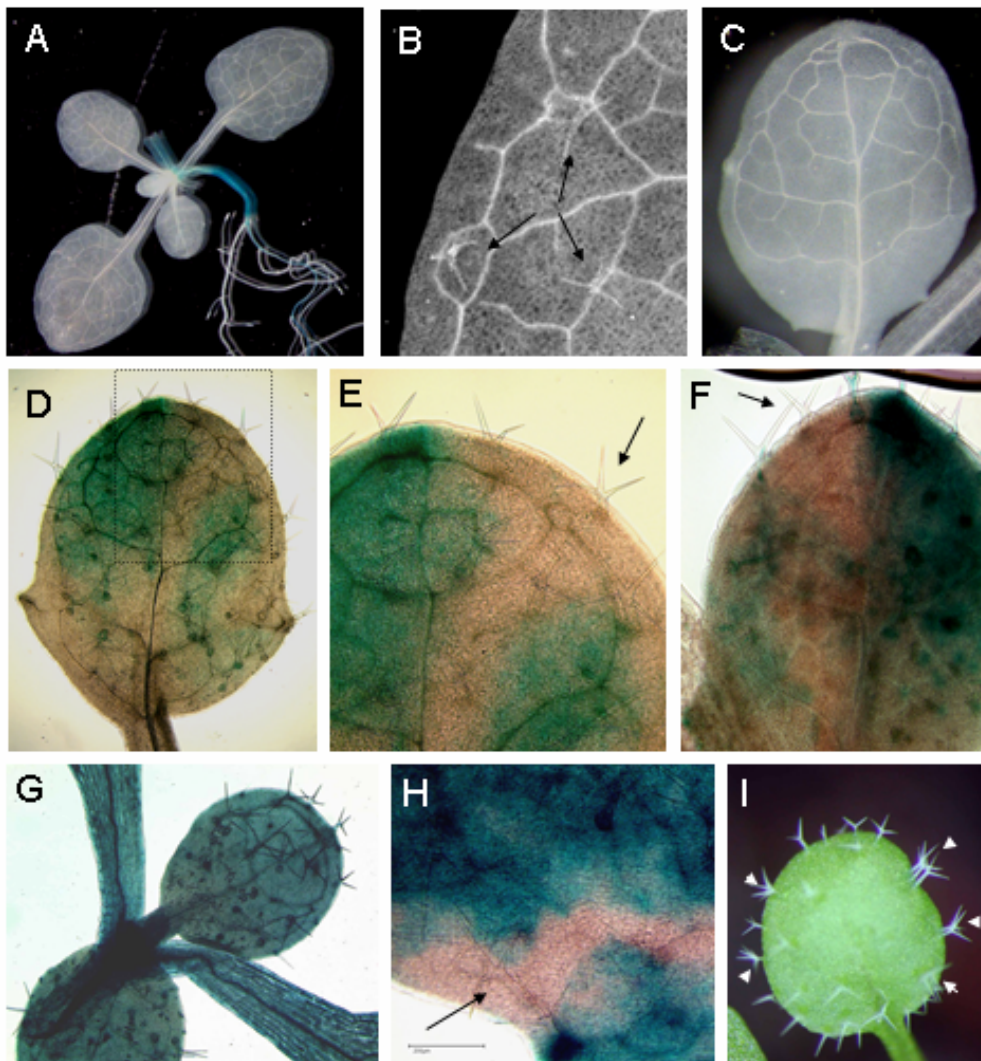


**Figure 17: Non-cell-autonomous action of *TTG1*.**

(A): GUS –staining of a rosette, which had been given a saturating heat shock treatment that was leading to the excision of the *LoxP*-flanked *TTG1*/*GUS* cassette on the entire leaves, staining is still visible at the hypocotyl, but is completely absent on the leaves. Cotyledons have been removed.

(B): Detail of leaf number one depicted from (A) showing three trichomes (arrows).

(C): Leaf number four, showing no trichomes.

(D): Leaf showing GUS-positive and –negative sectors after heat-shock treatment with trichomes on both, *TTG1*-positive (= blue) and *TTG1*-negative (= unstained) tissue.

(E): Margination of (D) showing a *ttg1* trichome several cells away from *TTG1*<sup>+</sup> trichomes.

(F): Further example of *ttg1* trichome (arrow)

(G): *TTG1-LOX* plant before heat shock treatment, which shows overall GUS-staining and trichome formation

(H): Further example of a *ttg1* trichome (arrow) surrounded by *TTG1*<sup>+</sup> sectors.

(I): First leaf of a *35S::GFPTTG1* transgenic plant showing strong trichome clustering (white arrows).

Because trichome-initiation and pattern-formation take place at very early stages during leaf-development it is important to obtain early recombination events (Hülkamp *et al.* 1994, Lloyd *et al.* 1994, Larkin *et al.* 1996). The time point of such a recombination is monitored by the size of the GUS-negative sector. The earlier the recombination event took place, the larger will be the resulting sector. All heat-shock treatments were performed with seedlings where the first two leaves were barely visible and approximately 1 mm in size.

Fig. 17D – E and H show some of the *GUS*-negative sectors, where *TTG1* is absent, having trichomes. However the *GUS*-positive sectors, containing *TTG1*, are several cells away (Fig. 17D – E & H). This means that *TTG1* is able to act non-cell-autonomous.

### **B 2.6. TTG1-YFP-fusion is able to move**

To analyse if the *TTG1* protein can move I expressed *TTG1*-YFP under the control of the phosphoenol-pyruvat-carboxylase promoter (*pPCAL*) from *Flaveria trinerva*. This promoter is active in a mesophyll-specific manner in tobacco (Stockhaus *et al.* 1994). To test if the same is true for *Arabidopsis* mGFP5-ER (*GFP5*) was expressed under the control of *pPCAL*. *GFP5* localises to the endoplasmatic reticulum (ER) and is strictly cell-autonomous (Crawford & Zambryski 2000). CLSM-analysis of transverse sections of leaves of *pPCAL::GFP5* plants show that *GFP5*-fluorescence can be found only in subepidermal tissues whereas untransformed WT plants did not show ER-specific fluorescence (Fig. 18D – F & 18A-C). Thus, the expression pattern of *pPCAL* resembles what was described for tobacco (Stockhaus *et al.* 1994).

Sections of Col plants expressing *TTG1-YFP* under the *PCAL* promoter showed nuclear fluorescence in subepidermal tissue and quite intensive also in trichomes (Fig 18G - I). To further investigate this, *pPCAL::TTG1-YFP* and *pPCAL::GFP5* plants were studied for epidermal fluorescence. The *pPCAL::GFP5* lines did not show any ER-specific fluorescence of pavement cells or trichomes (data not shown). However *pPCAL::TTG1-YFP* resulted in a clear nuclear fluorescence in trichomes, but no YFP-specific fluorescence could be detected in ordinary pavement cells in all stages during leaf development (Fig. 18J - L). It cannot be distinguished from these experiments if *TTG1*-YFP is selectively transported into trichomes, stabilised there or if the concentration of *TTG1*-YFP in pavement cells is below the detection level.

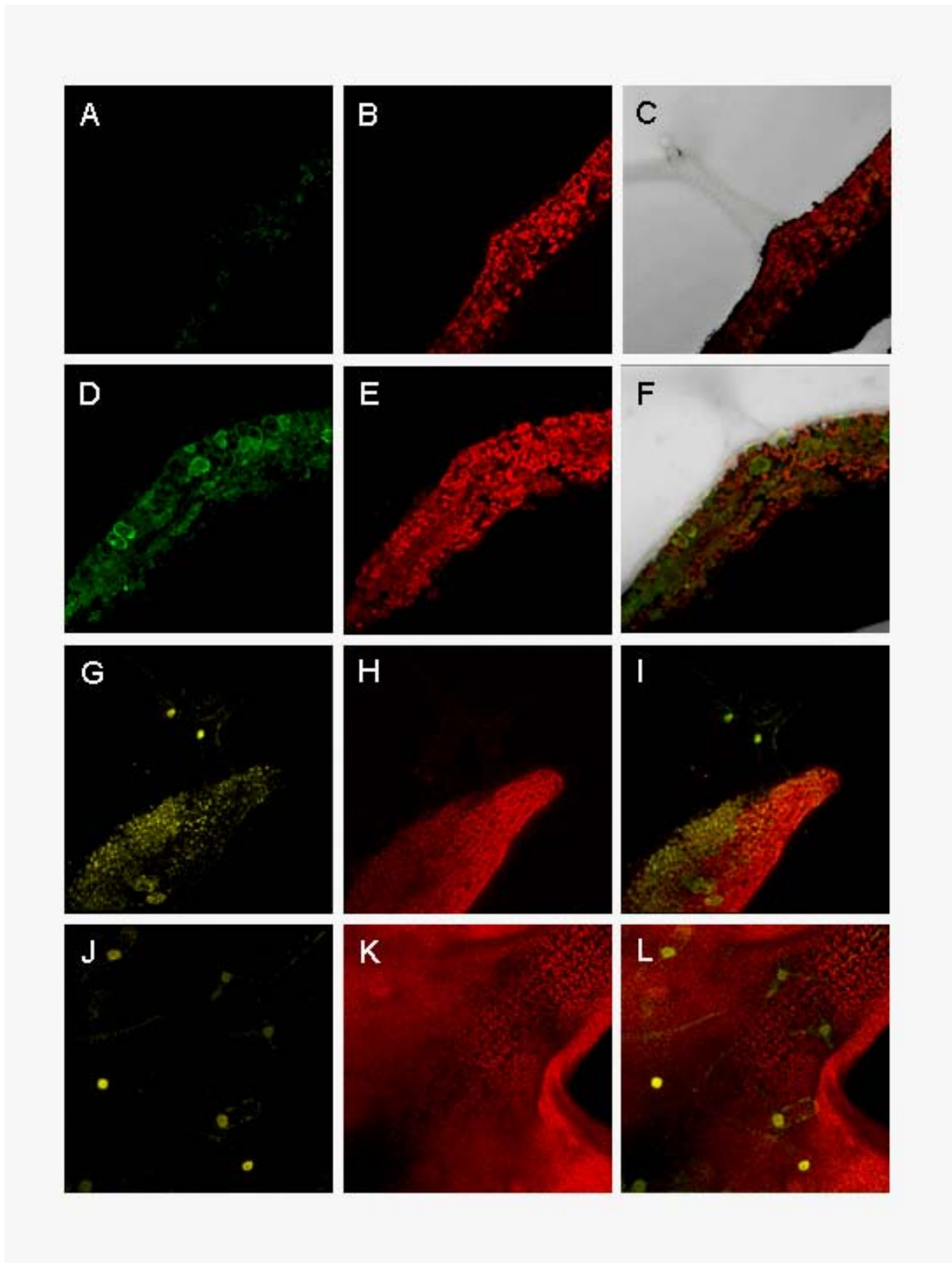


Figure 18: TTG1-YFP fusion moves between cells. description is given on the next page.

To further corroborate the specificity of *pPCAL*, the *GL3*-CDS was expressed under its control. *GL3* encodes for a 70.9 kD protein and is normally expressed at low levels in the trichome-initiation-zone of young leaves (Zhang *et al.* 03). *pPCAL::GL3* was not able to rescue the *gl3* mutant in 21 independent transgenic lines, whereas the ubiquitous expression with *35S::GL3* resulted in complementation of *gl3* or even excess trichome formation, suggesting that the *PCAL* promoter is not active in the epidermis (data not shown).

Comparison of *ttg1-13* plants expressing either *pPCAL::TTG1* or *pPCAL::TTG1-YFP*, showed that the latter could not rescue the *ttg1-13* mutation as effectively as the unfused version (84.8 % versus 36.3% of WT TIS, respectively, see table 2). Because *pTTG1::TTG1-YFP* is able to give rise to a normal number of trichomes in the same background (table 2) it is unlikely that the fusion is less active than *TTG1* itself but rather is less mobile compared to *TTG1*. This also suggests that the non-cell-autonomy is a result of the mobility of the *TTG1* protein and/or its mRNA and not an indirect *TTG1*-dependent effect.

---

← **Figure 18: TTG1-YFP fusion moves between cells.**

CLSM micrographs of WT and *pPCAL::GFP5* and *pPCAL::TTG1-YFP* plants

**(A) – (I):** Transversal section through the leaf blade.

**(A) – (C):** Untransformed WT plant. (A) GFP-specific signal. (B) Chlorophyll specific signal. (C) Merge of GFP, chlorophyll and throughlight.

**(D) – (F):** *pPCAL::GFP5* in WT. (D) GFP-signal showing ER-specific fluorescence. (E): chlorophyll specific fluorescence. (G): merge of GFP, chlorophyll and throughlight. Please note that the trichome and epidermis does not show any GFP-signal.

**(G) – (I):** *pPCAL::TTG1-YFP* in WT. (G) YFP signal is detected in subepidermal tissue and in trichomes. (H) chlorophyll specific signal. (I) merge of YFP and chlorophyll fluorescence.

**(J) – (K):** View from above on a *pPCAL::TTG1-YFP* plant. (G) YFP specific signal, please note that the fluorescence is strong in trichome nuclei but not detectable in other epidermal cells. (H) Chlorophyll specific signal. (I) merge of (G) and (H).

### B 2.7. TTG1-YFP constructs show pattern defects

The *TTG1YFP*-fusion additionally showed patterning defects in transgenic plants under the control of pPCAL or the endogenous promoter in both, *ttg1* mutant or WT background. This is monitored by the frequency of trichome clusters. *pTTG1::TTG1-YFP* in *ttg1-13* background resulted in 3.8% cluster frequency, whereas RLD WT or transgenic plants that contained the unfused *TTG1* under the control of the same promoter show no clusters at all (table 1). In the *Ler* background *pTTG1::TTG1* develop on average 7.8 TIS compared to 8 TIS in untransformed *Ler*. However *pTTG1::TTG1YFP* produced 13.4 TIS, which is an increase of about 67%, and 7.6% of these appeared in clusters in contrast to a cluster frequency of 0.3% in *Ler* (table 2). An increase in cluster frequency was also observed in plants carrying *35S::TTG1-YFP* or *35S::GFP-TTG1*, but not in plants with only *35S::TTG1* (Figure 17I and data not shown). Even though I cannot generally exclude that the fusion to YFP alters TTG1 activity, this suggests that the mobility of TTG1 is important for proper pattern formation and interference with the mobility leads to defects during this process.

Construct	Background	TIS	SD <sub>TIS</sub>	Trichome cluster	n
-	RLD	29.5	±3.8	0	561
<i>pTTG1::TTG1</i>	<i>ttg1-13</i>	27.2	±2.4	0	542
<i>pTTG1::TTG1-YFP</i>	<i>ttg1-13</i>	33.5	±3.7	3.8 %	805
<i>pPCAL::TTG1</i>	<i>ttg1-13</i>	25.0	±2.6	2.1 %	579
<i>pPCAL::TTG1-YFP</i>	<i>ttg1-13</i>	10.7	±3.6	4.5 %	320
<i>pTTG1::TTG1<sup>im</sup></i>	<i>ttg1-13</i>	58.5	±11,1	15.1%	1236
<i>pTTG1::NLS-TTG1</i>	<i>ttg1-13</i>	31.7	±3.2	4.1%	865
<i>35S::TTG1(LoxP)</i>	<i>ttg1-13</i>	20.5	±1.8	0	452
<i>pGL2::TTG1-YFP</i>	<i>ttg1-13</i>	28.3	±3.5	2.8%	680
-	<i>Ler</i>	8.0	±2.0	0.3%	321
<i>pTTG1::TTG1</i>	<i>Ler</i>	7.8	±1.4	0	187
<i>pTTG1::TTG1-YFP</i>	<i>Ler</i>	13.4	±1.4	7.6%	322
<i>pGL2::NLS-TTG1</i>	<i>Ler</i>	10.3	±1.6	0	206

**Table 2: Quantification of trichome initiation sites and nest-frequency in transgenic lines.**

Trichomes on the first two leaves of at least ten 10 day old plants grown at the same place at the same time were counted. TIS = trichome initiation site per leaf, a TIS may contain more than one trichome, SD<sub>TIS</sub> = standard deviation for TIS, n = number of TIS counted.

## B 2.8. Blocking TTG1 mobility leads to strong pattern defects

### B 2.8.1. Exchanging endogenous TTG1 with an immobile TTG1

The observation that *TTG1-YFP* fusions showed patterning defects that are absent when doing the same experiments with the unfused *TTG1-CDS* gave a first hint that the mobility of TTG1 is important for proper trichome pattern formation. Therefore I tried to block TTG1 movement by fusing it C-terminally to a GFP-GUS fusion. However in more than 50 lines I could not observe any rescue of the *ttg1* mutant phenotype (data not shown). Moreover in those lines the GUS-signal was barely detected in the nucleus of plants carrying a 35S::*TTG1-GFP-GUS* construct (data not shown). Therefore I added an N-terminal nuclear localisation signal (NLS) (see above, Chytilova *et al.* 1999). The *NLS-TTG1* fusion (without *GFP-GUS*) leads to the formation of trichomes when expressed in the *ttg1-13* background (31.7 TIS compared with 29.5 TIS in RLD WT), indicating that the NLS-sequence does not impair the activity of TTG1 (see table 2).

The block of TTG1 mobility is monitored by incapability to rescue the *ttg1-13* mutant when the *NLS-TTG1-GFP-GUS* construct is expressed under the control of *pPCAL*. In 12 independent transgenic lines I could not find a single trichome on the first four leaves (data not shown).

The *NLS-TTG1-GFP-GUS* (*TTG1<sup>im</sup>*) fusion was next expressed under control of the endogenous TTG1 promoter in *ttg1-13* mutant plants, thereby allowing the transcriptional regulation of *TTG1*. The just emerging first leaves in 16 of 40 independent lines showed extremely dense trichome-formation, especially at the edges (Fig. 19A). During expansion of the leaf blade the trichome density decreases (Fig. 19 B, C shows a weaker phenotype). Besides strong patterning defect, the trichomes exhibited a very strongly distorted and blown-up phenotype, resembling the phenotype of plants overexpressing *GL3* cDNA in *ttg1-1* background and the phenotype of the recently identified *gl3-sst* allele (Fig. 19D – F and Zhang *et al.* 03, Esch *et al.* 03). Agar-imprints of the adaxial leaf surface showed that there is an excess trichome-initiation because of local outgrowth of cells, resembling young trichomes that are never seen in fully developed leaves of WT- or *ttg1-13* plants (Fig. 19D & E and data not shown). It turned out that the number of these trichome initiation sites (TIS) on the first two leaves is around twice as high as the number of trichomes of WT plants of the same age (table 1). In addition the frequency of clusters is about 15 % (RLD-

WT: 0%) and those quite often contain more than just two trichome cells (Fig. 7D & 7E and table 2).

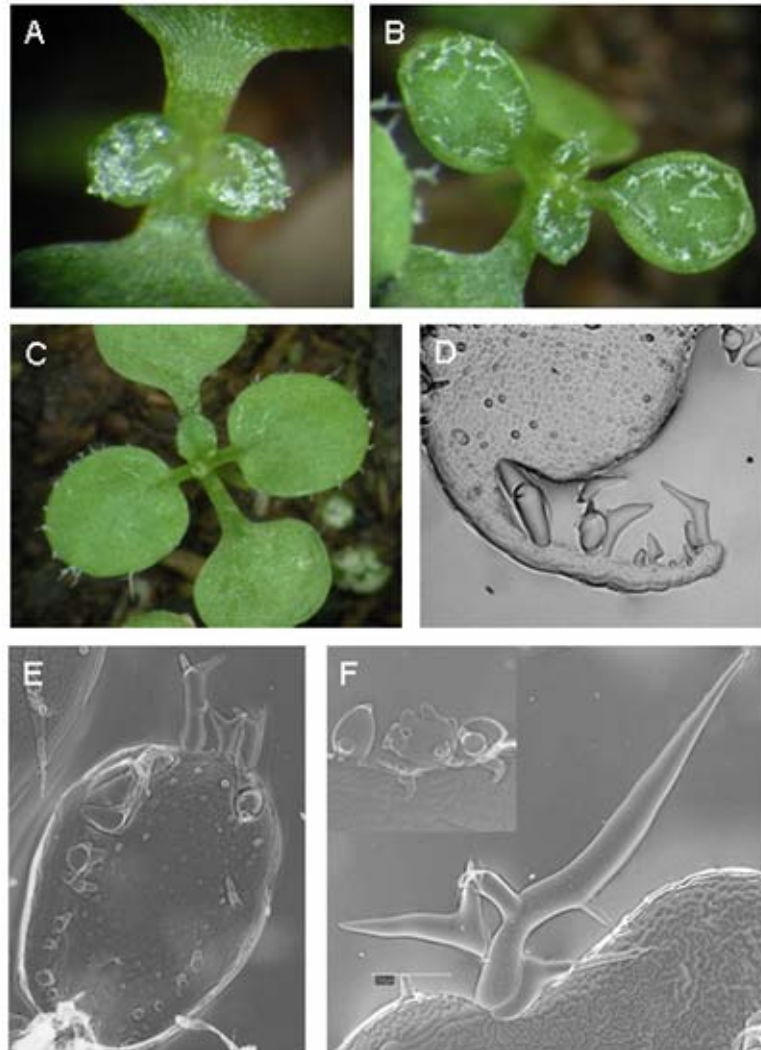


**Figure 19: Trichome phenotype of immobilised TTG1 (TTG1<sup>im</sup>).**

(A) – (F): Phenotypic analysis of *pTTG1::TTG1<sup>im</sup>* in the *ttg1-13* mutant background.

(A): Young seedling with the first two just outgrowing leaves showing very dense trichome formation.

(B): Young seedling where the first two leaves have grown out. Trichome density decreases.

(C): Weaker phenotype

(D) – (F): Trichome morphology. (D): Trichomes show both, patterning and morphogenesis defects.

Cluster formation and trichomes with bloated phenotype and initiated trichome cells that do not grow out of the leaf surface. (E): Young leaf showing several bloated trichomes at the margin and many initiated trichomes in the centre. (F): Trichomes with both bloated stalk and many blunted branches (above) or with a spine-like appearance and aberrant branching.

13 independent transgenic *Ler* plants with  $pTTG1::TTG1^{im}$  had either no phenotype, or showed a more negative effect on trichome development, resulting in reduced trichome number and branching (data not shown).

### B 2.8.2. Dependency of $TTG^{im}$ -phenotype on endogenous $TTG1$ function

Because it is not clear if the distorted trichome phenotype seen in the *ttg1-13* plants expressing  $TTG1^{im}$  is due to an incomplete rescue or evokes a “new” phenotype, those lines were crossed with different *ttg1* alleles and with RLD-WT plants to see if the trichomes of the descendants resemble more WT phenotype, or if the distortion is a dominant phenotype of the fusion protein.

In fact there was an allelic series where the degree of the distortion corresponds to the strength of the *ttg1* mutant allele. *ttg1-1*, a strong allele, showed a still strong distortion; in *ttg1-10*, a weak allele, only some distorted trichomes appeared and in another weak allele, *ttg1-9*, I could not find any distortions (compare Fig. 19A with Fig. 20A - C).

The number of outgrowing trichomes was also dependent on the activity of endogenous  $TTG1$ . Whereas in the *ttg1-13* background this number was quite low, it increased with the activity of the remaining  $TTG1$  allele in the different mutant backgrounds, with still few in *ttg1-1* and increasingly in *ttg1-9* and *ttg1-10* (Fig. 20A - C). In addition, the weak *ttg1-10* mutant was directly transformed with  $pTTG::TTG1^{im}$ . Some lines showed the strong distortion phenotype that was also observed in *ttg1-13* background, with the difference that an excess of trichomes grew out of the leaf surface (Fig. 20D). This indicates that the distortion of trichomes is not due to a weak rescue but represents a new phenotype.

The most dramatic effect showed the offspring of the cross with the corresponding RLD-WT that resulted in plants that exhibit a very extreme overproduction of trichomes on the leaves (Fig. 20F), which I never observed, if  $TTG1^{im}$  is directly transformed. Again the trichomes no longer showed the distorted and blown-up phenotype but looked rather normal, with only a slight increase in branching (Fig. 20F). These plants were similar to WT plants expressing 35S::*GL3* together with 35S::*GL1* (Zhang *et al.* 03) with the exception that in the case of  $TTG1^{im}$  no trichomes are formed on hypocotyl or cotyledons. The leaves did not expand properly and plants were dying after the outgrowth of the third and fourth leaf. This is also observed in other

transgenic plants where trichome-overproduction takes place (Larkin *et al.* 1994, Schnittger *et al.* 1999).



**Figure 20: Effect of  $pTTG1::TTG1^{tm}$  in different  $ttg1$  and other mutant backgrounds.** A description is given on the next page.

### 2.8.3. Dependency of *TTG1<sup>im</sup>*-induced patterning and trichome-morphogenesis effects on other trichome regulators

Because the phenotypes observed with *TTG1<sup>im</sup>* resembled that of *GL3* overexpression, the question was, if these effects are dependent on *GL3* function. Therefore *gl3-1 ttg1-1* double mutants, who are completely glabrous, were transformed with *pTTG1::TTG1<sup>im</sup>*. Double mutant plants carrying the *pTTG1::TTG1<sup>im</sup>* develop trichomes, but the distorted and blown-up phenotype observed with *pTTG1::TTG1<sup>im</sup>* in the *ttg1* single mutant background was not observed (Fig. 20 I). Instead, the outgrown trichomes looked like *gl3* or WT-trichomes with branch number ranging from unbranched to three-branched (Fig. 20 I). This shows that the distorted phenotype is dependent on the *GL3* gene, but also indicates that *TTG1<sup>im</sup>* is able to rescue the *gl3* trichome phenotype to some extent, because *gl3* trichomes produce only up to two branches (Hülkamp *et al.* 1994).

The *try cpc* double mutant produces large clusters of trichomes that develop due to successive induction of trichome-neighbouring cells into trichomes (Schellmann *et al.* 2002). These *try cpc* trichome-clusters are regularly patterned over the leaf surface. To test the role of *TTG1* during this process the *try cpc ttg1-13* triple mutant, who develop few trichomes at the leaf margins (see Fig. 13 B & C), was transformed with either *pTTG1::TTG1* or with *pTTG1::TTG1<sup>im</sup>*.

#### ← Figure 20: Effect of *pTTG1::TTG1<sup>im</sup>* in different *ttg1* and other mutant backgrounds.

(A) – (C) Two-week-old seedling of the offspring of *pTTG1::TTG1<sup>im</sup>* in the *ttg1-13* deletion allele with different *ttg1* alleles. (A) Cross with *ttg1-1*, showing a bloated trichome phenotype. (B) Cross with *ttg1-9* showing some distorted and some overbranched trichomes, please note that trichome outgrowth is partially rescued. (C) Cross with *ttg1-10* with several overbranched trichomes and enhanced outgrowth of trichomes.

(D) *ttg1-10* mutant with directly transformed *pTTG1::TTG1<sup>im</sup>* showing enhanced outgrowth of bloated trichomes.

(E) – (H) Two-week-old seedlings. (E) RLD WT. (F) Offspring of *pTTG1::TTG1<sup>im</sup>* in the *ttg1-13* allele with RLD WT, plants show strongly enhanced trichome formation on the leaves.

(G): *pTTG1::TTG1<sup>im</sup>* in a *try cpc ttg1-13* mutant background. (H): *35S::GL3* in a *try cpc ttg1-13* mutant background.

(I): *pTTG1::TTG1<sup>im</sup>* in a *ttg1-1 gl3-1* mutant background, please note that the bloated and distorted phenotype is absent.

(J) – (M): GUS-staining of two-week-old seedlings. (J) *pGL2::GUS* in a WT background. (K) *pGL2::GUS* together with *pTTG1::TTG1<sup>im</sup>*, please note the staining in the hypocotyl. (L) *pTRY::GUS* in a WT background. (M): *pTRY::GUS* together with *pTTG1::TTG1<sup>im</sup>*. Please note that the hypocotyl and the cotyledons show staining around the vasculature, which is not seen in the WT.

Whereas *pTTG1::TTG1* restored the *try cpc* double mutant phenotype (data not shown), *pTTG1::TTG1<sup>im</sup>* resulted in enhanced trichome production, however the large cluster phenotype was lost (Fig. 20 G). Therefore *TTG1* in fact seems to play a role in the formation of the large trichome clusters in *try cpc*. If *try cpc ttg1-13* was transformed with *35S::GL3* this resulted in the same phenotype as *pTTG1::TTG1<sup>im</sup>* in this background (Fig. 20 H), indicating that *pTTG1::TTG1<sup>im</sup>* is activating *GL3*.

#### B 2.8.4. Immobilised TTG1 induces ectopic trichome-specific reporters

To test whether the enhanced trichome production that is observed together with the *pTTG1::TTG1<sup>im</sup>* construct is reflected in ectopic expression of trichome specific genes, a line expressing *pTTG1::TTG1<sup>im</sup>* in a *ttg1-13* background was crossed to *Ler* plants expressing the trichome-specific *pGL2::GUS* or *pTRY::GUS* marker constructs (Szymanski *et al.* 1998a & Schellmann *et al.* 2002). The *pGL2::GUS* construct contains the promoter fragment of the *GLABRA2* gene together with the 5' UTR. *GL2* is supposed to have a role in differentiation of trichomes and seems to be a target gene of the initial trichome patterning genes (Szymanski *et al.* 1998b). The *TRY* gene plays a role early in trichome patterning (Hülkamp *et al.* 1994, Schnittger *et al.* 1999, Schellmann *et al.* 2002).

The use of these GUS-reporters is possible because the GUS-reporter of the *TTG1<sup>im</sup>*-fusion does not result in any detectable GUS-staining (data not shown). While *pTRY::GUS* is active in all epidermal cells of the trichome-patterning zone in young leaves and later on becomes specific for trichomes in the WT background (Fig. 20 L and Schellmann *et al.* 2002), an ectopic expression in cells around the vasculature of cotyledons and hypocotyl is found in the lines with *pTTG1::TTG1<sup>im</sup>* (Fig. 20M).

*pGL2::GUS* is more restricted to trichomes and is thought to act later in trichome formation (Fig. 20J and Szymanski *et al.* 1998b). In *pTTG1::TTG1<sup>im</sup>* the *GL2::GUS* activity was additionally observed in the hypocotyl that was not observed in the segregating WT-background plants (compare Fig. 20 J & K). However *GL2* and *TTG1* seem to have a role in the stomata patterning of the hypocotyl and the observed GUS-staining may be due to an enhancement of the endogenous *GL2* activity (Berger *et al.* 1998).

Therefore *pTTG1::TTG1<sup>im</sup>* is able to ectopically activate trichome-specific reporters, although no ectopic trichomes develop on those organs.

### **B 2.8.5. Dominant negative effect of trichome-specific expression of the immobilised TTG1**

If *pTTG1::TTG1<sup>im</sup>* is able to promote ectopic *GL2* expression, what would happen if *TTG1<sup>im</sup>* would be expressed under this strong trichome-specific promoter? This construct was no longer able to rescue the *ttg1* mutant, although expression of *TTG1* or *NLS-TTG1* under *pGL2* resulted in a complete rescue of *ttg1-1* (Martina Pesch, unpublished observation and table 2).

More striking was the effect in WT. Plants had glabrous leaves and in addition showed enhanced root hair production (Fig. 21A - C), which resembles the *ttg1* mutation. This effect is unlikely to be caused by co-suppression because the seed coat was not affected.

This dominant negative phenotype could be explained for example by the downregulation of the activator *GLI*, or the upregulation of negative regulators, like *TRY*. Crosses of the transformants with a *pGL1::GUS* line showed the same basic expression pattern that is also observed in WT (Fig. 21J & K, Larkin *et al.* 1993). *pTRY::GUS* expression remained unchanged (the same result was obtained with *pETC1::GUS* or *pCPC::GUS*), making it very unlikely that the observed phenotype is due to a change in the expression of the trichome patterning genes (Fig. 21L & M).

### **B 2.8.6. The dominant negative effect of *GL2::TTG1<sup>im</sup>* is dependent on TRY/CPC**

Although *pGL2::TTG1<sup>im</sup>* does not induce ectopic *TRY* or *CPC* reporter gene expression it possible that the dominant negative phenotype is caused due to an interaction of *TTG1* with the negative regulators *TRY* or *CPC*. Therefore *Ler* plants containing *pGL2::TTG1<sup>im</sup>* were crossed with *try*, *cpc* and *try cpc* mutants. F2-descendants were selected on kanamycin MS-plates, or on kanamycin + hygromycin MS-plates in the case of *cpc*. In the case of *try cpc* the formation of trichomes together with *pGL2::TTG1<sup>im</sup>* was observed (Fig. 21E) indicating that the dominant negative effect seen with this construct is dependent on the negative regulators.

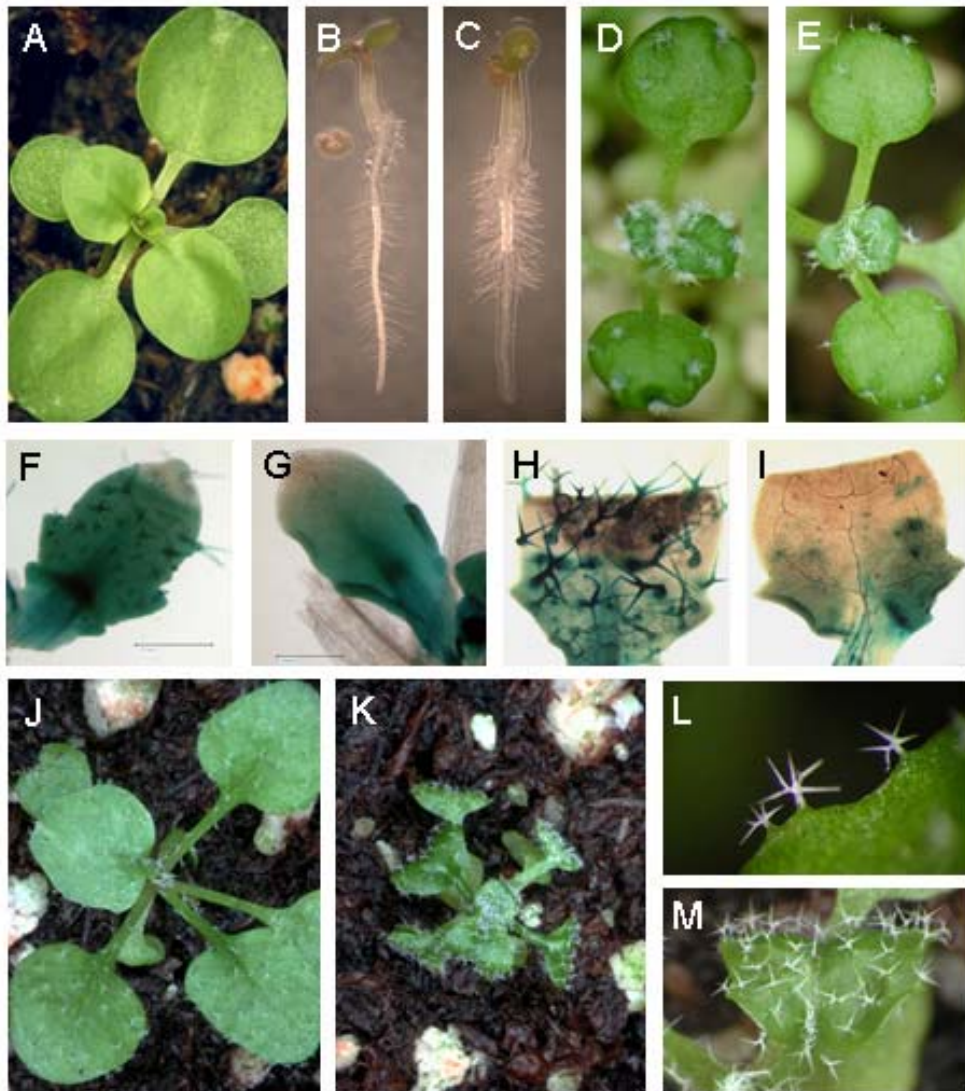


**Figure 21: Dominant negative effect of pGL2::TTG1<sup>im</sup>.**

(A) Transgenic Ler plant carrying pGL2::TTG1<sup>im</sup>, showing glabrous phenotype.

(B) & (C): Root phenotype, (B): Ler WT and (C): pGL2::TTG1<sup>im</sup> in Ler background.

(D): *try cpc* double mutant showing large trichome clusters.

(E): pGL2::TTG1<sup>im</sup> in *try cpc* double mutant background, please note that the large cluster phenotype is abolished.

(F) – (I): GUS staining. (F): pGL1::GUS in WT background, showing ubiquitous and stronger trichome-

activity (G) pGL1::GUS in pGL2::TTG1<sup>im</sup> background, same ubiquitous expression as in the (F).

(H) pTRY::GUS in WT background with weak ubiquitous and strong trichome-specific expression.

(I) pTRY::GUS in pGL2::TTG1<sup>im</sup> background with the same ubiquitous expression activity as in the WT (H).

(J) – (K): Four-week-old plants. (J) pGL2::GL3 plant in the WS-O background.

(K): Same magnification as (J) Offspring of the cross between pGL2::TTG1<sup>im</sup> and strong pGL2::GL3, showing rescue of the dominant negative phenotype of pGL2::TTG1<sup>im</sup>. Please note that growth is strongly retarded in comparison to (J).

(L): overbranched trichomes on a pGL2::GL3 line. (M): detail of the plant shown in (K) showing overbranched trichomes and impaired leaf-development

However the absence of *TRY* and *CPC* together with the expression of *pGL2::TTG1<sup>im</sup>* did not result in a *try cpc* double mutant phenotype with large clusters, but produced only some trichomes with some clusters having only few trichomes (Fig. 21E). This means that there is still some dominant negative effect on trichome formation in these lines.

### **B 2.8.7. *TTG1<sup>im</sup>* interacts with *GL3* but not with *GL1***

Previous genetic studies have suggested that the *GL3* gene acts either downstream of *TTG1* or together with *TTG1* at the same level (Payne *et al.* 2000, Esch *et al.* 2003). Moreover both gene-products show interaction in yeast-two-hybrid experiments (Payne *et al.* 2000). *GL1* did not show any interaction with *TTG1* in yeast-two-hybrid analysis, but has been shown to interact genetically (Payne *et al.* 2000, Esch *et al.* 2003, Larkin *et al.* 1999, Schnittger *et al.* 1999).

The *pGL2::TTG1<sup>im</sup>* crossed with *pGL2::GL1* did not change the dominant negative phenotype, indicating that there is no direct interaction of *GL1* and *TTG1* (data not shown). To test whether *TTG1* and *GL3* can interact *in planta* and rescue the observed trichome phenotype, I crossed *pGL2::TTG1<sup>im</sup>* with *pGL2::GL3*-lines (Plants were generated by Martina Pesch). The *pGL2::GL3* plants show a strongly overbranched trichome-phenotype (Fig. 21L). The cross with a strong allele of *pGL2::GL3* rescued the trichome phenotype completely (Fig. 21M), showing that *TTG1* and *GL3* are in fact interacting *in planta*. Weak *pGL2::GL3* alleles could not as effectively rescue the glabrous phenotype, indicating that the observed effect is concentration dependent (data not shown).

During further development of the F1 descendants I observed very strong developmental defects that resulted in curling of leaves and extreme dwarfism (compare Fig. 21J & K), thereby giving additional indication of the interaction of *GL3* and *TTG1*.

### B 3. DISCUSSION

Because cell differentiation in plants depends largely on positional information, cells have to communicate this information (for a summary see Benfey 2001, Szymkowiak & Sussex 1996). A special case for such a process is provided by the development of trichomes on the leaf surface of *Arabidopsis thaliana* (Hülkamp *et al.* 1994, Szymanski *et al.* 2000, Larkin *et al.* 2003). The pattern of trichome distribution is not random and it has been shown that cell lineage is rather unlikely to be involved and that there are no prepatterns, therefore trichome patterning can be described as *de novo* pattern formation and most likely depends on cell-cell communication (Hülkamp *et al.* 1994, Larkin *et al.* 1996, Schnittger *et al.* 1998 & 1999).

Communication between cells can be established by extracellular signalling, however this is somehow hindered in plants because of the existence of a rigid cell wall and this process has been described only for a few cases (Fletcher *et al.* 1999, Matsubayashi *et al.* 2001).

Instead, signalling in plants is established throughout specialised channels between their cells, the plasmodesmata that connect those cells with each other and allow the exchange of signaling molecules and even proteins (Jackson 2000, Heinlein 2002, Oparka 2003, Wu *et al.* 2002, Zambryski 2004).

#### B 3.1. Non-cell-autonomous action of TTG1

Protein movement has been observed in several pattern-formation processes in plants, including radial and epidermal patterning in the root of *Arabidopsis* (Nakajima *et al.* 2001, Wada *et al.* 2002). In both cases the expression patterns of the respective genes differ from the protein localisation and the mobility of the proteins seems to be restricted to the adjacent cell-file (Nakajima *et al.* 2001, Wada *et al.* 2002).

*TTG1* is involved in the epidermal pattern formation in the shoot and therefore it was examined if this is a non-cell-autonomous function of *TTG1*. First the non-cell-autonomy is shown in the performed *Cre-Lox* experiments where *TTG1* is locally excised, but trichome formation still takes place in sectors lacking *TTG1*. The quite large space between the place of *TTG1* expression, marked by the GUS-staining, and the site where trichomes are formed, indicates that the gene is able to act over a distance of several cells within the same cell-layer. However it should be

mentioned that trichome formation takes place very early during leaf-development when the trichomes are separated by not more than three to four epidermal cells, which makes it difficult to determine the exact range of *TTG1* action (Hülkamp *et al.* 1994, Larkin *et al.* 1996).

A second approach to test the non-cell-autonomous action of *TTG1* was to express it from the subepidermal layer. Therefore I used the well-characterised *PCAL* promoter that controls the leaf subepidermal expression of the phosphoenolpyruvat-carboxylase gene of *Flaveria trinerva* (Stockhaus *et al.* 1994). Several experiments indicate that this promoter is in fact also mesophyll specific in *Arabidopsis* (see Results). Therefore the observed rescue of the *ttg1-13* mutant by expression of *TTG1* under the *PCAL* promoter is a consequence of the non-cell-autonomous action of *TTG1*, which in addition shows that *TTG1* is able to function between cell-layers.

Detection of the *TTG1*-YFP fusion protein expressed in the subepidermis in trichome-cells favours the idea of non-cell-autonomous *TTG1* action and suggests that either *TTG1* protein or its mRNA or both are mobile and the non-cell-autonomous action is not an indirect effect. However the *TTG1* expression pattern does not hint towards a non-cell-autonomous function, because it is expressed in the entire trichome-patterning zone. But several cases of protein movement have been reported where the biological relevance of this mobility was somehow unclear because the genes are also expressed throughout their domains of action (Perbal *et al.* 1996, Sessions *et al.* 2000, Wu *et al.* 2003, Kim *et al.* 2003). One explanation for these paradox observations may be the postulated “fail-safe” mechanism, which ensures that cells adopt a certain fate that is promoted by those proteins, meaning that single cells that may exhibit a reduced expression of a certain gene will still obtain enough of the protein due to its mobility from neighbouring cells (Mezitt & Lucas 1996, Sessions *et al.* 2000, Kim *et al.* 2003).

### **B 3.2. Developmental relevance of *TTG1* mobility**

Several observations indicate that the *TTG1* mobility is relevant for the pattern formation process. The fusion of *TTG1* to YFP leads to reduced trichome number when expressed from the subepidermis compared with the unfused *TTG1* in the *ttg1* mutant background. The *TTG1*-YFP (65.8 kD) fusion has a remarkable larger size than *TTG1* alone (38 kD) and the reduced rescue most likely results from an impaired mobility of the fusion-protein. If *TTG1* mobility would be of

minor relevance, this should not impair the trichome pattern formation. However patterning defects were observed in transgenic plants expressing the TTG1-YFP fusion under the endogenous *TTG1*-promoter, but never in plants carrying the *pTTG1::TTG1* transgene. Enhanced cluster formation was observed, both in the *ttg1* mutant and in WT background. Furthermore, in some cases the distribution of the trichomes over the leaf epidermis is concentrated towards the margins and depleted from the centre if the fusion is expressed under the constitutive CaMV 35S promoter in WT. A similar distribution pattern is observed in *35S::GL1* plants, however those lines do not produce trichome clusters.

Cluster formation is also observed in weak alleles of *ttg1*. Therefore one may argue that the cluster formation is a consequence of a reduced activity of the fusion protein. This is unlikely because the number of trichomes of *pTTG1::TTG1-YFP* in *ttg1-13* is at least as high as in the corresponding WT situation. In addition trichomes in weak *ttg1* alleles show a reduction in branching and the seed coat differentiation is strongly impaired (Koorneef 1981, Larkin *et al.* 1994, Larkin *et al.* 1999). Both phenotypes are completely rescued by the fusion, which render it unlikely that the activity of TTG1-YFP is impaired. However it cannot be excluded that the fusion is leading to changes in protein function other than mobility. Yet the same trichome patterning defects are observed in a *35S::GFP-TTG1* fusion that also leads to the formation of the WT-number and morphogenesis of trichomes in the *ttg1-13* mutant.

The pattern formation and trichome morphology are strongly disturbed if the mobility of TTG1 is completely abolished. The loss of mobility was established by a fusion of TTG1 with GFP-GUS. In this case the addition of an NLS sequence is a prerequisite for the functionality of the fusion protein (TTG1<sup>im</sup>). The fusion of the NLS sequence to TTG1 alone does not result in such strong trichome patterning defects as seen in plants expressing *TTG1<sup>im</sup>*. *ttg1-13* plants expressing *pTTG1::NLS-TTG1* show rescued trichome-number and -morphology and seed coat colouring but resulted in an increased cluster formation (4.1%) that is also seen *ttg1-13* plants expressing *pTTG1::TTG1-YFP* (3.8%). TTG1-YFP is in fact impaired in the mobility compared to the unfused TTG1 and the same may be expected for NLS-TTG1. Previously it has been shown that the fusion of an NLS-sequence to GFP results in impaired mobility (Crawford and Zambryski 2000).

TTG1<sup>im</sup> is able to lead to trichome formation in the *ttg1* background. Yet the trichomes show strong morphological deviation from the WT leading to different distortions and a bloated

appearance of the cells. The number of trichome initiation sites (TIS) is doubled when compared with the WT and the cluster frequency is about 15%, which is even higher than in the *try* mutant (4.4% data from Schellmann *et al.* 2002). Although most of these TIS do not grow out in the *ttg1-13* mutant, this is the case if those lines are crossed with weaker alleles of *ttg1* or if the construct is directly transformed into weaker alleles. The most dramatic effect is observed if *TTG1<sup>im</sup>* is crossed to the corresponding WT, thereby adding a copy of the endogenous (and mobile) *TTG1*. This results in excess trichome formation. Therefore the immobilisation of TTG1 seems to result in hyperactivation of trichome formation. An increase in trichome number of around 50% is also observed in *Ler* plants expressing *pTTG1::TTG1-YFP* (24.5 versus 16.5 TIS on the first two leaves of *pTTG1::TTG1-YFP* and WT, respectively).

It cannot be ruled out that the biochemical function of TTG1 has been changed due to the fusion, and in fact the fusion to GUS can change the behaviour of a protein (Torii *et al.* 1998). One may argue for example that negative regulatory functions of TTG1 that are implied from previous analysis (Larkin *et al.* 1994, Larkin *et al.* 1999, Schnittger *et al.* 1999) are abolished due to the fusion. This seems unlikely because the trichome specific expression of *TTG1<sup>im</sup>* leads to a dominant negative phenotype. Those plants are devoid of any trichomes, showing that TTG1 is able to act as a negative regulator of trichome development. This phenotype can be complemented by co-expression of *GL3* or reduction of the negative regulators, which suggest that this fusion does not lead to an unspecific block of trichome cell differentiation. In addition a GUS-hybrid has previously been used as a tool to block cell-to-cell transport of the mobile KN1 protein (Kim *et al.* 2003).

According to these data one can postulate that the mobility of TTG1 is of functional relevance during the trichome pattern formation process. Possible explanations for the observed phenotypes will be given in the further discussion.

### **B 3.3. Is TTG1 actively transported?**

The issue of active protein transport is difficult to assess, because there exist no clear criteria for the subdivision into active or passive transport (Kim *et al.* 2003, Wu *et al.* 2003). However I think it is worth to discuss this question because it is of functional relevance.

The tobacco viral movement protein (MP) is the best-studied example of an actively transported protein and is known to increase the plasmodesmatal size exclusion limit (SEL) (Deom *et al.* 1987, Wolf *et al.* 1989) thereby allowing the passage of other non-specific reporter molecules (for review see Ghoshroy & Citovsky 1997). Another intensively studied example is the non-cell-autonomous homeodomain transcription factor KNOTTED1 (KN1) that increases the SEL and has the capacity to bind and traffic its own mRNA (Lucas *et al.* 1995). However MP- and KN1-GFP fusions differ in their distribution if expressed from a certain cell layer. Whereas the MP-GFP can be detected everywhere in the shoot apical meristem with the same intensity when expressed from the epidermal cell layer, KN1-GFP shows a gradient and ceases with increasing distance to the expressing tissue (Kim *et al.* 2002, Kim *et al.* 2003).

These findings together with other studies focusing on the dependency of intracellular localisation and intercellular mobility of proteins, lead to the suggestion that transport is a kind of default pathway and is highly dependent on the intracellular targeting (Crawford & Zambryski 2000, Wu *et al.* 2003). Wu *et al.* speculated that proteins that localised strictly to the nucleus are trapped in the cell and only proteins that have at least some cytoplasmic localisation will move just by diffusion (Wu *et al.* 2003). However NLS-GFP is not blocked in cell-to-cell transport (Crawford & Zambryski 2000 & 2001) and a mutated form of KN1, where the NLS is affected, results in even reduced mobility of the protein (Kim *et al.* 2002).

TTG1-YFP shows both nuclear and cytoplasmic localisation, yet the nuclear localisation appears to be predominant during early development and shifts towards a more cytoplasmatic localisation during further differentiation of the pavement cells. Unfused TTG1 leads to a more efficient rescue of *ttg1-13* than TTG1-YFP when expressed from the subepidermis, which may be an indication for a passive kind of transport. However the sizes of TTG1-YFP (65.8 kD) and of NLS-TTG1-YFP (72.4 kD), which is exclusively in the nucleus, are remarkably larger than that of NLS-2x-rsGFP (54.6 kD) that is blocked in transport (Crawford & Zambryski 2000 & 2001). This in turn would argue for an active transport of TTG1. But the experiments are not easy to compare because Crawford and Zambryski (2000) used biolistic transfection of tobacco plants in contrast to the stable transformants in *Arabidopsis* used in this study.

Another approach to test if TTG1 is actively transported would be to fuse TTG1 with a protein that is cell-autonomous and then see if this fusion is non-cell-autonomous. This experiment has been successfully carried out while fusing KN1 with GL1. This fusion rescues the *gl1* mutant

phenotype when expressed from the subepidermis, which was not observed if the experiment was done with *GL1* alone (Yae-Jean Kim & David Jackson unpublished results). The same experiment will be performed in collaboration with Yae-Jean Kim using TTG1 (instead of KN1) and then see if it can lead to a transport of GL1 from the subepidermis to epidermal cells. However if one assumes that only the intracellular localisation determines the intercellular mobility of a protein, a rescue of *gll* by subepidermal expressed TTG1-GL1 may be just a consequence of disturbing the nuclear localisation of GL1 (Szymanski *et al.* 1998b, Esch *et al.* 2003) and not an effect of an active transport mediated by TTG1.

A further observation may give an indication that the transport of TTG1 is specific with respect to trichomes. If TTG1-YFP is expressed from the subepidermis the YFP-signal in the epidermis seems to be restricted to trichomes. It is possible that the signal is only detected in trichomes because of the large nucleus and TTG1-YFP in the pavement cells is below the detection limit or is destabilised there. However this signal in trichomes is quite strong and comparable to the signal that is observed when the fusion is expressed under the endogenous *TTG1* promoter, which suggests that there may be a directional transport into trichomes or an active exclusion from other cells.

### **B 3.4. Intracellular localisation of TTG1**

The putative intracellular targeting of TTG1 was a matter of long debate (Walker *et al.* 1999, Larkin *et al.* 2003, Esch *et al.* 2003). A TTG1 ortholog from *petunia hybrida*, AN11, has been shown in cell fractionation experiments to be exclusively localised in the cytoplasm (de Vetten *et al.* 1997). Therefore it was likely that TTG1 would also act in the cytoplasm, may be by stabilising the trichome-activating complex prior to nuclear localisation (Larkin *et al.* 2003).

However all other members of the trichome patterning system encode for transcription factors and all of them localise to the nucleus as shown for GFP-fusion proteins (Oppenheimer *et al.* 1991, Szymanski *et al.* 1998b, Payne *et al.* 2000, Schellmann *et al.* 2002, Wada *et al.* 2002, Esch *et al.* 2003). Moreover TTG1 and GL3 strongly interact in yeast-two-hybrid analysis and GL3 in addition interacts also with GL1 and TRY (Payne *et al.* 2000, Esch *et al.* 2003). Therefore it is assumed that the postulated activator complex is active in the nucleus.

This is in agreement with my observation that TTG1-YFP localises to the nucleus. However I observed that the localisation of TTG1 seems to be differently distributed during leaf development. Trichomes showed, beside a weak cytoplasmic signal, a clear nuclear localisation, whereas pavement cells were losing the nuclear signal during further development.

The relevance of this change in intracellular localisation during leaf development is unclear, but may explain the difference between our results and those reported by de Vetten *et al.* (1997).

Like *AN11*, *TTG1* has also a role in the regulation of anthocyanin biosynthesis and this process is not dependent on trichome development, because the *gl1* mutant has no defect in anthocyanin production (personal observation). An interesting explanation for the observed differences in intracellular localisation may be that the nuclear transport of TTG1 into the nucleus is part of the regulation of the respective process. In this context it may be interesting to follow the TTG1-YFP targeting in older pavement cells when the anthocyanin pathway is activated, for example by UV-irradiation. However it is unlikely that the transport into the nucleus would be the only regulatory mechanism, because plants expressing *NLS-TTG1* do not produce ectopic anthocyanin (personal observation).

Sompornpailin *et al.* (2002) have shown that a close ortholog of *TTG1*, *PFWD* from *Perilla frutescens* shows both nuclear and cytoplasmic localisation in onion epidermal cells. Interestingly this localisation shifted towards a more nuclear localisation if in addition a bHLH gene similar to *GL3* was co-expressed (Sompornpailin *et al.* 2002). Therefore one possible explanation that the TTG1-YFP signal remains nuclear in trichomes is that this localisation depends on *GL3* and/or *EGL3* which are both expressed throughout the trichome patterning zone in the young leaf and later concentrate in the developing trichomes (Zhang *et al.* 2003). This is in agreement with the observation that the nuclear signal of TTG1-YFP is weaker in *gl3* mutant background. In addition this indicates that TTG1 does not contain an own nuclear localisation signal, but is localised into the nucleus by the strong interaction with the nuclear localised *GL3*.

### **B 3.5. Interaction of TTG1 with other patterning genes**

Genetic and biochemical analysis have indicated that the trichome patterning factors interact and form an activating complex or an inhibiting complex (Larkin *et al.* 1994, Schnittger *et al.* 1998, Schnittger *et al.* 1999, Larkin *et al.* 1999, Payne *et al.* 2000, Schellmann *et al.* 2002, Esch *et al.*

2003). Yeast two-hybrid analyses have shown that TTG1 interacts with GL3 and EGL3 but not with GL1 (Payne *et al.* 2000). This is in agreement with my observation that the dominant negative effect of *pGL2::TTG1<sup>im</sup>* is rescued by *pGL2::GL3*, but not by *pGL2::GL1*. Furthermore the aberrant growth of the offspring of the cross between *pGL2::TTG1<sup>im</sup>* and *pGL2::GL3* indicates that both gene products synergistically interact *in planta*.

The change in intracellular localisation of TTG1-YFP in trichomes from nuclear in WT to more cytoplasmatic in the *gl3* mutant background gives a further hint for the interaction of TTG1 and GL3. Moreover the phenotypes of *pTTG1::TTG1<sup>im</sup>* in both *ttg1* and WT background resemble the overexpression phenotype of *GL3*, leading to bloated and distorted trichome morphology in the *ttg1* mutant background, and an enhanced trichome production in the WT background. Trichome-specific overexpression of *GL3* is able to produce a bloated and distorted trichome phenotype also in the WT (Viktor Kirik unpublished results). In fact, the striking phenotype in the *ttg1* background is dependent on the presence of *GL3*. This is shown by the loss of the distorted trichome phenotype, if *pTTG1::TTG1<sup>im</sup>* is expressed in the *ttg1 gl3* double mutant background. However this does not only lead to a reduction of the distorted trichome phenotype but was able to partially rescue the branching defect of *gl3* mutant trichomes. This may be explained due to a partial redundancy of *GL3* with *EGL3*, which may compensate for *GL3* in those lines if *EGL3* is activated by *pTTG1::TTG1<sup>im</sup>*. Therefore it would be necessary to test if *pTTG1::TTG1<sup>im</sup>* is still able to produce trichomes in the *ttg1 gl3 egl3* triple mutant. However the observation that trichome-specific expression of the *pGL2::TTG1<sup>im</sup>* leads to a negative effect instead of an enhanced phenotype indicates that TTG1 does not only promote the *GL3* pathway.

An interaction was observed between TTG1<sup>im</sup> and the negative regulators TRY and CPC. The dominant negative effect of *pGL2::TTG1<sup>im</sup>* that leads to glabrous leaves is reduced in the absence of *TRY* and *CPC*. An activation of *TRY* by *TTG1* has been postulated previously (Schnittger *et al.* 1999, Larkin *et al.* 1999). However the expression of *pTRY::GUS* or *pCPC::GUS* remained unchanged in the *pGL2::TTG1<sup>im</sup>* lines. Therefore it is likely that TTG1<sup>im</sup> and TRY/CPC interact and the dominant negative phenotype is caused by this interaction. Although no strong direct interaction between TTG1 and TRY or CPC has been reported in yeast-two hybrid assays (Esch *et al.* 2003, Katja Wester unpublished results), this interaction may take place indirectly through a multi protein complex that may be stabilised by TTG1<sup>im</sup>. If one assumes that the negative regulators need to move out of the cell where they are expressed, and acts as inhibitors (Wada *et*

*al.* 2002, Lee & Schiefelbein 2002, Larkin *et al.* 2003), such a binding to a complex would lead to an inhibition of trichome development.

The genetic interaction between *TTG1* and the negative regulators is furthermore shown in the triple and quadruple mutants of *ttg1* with *try cpc* and either *etc1* or *etc2*. Because those plants produce synthetic trichome phenotypes this suggests that *TTG1* and the negative regulators act at the same level and this is consistent if one assumes that they can interact.

### **B 3.6. Is the role of TTG1 in agreement with an activator-inhibitor system?**

The activator-inhibitor model explains the generation of a stable spacing pattern in a two dimensional field. The activator acts in an autocatalytic feedback loop, whereas the inhibitor counteracts this positive regulation by providing a negative feedback loop, which complements the activator (Meinhardt & Gierer 2000). An important difference between the activator and the inhibitor is their different diffusion rate that needs to be higher for the inhibitor.

One problem, if this model is applied to the trichome patterning system is, to clearly define the involved components as activator or inhibitor. A particular case is the *TTG1* gene because of its double function in trichome patterning (Larkin *et al.* 1994, Larkin *et al.* 1999, Schnittger *et al.* 1999).

First I want to summarise arguments for the assumption that *TTG1* acts as an activator during trichome development. The deletion of *TTG1* leads to a complete loss of trichomes, therefore *TTG1* is required to produce trichomes in the WT (Koorneef 1981, Walker *et al.* 1999). If the activity of *TTG1* is reduced this leads to a reduction in trichome-number and –cell-differentiation (Larkin *et al.* 1994, Larkin *et al.* 1999). In this case trichomes do not complete their morphogenetic program, e.g. they are underbranched (Larkin *et al.* 1994, Larkin *et al.* 1999, Schnittger *et al.* 1999).

Second, what are the arguments to categorize *TTG1* as a negative regulator? The indications for this came from the analyses of weak *ttg1* mutants that showed the formation of trichome clusters (Larkin *et al.* 1994, Larkin *et al.* 1999, Schnittger *et al.* 1999). This means that those plants are defective in lateral inhibition, and this effect can even be enhanced if in addition the activity of *TRY* is reduced (Schnittger *et al.* 1999). *TRY* has been shown to be a negative regulator of trichome development because in the *try* mutant clusters of trichomes are formed, and the ectopic

expression of *TRY* leads to glabrous leaves (Hülskamp *et al.* 1994, Schellmann *et al.* 2002). In addition the loss of *TRY* leads to enlarged and overbranched trichomes and it has been shown that *TRY* belongs to a subfamily of partially redundant genes that all mediate lateral inhibition during trichome development (Schellmann *et al.* 2002, Kirik *et al.* 2004a & 2004b). The observation that *ttg1* is involved in lateral inhibition has been explained with the activation of *TRY* by *TTG1*, meaning that a loss in *TTG1* activity would also lead to a decrease in *TRY* activity (Schnittger *et al.* 1999). However this is what would be expected in the activator-inhibitor model because the inhibitor activity (in this case *TRY*) depends on the activator (in this case *TTG1*) (Schnittger *et al.* 1999). Therefore *TTG1* does not seem to be an inhibitor of trichome cell fate *per se*.

The fact that the need for *TTG1* can be bypassed by overexpression of other activators have suggested that *TTG1* plays a more modulating role during trichome development and may therefore not be classified in terms of being an activator or an inhibitor (Schnittger *et al.* 1999, Payne *et al.* 2000). But how could such a modulatory role look like? *TTG1* has been shown to interact with the *GL3* protein (Payne *et al.* 2000). The *GL3* gene has been shown to be a limiting factor for trichome initiation. Together with its close and partially redundant homologue *EGL3*, *GL3* overexpression leads to enhanced trichome formation (Payne *et al.* 2000, Zhang *et al.* 2003), whereas neither 35S::*GL1* nor 35S::*TTG1* results in enhanced trichome production on the leaf (Larkin *et al.* 1994, Payne *et al.* 2000, my own observation).

Interestingly the expression of the immobilised *TTG1* under its own promoter reflects all aspects of *GL3* overexpression. This indicates that *TTG1<sup>im</sup>* leads to a stronger activation of *GL3*, which suggests a role of *TTG1* as a positive modulator. In the activator-inhibitor model the activator needs to act in a more immobile manner, at least with respect to the inhibitor. However my observations suggest that *TTG1* acts non-cell-autonomously in the range of several cells and is itself mobile. On the other side the immobilisation of *TTG1* leads to enhanced trichome-initiation as may be expected for an activator in the Meinhardt-model. However the addition of an endogenous, and mobile, copy of *TTG1* does even enhance the effect, leading to excessive trichome development. Therefore the assumption that the immobilisation itself leads to stronger activation does not seem to hold true with respect to trichome pattern formation.

However taking a look at the trichome-morphology there are striking differences. The bloated and distorted phenotype is reduced with increasing activity of endogenous/mobile *TTG1*, shown by the phenotypes of the descendants of the crosses of *pTTG1::TTG1<sup>im</sup>* in the *ttg1-13* background with weaker *ttg1* alleles and the WT. This could be interpreted as a rescue if the bloated and

distorted phenotype would be regarded as a weak complementation of *ttg1*. However the fact that weaker alleles of *ttg1* combined with *pTTG1::TTG1<sup>im</sup>* show overbranching, which is also observed if *GL3* is trichome-specifically expressed, indicates that these phenotypes correspond to higher trichome-promoting activities in those cells. Whereas the bloating and distortion is decreasing, the outgrowth of trichomes is increasing. On the other hand the overbranching is again reduced if a complete *TTG1* allele is added, but now a dramatic increase in trichome formation takes place. This suggests that the intracellular promotion of trichome cell fate is enhanced in those lines where *TTG1* is strictly cell-autonomous. This trichome promoting activity shifts from a cell-intrinsic function if *TTG1* is completely cell-autonomous towards a spread of this trichome promoting activity over the whole leaf if a part of *TTG1* is mobile and another part is immobile. But this also implies that *TTG1* has some negative regulatory function because otherwise the immobilisation together with the mobile copy of *TTG1* should lead to an increase in trichome-initiation AND the formation of bloated or overbranched trichomes. In summary these observations suggest that the effect of *TTG1* action, meaning that *TTG1* is activating or inhibiting trichome cell fate, is highly dependent on its concentration in the cell. How could this effect be explained according to the activator-inhibitor model?

### **B 3.7. Another view on the Meinhardt-model**

In the conventional description of the Meinhardt-model, the activator-inhibitor system, small fluctuations of the activator lead to an autocatalytic amplification of the activator concentration in a given cell. At the same time the activator induces the inhibitor in the same cell. This inhibitor will then, in contrast to the less mobile activator, diffuse out of the cell and antagonize the cell fate that is promoted by the activator in the neighbouring cells. This process is called lateral inhibition.

*TTG1* action suggests a different kind of looking at the model. In the following scenario I will describe a model that is also dependent on only two components, an activator (*GL3*) and a substance that is needed for the autocatalytic process (*TTG1*), thereafter called activator-substance system. For a schematic description see Fig. 22. Just as in the lateral inhibition scenario, all cells in the patterning zone are identical according to the concentration of the involved components. Already a small increase in *GL3* concentration in a given cell will lead to

an increased localisation of TTG1 in the nucleus due to the strong interaction between GL3 and TTG1 and the nuclear localisation of GL3. This in turn results in a decrease in cytoplasmic concentration of TTG1 in this cell, thereafter called trichome initiation cell (TIC). Therefore the cytoplasmic TTG1 concentration in the TIC is lower than in the neighbouring cells. Because TTG1 is mobile it will diffuse from the surrounding cells into the TIC. This will lead to a reduced concentration of TTG1 in the neighbour cells, which makes it difficult for those cells to adopt TIC fate themselves. At the same time the concentration of TTG1 in the existing TIC is increasing and leads there to a stabilisation of the trichome cell fate. A schematic description of this process is given in Fig. 22.

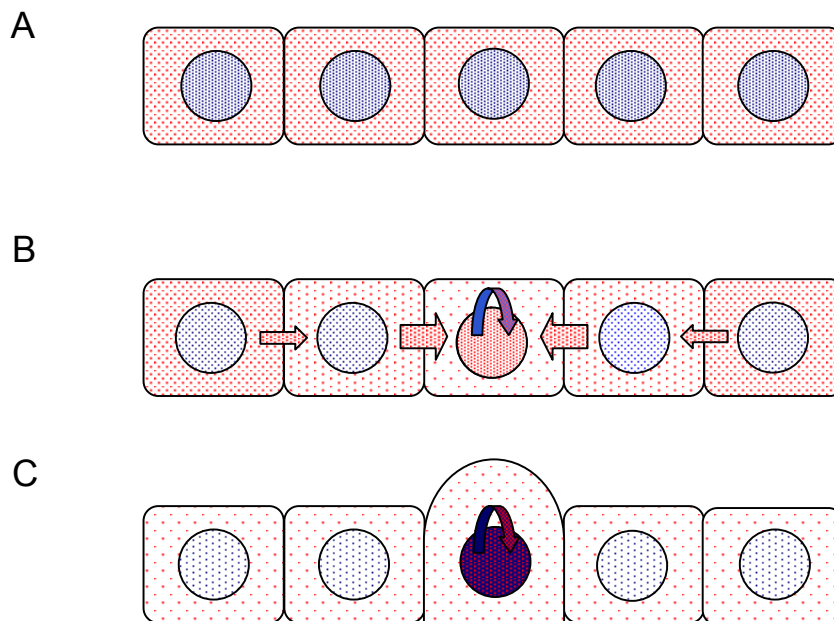


**Figure 22: Model to explain the early steps in pattern formation.** TTG1 is shown in red and GL3 is shown in blue. (A) Initially both components are equally distributed among all cells. The GL3 is found in the nucleus, whereas TTG is also found in the nucleus and the cytosol. (B) Due to a minute increase of GL3 TTG1 follows, because of the strong interaction, into the nucleus and acts there in the autocatalytic feedback loop. Because of the mobility of TTG1 it will be depleted in the cytoplasm of this cell and from the surrounding cells. (C) This will lead to a stabilisation of the autocatalytic feedback loop and at the same time mediates a lateral inhibition because the concentration of TTG1 in the surrounding cells is decreasing, which prevents the generation of a new trichome there.

This mechanism will also lead to a lateral inhibition as observed in the activator-inhibitor system. In both cases cells are competing to acquire a certain cell fate. However the activator-substance system is not based on a direct production of an inhibitor, but on the depletion of a substance needed for the autocatalytic process. In fact it has been shown that this kind of depletion mechanism can be regarded as a special case of the lateral inhibition mechanism, but was assumed unlikely to take place in biological systems (Koch & Meinhardt 1994, Meinhardt & Gierer 2000).

Which results account for this mechanism?

First *TTG1* is expressed throughout the patterning zone. In contrast to the other components of the patterning system *TTG1*-expression is not increasing in developing trichomes, however judged by the TTG1-YFP signal, the concentration of TTG1 in trichome-nuclei is higher than in the non-trichome cells.

Second TTG1 is required for the formation of trichomes in the WT, but it can be bypassed if other activators are overexpressed or the inhibitor-activity is decreased. Therefore it bears the criteria of a substance that is involved in the autocatalytic feedback loop, but is itself not strictly necessary for the promotion of trichome cell fate.

Third TTG1 acts non-cell-autonomous BUT acts as a positive regulator in the trichome patterning system. According to the activator-inhibitor model the activator should at least be less mobile than the inhibitor. However TTG1 seems to act non-cell-autonomous over a range of several cells, which would not be expected for the activator in the activator-inhibitor system.

Fourth TTG1 and GL3 strongly interact and GL3 seems to be responsible for the nuclear localisation of TTG1. This may account for a very simple mechanism of TTG1 depletion in the cytoplasm if the concentration of GL3 is slightly increasing. GL3 encodes for a transcription factor, is nuclear localised and is a limiting factor in the trichome formation (Payne *et al.* 2000, Zhang *et al.* 2003).

Fifth TTG1-YFP is predominantly detected in trichomes if expressed from the subepidermis, which could be explained by a depletion mechanism. This means the higher concentration of GL3 in trichomes (Zhang *et al.* 2003) would lead to a stronger attraction of TTG1-YFP than in the other epidermal cells.

Sixth if the inhibitors TRY and CPC are taken away in the trichome patterning system this leads to a successive outgrowth of trichome cells forming large clusters of trichome cells, but not to a

simultaneous outgrowth of trichome cells at the same time (Schellmann *et al.* 2002). Therefore the basic pattern is already established before the action of TRY and CPC, which is reflected by the ordered pattern of the large clusters in the *try cpc* double mutant on the leaf surface (see for example Fig. 13A). This indicates that the activator-inhibitor mechanism, involving TRY and CPC as inhibitors, does not account for the primary pattern process.

Seventh if the mobility of TTG1 is impaired this leads to a disturbed pattern formation. This is reflected by the formation of trichome clusters, which would be a consequence if the depletion of TTG1 from the cells surrounding a trichome-initiation cell is less effective. This would result in higher concentrations of TTG1 in the cells and thus allow the promotion of trichome cell fate.

Eighth if the mobility of TTG1 is completely blocked, this results in the formation of many trichome-initiation sites (TIS) and a high frequency of cluster formation. However most of these TISs do not grow out of the leaf surface, meaning that they do not acquire a complete trichome cell fate. This could also be explained by the depletion mechanism. If TTG1 is immobile several cells will still bear a higher concentration of TTG1 because TTG1 will not diffuse out of the cell, which would explain the higher number of TISs. At the same time this also prevents that the concentration of TTG1 in a TIS is increasing to fuel the autocatalytic process, which would lead to the outgrowth of a trichome. Moreover this effect is dependent on GL3 indicating that GL3 acts together with TTG1 in the autocatalytic process.

Ninth if immobile TTG1 and mobile TTG1 act together this leads to an extreme overproduction of trichomes. In this case, the immobile TTG1 prevents a depletion of its own concentration in a certain cell and in addition the mobility of the endogenous TTG1 can trigger the autocatalytic feedback-loop.

Taken together I think there are several arguments that account for a depletion mechanism of TTG1. This mechanism allows a very simple generation of a stable spacing pattern of the trichomes. In a second step the activator-inhibitor system would further stabilise this prepattern.

**B 3.8. Outlook**

An interesting aspect in the non-cell-autonomous action of TTG1 is the putative specificity of movement. Conversely, for example AN11 seem to act in a cell-autonomous manner in *Petunia* (A. Walker, unpublished results). If AN11 would function in a cell-autonomous way in *Arabidopsis* this may serve as an excellent tool to analyse the features of protein transport. Another ortholog of *TTG1*, *PFWD*, has been shown to induce ectopic trichomes when overexpressed in *Arabidopsis* (Sompornpailin *et al.* 2002). Because the ectopic expression of *TTG1* does not result in an overproduction of trichomes both proteins have to differ in their function or activity and it is tempting to speculate that it might be their ability to move. This would allow the elucidation of domains of the proteins that are either responsible for mobility or for non-mobility.

## MATERIAL AND METHODS

### MATERIAL

#### Chemicals, antibiotics

All used chemicals and antibiotics in analytical quality have been used from Sigma (Deisenhofen), Roth (Karlsruhe) and Appligene (Heidelberg).

#### Enzymes and molecularbiological materials

Restriction enzymes were used from MBI-fermentas (St.Leon-Rot), New England Biolabs (Frankfurt/Main) and Roche (Mannheim). Primers were generated by ARK Scientific and Invitrogen (Karlsruhe).

#### Cloning vectors

The following vectors were used in this work:

pBluescript KS (pBS) (stratagene) for standard clonings and PCR-product clonings (see above)

pGEM-T easy (Promega) for PCR-product clonings

pEN1a vector (Invitrogen) was used as a donor in gateway based clonings

pAM-PAT-GW as a binary gateway target vector containing a CaMV 35S promoter cassette and BASTA resistance (GenBank accession AY027531)

pBA005 binary vector containing a CaMV 35S promoter cassette and BASTA resistance (Kost *et al.* 1998)

pGTV-hpt, binary vector containing a hygromycin resistance

pCAMBIApGL2 containing a GL2 promoter cassette and a hygromycin resistance (created by Jaideep Mathur)

pBIN19 containing the GLABRA2 promoter and kanamycin resistance (Szymanski *et al.* 1998b)

### **Bacterial strains**

For standard clonings the *Escherichia coli* strains DH5 $\alpha$  and XL1blue were used. For gateway cloning of destination vectors the DB3.1 strains were used which are resistant to the *ccdB* gene. For plant transformation *Agrobacterium tumefaciens* strains GV3101 were used. The gateway cloning required the usage of a modified strain of GV3101, pMP90RK.

### **Plant lines**

In this study Landsberg *erecta* (*Ler*), *Colombia* (*Col*), *Wassilewskaja* (*WS-O*) and *RLD* ecotypes were used. The mutant alleles of *sti* are in *Ler* background (Hülkamp *et al.* 1994). The *cpr5-T1* is in *WS-O* background (Kirik *et al.* 2001). *ttg1-1* is in *Ler* (Koorneef 1981), *ttg1-9* and *ttg1-10* in *Col* (Larkin *et al.* 1999), *ttg1-13* in *RLD* (Walker *et al.* 1999). *gl1-1*, *gl3-1* and *try* mutant are in *Ler* (Oppenheimer *et al.* 1991, Hülkamp *et al.* 1994). The *cpc* mutant is a T-DNA insertion line in *WS-O* (Wada *et al.* 1997). The *etc1* and *etc2* mutants are both T-DNA insertion lines in *Col* (Kirik *et al.* 2004a, 2004b).

## **METHODS**

### **RNA isolation**

Young rosette plants with four to five leaves were used. Plants were homogenised with a mortar and pestle under constant addition of liquid nitrogen and the powder transferred into a 2-ml-tube. 250  $\mu$ l extraction buffer (1M Tris/HCl pH 7.4, 1% SDS, 5mM EDTA) was added and directly mixed with 500  $\mu$ l PCI (Phenol-chloroform/isoamyl alcohol, 24+1) and immediately mixed. After centrifugation at 13 krpm the aqueous (=upper) phase carefully transferred into a new 1.5-ml-tube and again immediately mixed with 500  $\mu$ l PI and thoroughly vortexed. After centrifugation (5 min. 13 krpm) the upper phase was transferred into a new 1.5-ml-tube and mixed with Chloroform (Cl) and again centrifuged (5 min. 13 krpm). This step was repeated for one time. The resulting aqueous phase was transferred into a new 2-ml-tube and 50  $\mu$ l sodium-acetate and 1500  $\mu$ l 100% EtOH added, carefully mixed and incubated for at least one hour at  $-70^{\circ}\text{C}$ . In this step the RNA (and DNA) will precipitate and can be pelleted by centrifugation (10 min, 13 krpm,  $4^{\circ}\text{C}$ ). After careful removing the supernatant the pellet was dried and resolved

afterwards in 200 µl DEPC-treated H<sub>2</sub>O, mixed with 200 µl 4M LiCl and incubated over night at 4°C. During this step the RNA will be specifically precipitated. After centrifugation (15 min. 13 krpm, 4°C) the pellet is washed with 1 ml 2 M LiCl solution and again centrifuged (10 min. 13 krpm, 4°C). The supernatant was carefully removed and the pellet rinsed with 70% EtOH. After centrifugation the pellet was dried and resolved in 50 µl H<sub>2</sub>O.

### **Reverse transcription**

Prior to reverse transcription residues of genomic DNA were removed using the DNA-free kit from Ambion (Ambion AMS biotechnology) was used according to the manufacturer's manual. Reverse transcription of isolated RNA was performed using the SUPERScript II RNase H<sup>+</sup> Reverse Transcriptase kit from GibcoBRL (Life Technologies/GibcoBRL, Cleveland USA) according to the manufacturer's manual.

After reverse transcription residual RNA was removed by adding 5 units of RNase H (MBI-Fermentas) and incubated for 30 minutes at 37°C.

### **Semiquantitative RT-PCR**

The expression levels of STI-overexpressing plants were estimated by semiquantitative RT-PCR analysis. RT-PCR was carried out with Titan One tube RT-PCR mix (Roche Diagnostics, Indianapolis, USA). The primer pair SNT-70-forward (5'-CGA CGG TAT CGA TAA GCT TG-3') and SNT-70-reverse (5'-ACA CCT AAA ACC ACC GAA G-3') was designed to only amplify the 35S:STI transcript. No transcript was detected in wild-type plants after 35 cycles.

### **Genomic DNA preparation**

For PCR analysis CTAB-preparation of genomic DNA was performed (Rogers & Bendich 1988). For southern blotting the following protocol was used. One gram of plant material (around 10 six week old rosettes) was grinded with mortar and pestil and continuous addition of liquid nitrogen. To the homogenised powder 4ml of extraction buffer (2%(w/v) CTAB, 1.4M NaCl, 20mM EDTA, 100mM Tris/HCl pH 8.0, 0.2% β-mercaptoethanole) was added and incubated at 65°C for 30 minutes. After addition of 4ml Chloroforme/Isoamylalcohol (24:1) and careful shaking, the probes were centrifuged for 15 minutes at 4000 rpm. The aqueous phase was

transferred into a new tube and mixed with 3 ml isopropanol and centrifuged for 15 min. at 4000 rpm. The upper was again transferred into a new tube and mixed with 3 ml Isopropanol and the precipitate gained by centrifugation for 20 min. at 4000 rpm. The supernatant was removed and the pellet rinsed with 70% EtOH with 10 mM ammonium acetate. After centrifugation and rejection of the supernatant the pellet was dried and afterwards resolved in 250  $\mu$ l H<sub>2</sub>O and transferred into a 1.5 ml tube. After addition of 5  $\mu$ l RNase (10 mg/ml) for 30 min at RT, the solution was mixed again with 150  $\mu$ l Phenol/Chloroform. The mixture was centrifuged (16000 rpm, 5 min.) and the upper phase transferred into a new 1.5-ml-tube and mixed with Chloroform. After centrifugation (2 min. 16 krpm) the upper phase was transferred into a new 1.5-ml-tube and mixed with 1/10 vol. Na-acetate and 1 vol. Ethanol and incubated at 4°C for at least 15 min. . After centrifugation the pellet was rinsed with 70% EtOH and again centrifuged. The supernatant was removed and the pellet was dried and resolved in Tris/HCl pH 8.0 over night at 4°C.

### **Plasmid DNA preparation from bacteria**

Plasmid preparation was performed using a column pEQ-LAB Plasmid Miniprep KitI (PEQLAB Biotechnology GmbH, Erlangen) according to the manufacturers protocol. Plasmid DNA from *Agrobacteria* was isolated using Qiagen plasmid miniprep kit

### **DNA-manipulation**

DNA manipulation and cloning were carried out according to Sambrook and Russel (2001) or Ausubel *et al.* (1994), using standard procedures. All polymerase-chain reaction (PCR)-amplified fragments were sequenced prior to further investigation. Sequencing was carried out on an ABI 310 Prism (Perkin-Elmer Applied Biosystems, Foster City, CA) sequencing equipment according to the manufacturer's instructions. Sequencing reactions were performed using Big-Dye kit 1.1 (Perkin Elmer Applied Biosystems, Foster City, CA). PCR-Primers and constructs were designed using the VectorNTI-suite 7.1 software (InforMax, Paisley PA4 9RF United Kingdom).

### **Cloning of the STI cDNA**

Primers for amplification and sequencing of gene candidates were also created based on the sequence information provided by TIGR. The *STI*-transcribed sequence was amplified using the 5'-TGAAAACGCGAAGCTGAGAGAG-3' and 5'-CGAACAGGAGTTCCCTTG-3' primer pair from cDNA obtained by oligo(dT)-primed RT of RNA isolated from rosettes with four to five leaves. The 3' end was obtained using the oligo(dT) primer and the gene-specific nested primers 5'-CTGATAAAGACACACCTGGATCG-3' and 5'-ATCGCCAAACTAACGTAGC-3'. 5'-RACE PCR was performed with the 5'-RACE System for Rapid Amplification of cDNA Ends, version 2.0 (Life Technologies/Gibco-BRL, Cleveland) according to the manufacturer's instructions using the specific nested primers 5'-CATTAACACTAGCTTGCGTCCAC-3' and 5'-CTCTTCTTCTTACCATTCTTAG-3'. It yielded no products related to the *STI* gene. The sequence of the 5' region, including 120 bp of upstream untranslated sequence, was obtained using the 5'-TTGCACAGGTTTTGAAATGTCAG-3' and 5'-CTCTTCTTCTTACCATTCTTAG-3' primer pair.

### **Constructs**

#### CPR5-rescue construct

The BAC-clone MXK3 (Accession number: AB019236) was digested with BamHI and the resulting 6340-bp BamHI fragment containing 3.407 bp 5' and 500 bp 3' of the gene was subcloned into pBS into the BamHI site. To generate the rescue construct the BamHI fragment was again BamHI digested and ligated into the same site in pGTV-hpt binary vector.

#### 35S::STI & 35S::GFPSTI

*STI*-cDNA was PCR-amplified from +1 till +1871 using the already subcloned *STI*-cDNA in *STI*-pBS to generate a 5' *NaeI* site (5'-GAAGAAGCCGGCAAAATGTCAGGTTTCGAG-3', 5'-CGCACCTTGACTGAATGGTC-3') that is found in the 3' in frame of the *GFP*-sequence in pBA005 vector (Kost *et al.* 1998). This PCR product was subcloned in pBluescript, leading to *STI*73pBS. Correct clones were digested with *PstI* and *SacI* and the 3' part of *STI* from *STI*-pBS was ligated to it using the same REs, thereby making use of the entire *PstI* site at position +1782. PBA005 was digested using *XhoI* and *SacI* restriction enzymes and ligated into the same sites of pBS, thereby generating GFP-talin-pBS. GFP-talin-pBS was digested with *SacI* and partially with *NaeI*, the right band was isolated and ligated with *STI*73pBS-digested with the same REs.

Positive clones were sequenced to confirm the accuracy of the fusion using 5'RAC2-3 antisense *STI*-primer (5'-TCTTCTTCCTTACCATTCTTAG-3').

#### pTTG1::GUS & pTTG1-pAM-PAT

The *TTG1* promoter was isolated from *Arabidopsis thaliana* ecotype landsberg *erecta* (*ler*) with polymerase chain reaction (PCR)-amplification from genomic DNA (gDNA) using Hifi-Polymerase kit from Roche (REF) starting at position –2227 till –1 bp from the START-codon of the *TTG1*-ORF including the 110 nucleotides of the 5'UTR of the corresponding cDNA (FWD: 5'-AAAGCTTAACCGAGAATGTCTCCCGACTTCTAT-3'; REV: AGTCGACTCAAACTCTAAGGAGCTGCATTTG-3') and subcloned into pGEM-T vector, thereby generating pTTG-pGEM. To the 5' of the PCR-product was added an *AscI* site by ligating an oligo-linker into the *SpeI* site of the vector multiple cloning site (oligo: 5'-CTAGA | ATGGCGCGCCAT | T-3'). To generate the pTTG:  $\beta$ -*Glucuronidase*(GUS) construct the TTG-pGEM was digested with *AscI* and *SalI* and ligated into the binary gateway vector pAM-PAT-GW-GUS (pAM gene bank accession AY02531) by exchanging the existing 35S-promoter into the *AscI* and *XhoI* sites. The same procedure was performed to create pTTG-pAMPAT including the gateway recombination cassette flanked by the *attR1* and *attR2* sequences and containing the *ccdB* gene and a chloramphenicol resistance (INVITROGENE).

#### pPCAL::GFP5 & pPCAL-pAM-PAT

The pPCAL:GFP5 was created by exchanging the *HindIII* – *XbaI*<sup>blunted</sup> 35S-promoter-fragment of the mGFP5-ER vector (created by Arp Schnittger) with a *HindIII* – *SmaI* fragment of ppcA-L-Ft 5' pBS (Stockhaus *et al.* 1994). To create the pPCAL-pAMPAT binary vector the 2117 bp fragment included in the pPCAL-pBS was digested 5' with *HindIII* and ligated together with an oligonucleotide-linker to generate an *AscI* restriction site. Thereafter the *AscI* – *XhoI*-fragment was inserted into pAM-PAT using the same REs.

#### pGL2::NLS-GFP-GUS

The pGL2::NLS-GFP-GUS construct was created by digesting pBGF-O (pBGF-O was a gift from David Galbraight and contains a stuffer-nuclear localisation signal (NLS) from *Nicotiana tabacum* fused in front of a green fluorescing protein (GFP) and a beta-glucuronidase (GUS) gene; a detailed description of the GFP-GUS reporter has been published by Quaedvlieg *et al.* 1998) with *SmaI* and *BamHI* and inserting a *HindIII*<sup>blunted</sup>-*BamHI*pGL2 promoter fragment from pGL2pUC118 (Szymanski *et al.* 1998b).

The used *TRY:GUS* and *GLI:GUS* (pGGE4) lines have been described previously (Schellmann *et al.* 2002, Larkin *et al.* 1993).

#### NLS-TTG1-GFP-GUS (TTG1<sup>im</sup>)

To create the NLS-TTG1-GFP-GUS-fusions *TTG1pUC18* (Schellmann *et al.* 2002) was PCR-amplified using *Pfu*-polymerase to add *SalI* 5' (5'-AGTCGACAATGGATAATTCAGCTCCAG A-3') and *XhoI* 3' and delete the STOP-codon (5'-ACTCGAGACTCTAAGGAGCTGCATTTT-3') and subcloned into *SmaI*-site of pBluescript (pBS). Correct clones were digested with *SalI* and *XhoI* and ligated to the *SalI* site in pGL2::NLS-GFP-GUS thereby creating pGL2:TTG<sup>im</sup>. This fusion was excised with *XbaI* and *SpeI*, including the Cauliflower mosaic virus-terminator (CaMV-pA) and ligated to the *XbaI* site of pBS to create TTG<sup>im</sup>pBS. From there an *XbaI* – *SpeI* fragment was afterwards brought into the *XbaI* site of pENTRY1a (pEN) vector to enable gateway recombination with pTTG-pAMPAT and pPCAL-pAMPAT.

#### NLS-TTG1

To create the *NLS-TTG1* fusion *TTG1pUC18* was again *Pfu*-PCR-amplified with the same forward-primer that was used to build TTG1<sup>im</sup>, the reverse primer contains a *SacI* site and keeps the STOP codon (5'-AGAGCTCTGCACCTCACACTCTAAGGA-3'). After subcloning into pBS using the *SmaI* restriction site a *SalI* NLS-fragment from TTG1<sup>im</sup>pBS was ligated into the corresponding site to generate NLS-TTG1pBS. To obtain pGL2::NLS-TTG1 an *XhoI-SacI*-fragment from NLS-TTG1pBS was introduced in-between *SalI* and *SacI* of pGL2pCAMBIA, which was a gift from Jaideep Mathur.

#### TTG1-YFP & GFP-TTG1

To create the *TTG1-YFP* fusion an *NcoI-NotI*-fragment from pEYFP vector (Clontech) was replacing the TTG<sup>im</sup> in TTG<sup>im</sup>pBS thereby leading to eYFPpBS. This was done to include more in-frame 5'-REs in front of the AUG-start codon of eYFP. TTG1pUC18 was again PCR-amplified to add *SalI* 5' and *XhoI* 3' of the CDS thereby deleting the internal STOP-codon (fwd-primer: 5'-AGTCGACATGGATAATTCAGCTCCAGA-3', rev-primer: 5'-ACTCGACAACCTC TAAGGAGCTGCATTT-3') and ligated into the *SalI* site of pUC18 where in turn an *XbaI-SacI* eYFP-fragment from eYFPpBS was fused C-terminally to TTG1 using the same sites thereby creating TTG1-YFPpBS. The fusion was digested using *XhoI* and *EcoRI* and ligated into pEN1a *SalI-EcoRI* thereby replacing the *ccdB*-gene and leading to TTG1YFPpEN. To create 35S-, pTTG-, pPCAL- TTG1-YFPpAMPAT, TTG1YFPpEN was recombined with pAM-PAT, pTTG-

pAMPAT, pPCAL-pAMPAT respectively, following manufacturer's manual (INVITROGEN). The *TTG1* was PCR-amplified

#### NLS-TTG1-YFP

Digesting TTG1<sup>im</sup>pBS with SmaI and HindIII and ligating the thereby received fragment between XmnI and HindIII of TTG1YFPpEN established the NLS-TTG1-YFP fusion (NLS-TTG-YFPpEN). Gateway recombination was performed to get the 35S-, pPCAL-, and pTTG1-NLS-TTG1-YFP constructs.

The pPCAL-, pTTG-, pGL2- and 35S- TTG were created by PCR-amplification of TTG1pUC18 thereby adding the corresponding recombination-sites for direct recombination into pEN1a, which in turn is recombined with the corresponding binary gateway vectors.

#### GL3-constructs

The same was performed to obtain 35S:GL3 and pPCAL:GL3. To obtain pGL2::GL3 GL3pUC (Schellmann *et al.* 2002) was digested with *SaI* and ligated into the same site in pGL2pCAMBIA.

#### CRE-LOX-constructs

The vector backbone of the TTG1-*LoxP* construct, pCGNlox2b, was described in Sieburth *et al.* (1998). Arp Schnittger generated the 35S:TTG-NOSpA cassette. The corresponding heat-shock inducible *CRE*- line, a pCGNHCHN transformant, was crossed to the *ttg1-13* mutant line and homozygous for both, KAN-resistance and mutant phenotype isolated and crossed to TTG1-Lox lines.

### **Plant growth conditions**

Seeds were sown on humid freshly prepared *Arabidopsis* culture soil, covered with a plastic lid and stored for three to seven days at 4°C. Plants were grown at constant 16h light and 8h dark condition at constant temperatures at either 18°C or 23°C and the lid was removed after three to four days.

### **Crossing of plants**

Using fine-tweezers the anthers of flowers at a stage when the petals grew out of the sepals were removed. All remaining older and younger flowers were removed and the prepared flower was fixed on a wooden stick. After one to three days the stigma of the carpels were pollinated.

### **Plant transformation**

Plants were transformed according to the “floral dip” method (Clough & Bent 1998). To gain strong plants, these were allowed to grow at 18°C and till the first flowers appeared at stalks of approximately 10 cm in length. Four days before plant transformation a 5 ml preculture in YEB-medium of the Agrobacterial clone was incubated for two days at 29°C and 1 ml of this preculture was used to inoculate the final 200 ml culture. This culture was incubated again for two days at 29°C and afterwards precipitated at 5800 rpm for 12 minutes. The pellet was resuspended in a 5% Sucrose solution containing 0.05% Silwett L-77. Plants were dipped for approximately 20 seconds and afterwards covered with a lid. The lid was removed after two days and after that plants were treated as usual.

### **Seed sterilisation**

Before placing seeds on MS-agar-plates (1% Murashige-Skoog salts, 1% sucrose, 0.7% agar-agar, pH5.7, eventually with kanamycin (50µg/ml) or hygromycin (25µg/ml)) they were incubated for five minutes in 95% Ethanol (Rotisol) and afterwards incubated for 15 minutes in a 3% NaClO<sub>3</sub> solution containing 0.1% triton X-100. Afterwards seeds were washed two times with 0.01% Triton-X100 solution and than plated.

### **Heat-shock treatment**

To induce the CRE site-specific recombinase plants were prior to induction grown on MS-agar plates (see above) for approximately 8 days at 18°C under 16h light / 8h dark condition. Heat-shock was performed by putting the plates into an illuminated incubator at 41°C for ten minutes till up to two hours and afterwards immediately transferred back to the 18°C growth chamber.

### **Histochemistry**

GUS-activity was assayed according to Sessions & Yanofsky (1999). To allow complete penetration of X-Gluc-solution plants were vacuum infiltrated in staining buffer (0.2% Triton X-100, 50mM NaPO<sub>4</sub> (pH 7.2), 2mM potassium-ferrocyanide (K<sub>4</sub>Fe(CN)<sub>6</sub>\*H<sub>2</sub>O), 2mM potassium-ferricyanide (K<sub>3</sub>Fe(CN)<sub>6</sub>) containing 2mM X-Gluc (Roth) for approximately 15 minutes and

afterwards incubated at 37°C over night, in some cases for up to two days. Clearing was performed in 70% Ethanol solution at 37°C over night.

### **Fluoresceine diacetate- & propidium iodide staining**

To discriminate between living and dead cells in the *cpr5* analyses, tissue was stained either with fluoresceine diacetate (FDA) to detect living cells, or with propidium iodide (PI) that stains dead cells. This is possible because FDA –fluorescence is dependent on ATP. PI is diffusing into cells if the integrity of the cell membrane is lost and can be detected in the nucleus because PI interacts with DNA.

In both cases plant material was incubated for 5 minutes in H<sub>2</sub>O containing 100 µg/ml PI- and FDA, respectively. Afterwards the samples where washed with H<sub>2</sub>O and mounted on a slide and analysed under the microscope with UV excitation.

### **Microscopy**

Light and epifluorescence microscopy was performed using a LEICA-DMRE microscope using DIC optics (LEICA). Images were taken using a high resolution KY-F70 3-CCD JVC camera and a frame grabbing DISKUS software (DISKUS, Technisches Büro, Königswinter).

Confocal laser scanning microscopy (CLSM) was done with a Leica TCS-SP2 confocal microscope together with the Leica-software (Leica Microsystems, Heidelberg). Sections in steps of 1 or 2 µm were taken and eventually integrated by Leica Confocal Software Lite 2.05 (LCS, Leica Microsystems, Heidelberg).

For fluorescence microscopy plants were embedded with tab water and covered with a cover-slide. Transversal sections were carried out with plants embedded in 4% low-melting agarose and hand sectioned using a razor blade as described by Kim *et al.* (2003).

Images were assembled and processed using Adobe Photoshop 6.0 and Microsoft Power-Point software.

### **DNA-measurement**

Trichome nuclei were measured as described previously (Schnittger *et al.* 1998). 10 days old plants were fixed in 4% Paraformaldehyde in PBST-buffer and vacuum-infiltrated for

approximately 15 minutes and afterwards incubated at 4°C over night. Afterwards samples were washed with PBST and then incubated in a DAPI solution (10µg/ml) solved in PBST, containing 5% DMSO at 4°C over night. Samples were washed the next day two times with PBST and afterwards mounted in a 50% Glycerine solution and the samples and the slides were sealed with wet gloss. DNA-fluorescence measurement was performed as described in Hülkamp *et al.* 1994.

## REFERENCES

- Aeschbacher R, Schiefelbein JW, Benfey PN** (1994): The genetic and molecular basis of root development. *Annu Rev Plant Physiol Plant Mol Biol* **45**, 25–45
- Altschul SF, Gish W, Miller W, Myers EW, Lipman DJ** (1990) Basic local alignment search tool. *J Mol Biol* **215**: 403–410
- Ausubel F, Brent R, Kingston R, Moore D, Seidman J, Smith J, Struhl K** (1994): *Current Protocols in Molecular Biology*
- Bateman A, Birney E, Durbin R, Eddy SR, Finn RD, Sonnhammer EL** (1999) Pfam 3.1: 1313 multiple alignments match the majority of proteins. *Nucleic Acids Res* **27**, 260–262
- Bertram JG, Bloom LB, Turner J, O'Donnell M, Beechem JM, Goodman MF** (1998) Pre-steady state analysis of the assembly of wild type and mutant circular clamps of *Escherichia coli* DNA polymerase III onto DNA. *J Biol Chem* **273**, 24564–24574
- Bowling SA, Clarke JD, Liu Y, Klessig DF, Dong X** (1997): The cpr5 mutant of *Arabidopsis* expresses both NPR1-dependent and NPR1-independent resistance. *Plant Cell* **9**, 1573–1584
- Bowser J, Reddy ASN** (1997): Localisation of a kinesin-like calmodulin-binding protein in dividing cells of *Arabidopsis* and tobacco. *Plant J* **12**, 1429–1438
- Brown MS, Ye J, Rawson RB, Goldstein JL** (2000): Regulated intramembrane proteolysis: a control mechanism conserve from bacteria to humans. *Cell* **100**, 391–398
- Burk DH, Liu B, Zhong R, Morrison WH, Ye ZH** (2001) A katanin-like protein regulates normal cell wall biosynthesis and cell elongation. *Plant Cell* **13**: 807–827
- Berger F, Linstead P, Dolan L, Haseloff J** (1998): Stomata patterning on the hypocotyl of *Arabidopsis thaliana* is controlled by genes involved in the control of root epidermis patterning. *Dev Biol* **194**, 226–234
- Camilleri C, Azimzadeh J, Pastuglia M, Bellini C, Grandjean O, Bouchez D** (2002): The Arabidopsis TONNEAU2 gene encodes a putative novel protein phosphatase 2A regulatory subunit essential for the control of the cortical cytoskeleton. *Plant Cell* **14**, 833–845
- Carey CC, Strahle JT, Selinger DA, Chandler VL** (2004): Mutations in *pale aleurone color1* regulatory gene of the *Zea mays* anthocyanin pathway have distinct phenotypes relative to the functionally similar *TRANSPARENT TESTA GLABRA1* gene in *Arabidopsis thaliana*. *Plant Cell*
- Chen M, Pan Z-Q, Hurwitz J** (1992a) Sequence and expression in *Escherichia coli* of the 40-kDa subunit of activator 1 (replication factor C) of HeLa cells. *Proc Natl Acad Sci USA* **89**, 2516–2520
- Chen M, Pan Z-Q, Hurwitz J** (1992b) Studies of the cloned 37-kDa subunit of activator 1 (replication factor C) of HeLa cells. *Proc Natl Acad Sci USA* **89**, 5211–5215
- Chytilova E, Macas J, Galbraith DW** (1999): Green fluorescent protein targeted to the nucleus, a transgenic phenotype useful for studies in plant biology. *Annals of Botany* **83**, 645–654
- Clough SJ, Bent AF** (1998): Floral dip: a simplified method for agrobacterium-mediated transformation of *Arabidopsis thaliana*. *Plant J* **16**, 735–743
- Crawford KM, Zambryski PC** (2000): Subcellular localization determines the availability of non-targeted proteins to plasmodesmatal transport. *Curr Biol* **10**, 1032–1040

- Crawford KM, Zambryski PC** (2001): Non-targeted and targeted protein movement through plasmodesmata in leaves in different developmental and physiological states. *Plant Physiol* **125**, 1802-1812
- de Vetten N, Quattrocchio F, Mol J, Koes R** (1997): The *an11* locus controlling flower pigmentation in petunia encodes a novel WD-repeat protein conserved in yeast, plants, and animals. *Genes Dev* **11**, 1422-1434
- Dietrich RA, Delaney TP, Uknes SJ, Ward ER, Ryals JA, Dangi JL** (1994): *Arabidopsis* mutants simulating disease resistance response. *Cell* **77**, 565-577
- Deom CM, Oliver MJ, Beachy RN** (1987): The 30-kilodalton gene product of tobacco mosaic virus potentiates virus movement. *Science* **237**, 389-394
- Downes BP, Stupar RM, Gingerich DJ, Vierstra RD** (2003) The HECT ubiquitin-protein ligase (UPL) family in *Arabidopsis*: UPL3 has a specific role in trichome development. *Plant J* **35**, 729-742
- El Refy A, Perazza D, Zekraoui L, Valay JG, Bechtold N, Brown S, Hülskamp M, Herzog M, Bonneville JM** (2003): The *Arabidopsis* *KAKTUS* gene encodes a HECT protein and controls the number of endoreduplication cycles. *Mol Genet Genomics* **270**, 403-414
- Esch JJ, Chen M, Sanders M, Hillestad M, Ndkium S, Idelkope B, Neizer J, Marks MD** (2003): A contradictory *GLABRA3* allele helps define interactions controlling trichome development in *Arabidopsis*. *Development* **130**, 5885-5894
- Fletcher JC, Brand U, Running MP, Simon R, Meyerowitz E** (1999): Signaling of cell fate decisions by *CLAVATA3* in *Arabidopsis* shoot meristems. *Science* **283**, 1911-1014
- Folkers U, Berger J, Hülskamp M** (1997): Cell morphogenesis of trichomes in *Arabidopsis*: differential control of primary and secondary branching by branch initiation regulators and cell growth. *Development* **124**, 3779-3786
- Folkers U, Kirik V, Schöbinger U, Falk S, Krishnakumar S, Pollock MA, Oppenheimer DG, Day I, Reddy AR, Jürgens G, Hülskamp M** (2002): The cell morphogenesis gene *ANGUSTIFOLIA* encodes a CtBP/BARS-like protein and is involved in the control of the microtubule cytoskeleton. *EMBO J* **21**, 1280-1288
- Galway ME, Heckman J, Schiefelbein JW** (1997) Growth and ultrastructure of *Arabidopsis* root hairs: the *rhd3* mutation alters vacuole enlargement and tip growth. *Planta* **201**, 209-218
- Ghoshroy S, Citovsky V** (1997): Transport of proteins and nucleic acids through plasmodesmata. *Ann Rev Plant Physiol Plant Mol Biol* **48**, 27-50
- Greenberg JT, Guo A, Klessig DF, Ausubel FM** (1994): Programmed cell death in plants: a pathogen-triggered response activated coordinately with multiple defense functions. *Cell* **77**, 551-563
- Heinlein M** (2002): Plasmodesmata: dynamic regulation and role in macromolecular cell-to-cell signaling. *Curr Opin Plant Biol* **5**, 543-552
- Hoppe T, Rape M, Jentsch S** (2001): Membrane-bound transcription factors: regulated release by RIP and RUP. *Curr Opin Cell Biol* **13**, 344-348
- Hülskamp M, Misera S, Jürgens G** (1994): Genetic dissection of trichome cell development in *Arabidopsis*. *Cell* **76**, 555-566
- Hülskamp M, Folkers U, Grini P** (1998) Cell morphogenesis in *Arabidopsis*. *BioEssays* **20**, 20-29
- Hülskamp M, Schnittger A, Folkers U** (1999): Pattern formation and cell differentiation: Trichomes in *Arabidopsis* as a genetic model system. *Intern Rev Cytol* **186**, 147-178

- Hunt M, Delaney TP, Dietrich RA, Weymann KB, Dangi JL, Ryals JA** (1997): Salicylate-independent lesion formation in *Arabidopsis lsd* mutants. *Mol Plant Microbe Interact* **10**, 531-536
- Ilgenfritz H, Bouyer D, Schnittger A, Mathur J, Kirik V, Schwab B, Chua NH, Jürgens G, Hülskamp M** (2003): The *Arabidopsis STICHEL* gene is a regulator of trichome branch number and encodes a novel protein. *Plant Physiol* **131**, 643-655.
- Jackson D** (2000): Opening the communication channels: recent insights into plasmodesmal function. *Curr Opin Plant Biol* **3**, 394-399
- Johnson CS, Kovlevski B, Smyth DR** (2002): *TRANSPARENT TESTA GLABRA2*, a trichome and seed coat development gene of *Arabidopsis*, encodes a WRKY transcription factor. *Plant Cell* **14**, 1359-1375
- Kawai-Yamada M, Otori Y, Uchimiya H** (2003): Dissection of *Arabidopsis* Bax inhibitor-1 suppressing Bax-, hydrogen peroxide-, and salicylic acid-induced cell death. *Plant Cell* **16**, 21-32
- Kim GT, Shoda K, Tsuge T, Cho K-H, Uchimiya H, Yokoyama R, Nishitani K, Tsukaya H** (2002): The *ANGUSTIFOLIA* gene of *Arabidopsis*, a plant CtBP gene, regulates leaf-cell expansion, the arrangement of cortical microtubules in leaf cells and expression of a gene involved in cell-wall formation. *EMBO J* **26**: 1267-1279
- Kim J-Y, Yuan Z, Cilia M, Khalfan-Jagani Z, Jackson D** (2002): Intercellular trafficking of a KNOTTED1 green fluorescent protein fusion in the leaf and shoot meristem of *Arabidopsis*. *Proc Natl Acad Sci USA* **99**, 4103-4108
- Kim J-Y, Yuan Z, Jackson D** (2003): Developmental regulation and significance of KNOX protein trafficking in *Arabidopsis*. *Development* **130**, 4351-4362
- Kirik V, Schnittger A, Radchuk V, Adler K, Hülskamp M, Bäuml H** (2001): Ectopic expression of the *Arabidopsis AtMYB23* gene induces differentiation of trichome cells. *Dev Biol* **235**, 366-377
- Kirik V, Bouyer D, Schöbinger U, Bechtold N, Herzog M, Bonneville JM, Hülskamp M** (2001): *CPR5* is involved in cell proliferation and cell death control and encodes a novel transmembrane protein. *Curr Biol* **11**, 1891-1895
- Kirik V, Simon M, Hülskamp M, Schiefelbein J** (2004a): The *ENHANCER OF TRY AND CPC 1* gene acts redundantly with *TRIPTYCHON* and *CAPRICE* in trichome and root hair cell patterning in *Arabidopsis*. *Dev Biol* **268**, 506-513
- Kirik V, Simon M, Schiefelbein J, Hülskamp M** (2004b): *ENHANCER of TRY and CPC 2 (ETC2)* reveals redundancy in the region-specific control of trichome development of *Arabidopsis*. manuscript accepted pending revision in *Plant Mol Biol*
- Kirik V, Lee MM, Wester K, Herrmann U, Schiefelbein J, Hülskamp M** (2004c): Functional diversification of *AtMYB23* and *GLI* in trichome morphogenesis and initiation. Manuscript in preparation
- Koch AJ, Meinhardt H** (1994): Biological pattern formation: from basic mechanism to complex structures. *Reviews of Modern Physics* **66**, 1481-1507
- Koorneef M** (1981): The complex syndrome of *tig* mutants. *Arabid Inf Serv* **18**, 45-51
- Kost B, Spielhofer P, Chua N-H** (1998): A GFP-mouse talin fusion protein labels plant actin filaments in vivo and visualizes the actin cytoskeleton in growing pollen tubes. *Plant J* **16**, 393-401
- Kost B, Mathur J, Chua N-H** (1999): Cytoskeleton in plant development. *Curr Opin Plant Biol* **2**, 462-470
- Larkin JC, Oppenheimer DG, Pollock S, Marks MD** (1993): *Arabidopsis GLABRA1* gene requires downstream sequences for function. *Plant Cell* **5**, 1739-1748

- Larkin JC, Oppenheimer DG, Lloyd A, Papparozzi ET, Marks MD** (1994): The roles of *GLABROUS1* and *TRANSPARENT TESTA GLABRA* genes in *Arabidopsis* trichome development. *Plant Cell* **5**, 1739-1748
- Larkin JC, Young N, Prigge M, Marks MD** (1996): The control of trichome spacing and number in *Arabidopsis*. *Development* **122**, 997-1005
- Larkin JC, Walker JD, Bolognesi-Winfield AC, Grey JC, Walker AR** (1999): Allele-specific interactions between *tig* and *gll* during trichome development in *Arabidopsis thaliana*. *Genetics* **151**, 1591-1604
- Lee J-Y, Yoo B-C, Rojas MR, Gomez-Ospina N, Staehlin LA, Lucas WJ** (2003): Selective trafficking of Non-cell-autonomous proteins mediated by *NtNCAPP1*. *Science* **299**, 392-396
- Lee MM, Schiefelbein J** (2001): Developmentally distinct MYB genes encode functionally equivalent proteins in *Arabidopsis*. *Development* **128**, 1539-1546
- Lee ML, Schiefelbein J** (2002): Cell pattern in the *Arabidopsis* root epidermis determined by lateral inhibition with feedback. *Plant Cell* **14**, 611-618
- Lincoln JE, Craig R, Overduin B, Smith K, Bostock R, Gilchrist DG** (2002): Expression of the antiapoptotic p35 gene in tomato blocks programmed cell death and provides broad-spectrum resistance to disease. *Proc Natl Acad Sci USA* **99**, 15217-15221
- Lloyd AM, Walbot V, Davis RW** (1992): *Arabidopsis* and *Nicotiana* anthocyanin production activated by maize regulators *R* and *C1*. *Science* **258**, 1773-1775
- Lloyd AM, Schena M, Walbot V, Davis RW** (1994): Epidermal cell fate determination in *Arabidopsis*: patterns defined by a steroid-inducible regulator. *Science* **266**, 436-439
- Lucas WJ, Bouche-Pillon S, Jackson DP, Nguyen L, Baker L, Ding B, Hake S** (1995): Selective trafficking of *KNOTTED1* homeodomain protein and its mRNA through plasmodesmata. *Science* **270**, 1980-1983
- Luo D, Oppenheimer DG** (1999): Genetic control of trichome branch number in *Arabidopsis*: the roles of the *FURCA* loci. *Development* **126**, 5547-5557
- Mathur J, Chua NH** (2000): Microtubule stabilization leads to growth reorientation in *Arabidopsis thaliana* trichomes. *Plant Cell* **12**, 465-477
- Mathur J, Spielhofer P, Kost B, Chua N-H** (1999) The actin cytoskeleton is required to elaborate and maintain spatial patterning during trichome cell morphogenesis in *Arabidopsis thaliana*. *Development* **126**, 5559-5568
- Matsubayashi Y, Yang H, Sakagami Y** (2001): Peptide signals and their receptors in higher plants. *Trends Plant Sci* **6**, 573-577.
- McClinton RS, Sung ZR** (1997) Organization of cortical microtubules at the plasma membrane in *Arabidopsis*. *Planta* **201**, 252-260
- Meinhardt H, Gierer A** (1974): Application of a theory of biological pattern formation based on lateral inhibition. *J Cell Sci* **15**, 321-346
- Meinhardt H, Gierer A** (2000): Pattern formation by local self-activation and lateral inhibition. *Bioessays* **22**, 753-760
- Melaragno JE, Mehrotra B, Coleman AW** (1993): Relationship between endopolyploidy and cell size in epidermal tissue of *Arabidopsis*. *Plant Cell* **5**, 1661-1668
- Misera S, Muller AJ, Weiland-Heidecker U, Jürgens G** (1994): The *FUSCA* genes of *Arabidopsis*: negative regulators of light responses. *Mol Gen Genet* **143**, 242-252

- Mol J, Grotewold E, Koes R** (1998): How genes paint flowers and seeds. *Trends Plant Sci* **3**, 212-217
- Murashige T, Skoog F** (1962): A revised medium for rapid growth and bioassays with tobacco tissue cultures. *Physiologia plantarum* **15**, 473-497
- Nakajima K, Sena G, Nawy T, Benfey PN** (2001): Intercellular movement of the putative transcription factor *SHR* in root patterning. *Nature* **413**, 307-311
- Nesi N, Jond C, Debeaujon I, Caboche M, Lepiniec L** (2001): The *Arabidopsis TT2* gene encodes an R2R3 MYB domain protein that acts as a key determinant for proanthocyanidin accumulation in developing seed. *Plant Cell* **13**, 2099-2114
- Ohashi Y, Oka A, Ruberti I, Morelli G, Aoyama T** (2002): Entopically additive expression of *GLABRA2* alters the frequency and spacing of trichome initiation. *Plant J* **29**, 359-369
- Oparka KJ** (2003): Getting the message across: how do plant cells exchange macromolecular complexes? *Trends Plant Sci* **9**, 33-41
- Oppenheimer DG, Herman PL, Sivakumaran S, Esch JJ, Marks MD** (1991): A myb gene required for leaf trichome differentiation in *Arabidopsis* is expressed in stipules. *Cell* **67**, 483-493
- Oppenheimer D** (1998) Genetics of plant cell shape. *Curr Opin Plant Biol* **1**, 520-524
- Oppenheimer DG, Pollock MA, Vacik J, Szymanski DB, Ericson B, Feldmann K, Marks MD** (1997) Essential role of a kinesin-like protein in *Arabidopsis* trichome morphogenesis. *Proc Natl Acad Sci USA* **94**, 6261-6266
- Osterlund MT, Lay-Hong A, Deng XW** (1999): The role of COPI in repression of *Arabidopsis* photomorphogenic development. *Trends Cell Biol* **9**, 113-117
- Payne CT, Zhang F, Lloyd AM** (2000): *GL3* encodes a bHLH protein that regulated trichome development in *Arabidopsis* through interaction with *GL1* and *TTG1*. *Genetics* **156**, 1349-1362
- Perazza D, Herzog M, Hülskamp M, Brown S, Dorne AM, Bonneville JM** (1999): Trichome cell growth in *Arabidopsis thaliana* can be derepressed by mutations in at least five genes. *Genetics* **152**, 461-476
- Perbal MC, Haughn G, Saedler H, Schwarz-Sommer Z** (1996): Non-cell-autonomous function of the *Antirrhinum* floral homeotic proteins DEFICIENS and GLOBOSA is exerted by their polar cell-to-cell trafficking. *Development* **122**. 3433-3441
- Qiu JL, Jilk R, Marks MD, Szymanski DB** (2002): The *Arabidopsis SPIKE1* gene is required for normal cell shape control and tissue development. *Plant Cell* **14**, 101-118
- Quaedvlieg NEM, Schlaman HRM, Admiraal PC, Wijting SE, Stougaard J, Spaik H** (1998): Fusions between green fluorescent proteins and  $\beta$ -glucuronidase as sensitive and vital bifunctional reporters in plants. *Plant Mol Biol* **37**, 715-727
- Rate DN, Cuenca JV, Bowman GR, Guttman DS, Greenberg JT** (1999): The gain-of-function *Arabidopsis acd6* mutant reveals novel regulation and function of the salicylic acid signaling pathway in controlling cell death, defenses, and cell growth. *Plant Cell* **11**, 1695-1708
- Rodgers S, Wells R, Rechsteiner M** (1986) Amino acid sequences common to rapidly degraded proteins: the PEST hypothesis. *Science* **234**, 364-368
- Ryals JA, Neuenschwander UH, Willits MG, Molina A, Steiner H-Y, Hunt MD** (1996): Systemic acquired resistance. *Plant Cell* **8**, 1809-1819

- Schellmann S, Schnittger A, Kirik V, Wada T, Okada K, Beermann A, Thumfahrt J, Jürgens G, Hülskamp M** (2002): *TRIPTYCHON* and *CAPRICE* mediate lateral inhibition during trichome and root hair patterning in *Arabidopsis*. *EMBO J* **21**, 5036-5046
- Scheres B** (2001): Plant cell identity. The role of position and lineage. *Plant Physiol* **125**, 112-114
- Schiefelbein J** (2003): Cell-fate specification in the epidermis: a common patterning mechanism in the root and shoot. *Curr Opin Plant Biol* **6**, 74-78
- Schnittger A, Jürgens G, Hülskamp M** (1998): Tissue layer and organ specificity of trichomes formation are regulated by *GLABRA1* and *TRIPTYCHON* in *Arabidopsis*. *Development* **125**, 2283-2289
- Schnittger A, Folkers U, Schwab B, Jürgens G, Hülskamp M** (1999): Generation of a spacing pattern: The role of *TRIPTYCHON* in trichome patterning in *Arabidopsis*. *Plant Cell* **11**, 1105-1116
- Schnittger A, Schöbinger U, Stierhof YD, Hülskamp M** (2002): Ectopic B-type cyclin expression induces mitotic cycles in endoreduplicating *Arabidopsis* trichomes. *Curr Biol* **5**, 415-420
- Schnittger A, Schöbinger U, Bouyer D, Weinl C, Stierhof YD, Hülskamp M** (2002): Ectopic D-type cyclin expression induces not only DNA replication but also cell division in *Arabidopsis* trichomes. *Proc Natl Acad Sci U S A*. **99**, 6410-6415.
- Schnittger A, Weinl C, Bouyer D, Schöbinger U, Hülskamp M** (2003): Misexpression of the cyclin-dependent kinase inhibitor ICK1/KRP1 in single-celled *Arabidopsis* trichomes reduces endoreduplication and cell size and induces cell death. *Plant Cell* **15**, 303-315
- Schwab B, Folkers U, Ilgenfritz H, Hülskamp M** (1999): Trichome morphogenesis in *Arabidopsis*. *Philos Trans R Soc Lond B Biol Sci*. **355**, 879-83
- Sessions A, Yanofsky M, Weigel D** (2000): Cell-cell signaling and movement by the floral transcription factors *LEAFY* and *APETALA1*. *Science* **289**, 779-782
- Sieburth LE, Drews GN, Meyerowitz EM** (1998): Non-autonomy of *AGAMOUS* function in flower development: use of a *Cre/LoxP* method for mosaic analysis in *Arabidopsis*. *Development* **125**, 4303-4312
- Simpson P** (1997): Notch signalling in development – on equivalence groups and asymmetric developmental potential. *Curr Opin Genet Dev* **7**, 537-542
- Smirnova E, Reddy ASN, Bowser J, Bajer AS** (1998): A minus end-directed kinesin-like motor protein, KCBP, localizes to anaphase spindle poles in *Haemanthus* endosperm. *Cell Motil Cytoskeleton* **41**, 271-280
- Sompornpailin K, Makita Y, Yamazaki M, Saito K** (2002): A WD-repeat-containing putative regulatory protein in anthocyanin biosynthesis in *Perilla frutescens*. *Plant Mol Biol* **50**, 485-495
- Stockhaus J, Poetsch W, Steinmüller K, Westhoff P** (1994): Evolution of the phosphoenol-pyruvate carboxylase promoter of the C<sub>4</sub> dicot *Flaveria trinervia*: an expression analysis in the C<sub>3</sub> plant tobacco. *Mol Gen Genet* **245**, 286-293
- Szymanski DB, Marks MD** (1998a): *GLABROUS1* overexpression and *TRIPTYCHON* alter the cell cycle and trichome cell fate in *Arabidopsis*. *Plant Cell* **10**, 2047-2062
- Szymanski DB, Jilk RA, Pollock SM, Marks MD** (1998b): Control of *GL2* expression in *Arabidopsis* leaves and trichomes. *Development* **125**, 1161-1171
- Szymanski DB, Lloyd AM, Marks MD** (2000): Progress in the molecular genetic analysis of trichome initiation and morphogenesis in *Arabidopsis*. *Trends Plant Sci* **5**, 214-219

- Szymkowiak EJ, Sussex IM** (1996): What chimeras can tell us about plant development. *Annu Rev Plant Physiol Plant Mol Biol* **47**, 351-376
- Torii KU, McNellis TW, Deng X-W** (1998): Functional dissection of *Arabidopsis* COP1 reveals specific roles of its three structural modules in light control of seedling development. *EMBO J* **17**, 5577-5587
- Torres-Ruiz RA, Jürgens G** (1994): Mutations in the FASS gene uncouple pattern formation and morphogenesis in *Arabidopsis* development. *Development* **120**, 2967-2978
- Traas J, Bellini C, Nacry P, Kronenberger J, Bouchez D, Caboche M** (1995): Normal differentiation patterns in plants lacking microtubular preprophase bands. *Nature* **375**, 676-677
- Turing A** (1952): The chemical basis of morphogenesis. *Phil Trans B* **237**, 37-72
- Vos JW, Safadi F, Reddy ASN, Hepler PK** (2000): The kinesin-like calmodulin binding protein is differently involved in cell division. *Plant Cell* **12**, 979-990
- Wada T, Tachibana T, Shimura Y, Okada K** (1997): Epidermal cell differentiation in *Arabidopsis* determined by a Myb homolog, *CPC*. *Science* **277**, 1113-1116
- Wada T, Kurata T, Tominaga R, Koshino-Kimura Y, Tashibana T, Goto K, Marks MD, Shimura Y, Okada K** (2002): Role of a positive regulator of root hair development, *CAPRICE*, in *Arabidopsis* root epidermal cell differentiation. *Development* **129**, 5409-5419
- Walker AR, Davison PA, Bolognesi-Winfield AC, James CM, Srinivasan N, Blundell TL, Esch JJ, Marks MD, Gray JC** (1999): The *TRANSPARENT TESTA GLABRA1* locus, which regulates trichome differentiation and anthocyanin biosynthesis in *Arabidopsis*, encodes a WD40 repeat protein. *Plant Cell* **11**, 1337-1349
- Walker JD, Oppenheimer DG, Concienne J, Larkin JC** (2000): *SIAMESE*, a gene controlling the endoreduplication cell cycle in *Arabidopsis thaliana* trichomes. *Development* **127**, 3931-3940
- Webb M, Jouannic S, Foreman J, Linstead P, Dolan L** (2002): Cell specification in the *Arabidopsis* root epidermis requires the activity of *ECTOPIC ROOT HAIR 3*—a katanin-p60 protein. *Development* **129**, 123-131
- Weingartner M, Binarova P, Drykova D, Schweighofer A, David J-P, Heberle-Bors E, Doonan J, Bögre L** (2001): Dynamic Recruitment of Cdc2 to Specific Microtubule Structures during Mitosis. *Plant Cell* **13**, 1929-1943
- Weymann K, Hunt M, Uknes S, Neuenschwander U, Lawton K, Steiner HY** (1999): Suppression and restoration of lesion formation in *Arabidopsis* Lsd mutants. *Plant Cell* **7**, 2013-2022
- Wilhelmi LK, Preuss D** (1999): The mating game: pollination and fertilization in flowering plants. *Curr Opin Plant Biol* **2**, 18-22
- Wolf S, Deom CM, Beachy RN, Lucas WJ** (1989): Movement protein of tobacco mosaic virus modifies plasmodesmatal size exclusion limit. *Science* **246**, 377-379
- Wu X, Weigel D, Wigge PA** (2002): Signaling in plants by intercellular RNA and protein movement. *Genes Dev* **16**, 151-158
- Wu X, Dinneny JR, Crawford KM, Rhee Y, Citovsky V, Zambryski PC, Weigel D** (2003): Modes of intercellular transcription factor movement in the *Arabidopsis* apex. *Development* **130**, 3735-3745
- Zambryski P** (2004): Cell-to-cell transport of proteins and fluorescent tracers via plasmodesmata during plant development. *J Cell Biol* **162**, 165-168
- Zhang F, Gonzales A, Zhao M, Payne CT, Lloyd A** (2003): A network of redundant bHLH proteins functions in all *TGG1*-dependant pathways of *Arabidopsis*. *Development* **130**, 4859-4869

**Erklärung**

Ich versichere, dass ich die von mir vorgelegte Dissertation selbständig angefertigt, die benutzten Quellen und Hilfsmittel vollständig angegeben und die Stellen der Arbeit – einschließlich Tabellen, Karten und Abbildungen –, die anderen Werken im Wortlaut oder dem Sinn nach entnommen sind, in jedem Einzelfall als Entlehnung kenntlich gemacht habe; dass diese Dissertation noch keiner anderen Fakultät oder Universität zur Prüfung vorgelegen hat; dass sie – abgesehen von unten angegebenen Teilpublikationen – noch nicht veröffentlicht worden ist sowie, daß ich eine solche Veröffentlichung vor Abschluß des Promotionsverfahrens nicht vornehmen werde. Die von mir vorgelegte Dissertation ist von Prof. Dr. Martin Hülskamp betreut worden.

Daniel Bouyer

Veröffentlichungen:

***CPR5* is involved in cell proliferation and cell death control and encodes a novel trans-membrane protein.**

Kirik V, Bouyer D, Schöbinger U, Bechtold N, Herzog M, Bonneville JM, Hülskamp M  
*Curr Biol* 2001, **11**: 1891–1895

**The *Arabidopsis* *STICHEL* gene is a regulator of trichome branch number and encodes a novel protein.**

Ilgenfritz H, Bouyer D, Schnittger A, Mathur J, Kirik V, Schwab B, Chua NH, Jürgens G, Hülskamp M  
*Plant Physiol* 2003, **131**: 643-655

**LEBENS LAUF****Persönliche Daten**

Name Daniel Johannes Bouyer  
 Geburtsdatum 26.06.73  
 Geburtsort Villingen

**Schulbildung**

9/79 – 7/83 Grundschule am Warenberg, Villingen  
 9/83 – 7/89 Karl-Brachat-Realschule, Villingen  
 Abschluss: Mittlere Reife  
 9/89 – 7/92 Wirtschaftsgymnasium, Villingen  
 Abschluss: Allgemeine Hochschulreife

**Zivildienst und sonstige Tätigkeiten**

10/92 – 12/93 Zivildienst Städtisches Krankenhaus, Villingen  
 1/94 – 3/94 Mitarbeit beim Malteser Hilfsdienst, Villingen  
 4/94 – 7/94 Auslandsaufenthalt in Australien und Neuseeland

**Studium**

10/94 – 3/00 Albert-Ludwigs-Universität Freiburg  
 10/94 Deutsch und Biologie auf Staatsexamen  
 10/95 Diplom Biologie  
 6/96 – 3/97 Vordiplom  
 3/99 – 6/99 Diplomprüfungen Biologie  
 Hauptfach: Botanik / Pflanzenphysiologie  
 1. Biologisches Nebenfach: Genetik  
 2. Biologisches Nebenfach: Zellbiologie  
 Nichtbiologisches Nebenfach: Physikalische Chemie

7/99 – 3/00 Diplomarbeit im Fach Pflanzenphysiologie  
 Thema: "Analyse von *hebiba*, einer Reismutante, die Licht mit Dunkel verwechselt"

7/99 – 10/99 Hitachi Advanced Research Laboratory, Saitama, Japan  
 Abteilung Prof. Dr. Masaki Furuya  
 Stipendium des DAAD

10/99 – 3/00 Albert-Ludwigs-Universität Freiburg,  
 Abteilung Prof. Dr. Eberhard Schäfer  
 Betreuung PD Dr. Peter Nick

4/00 – 3/01 Eberhard-Karls-Universität Tübingen  
 Beginn der Promotionsarbeit  
 Institut für Entwicklungsgenetik, Prof. Dr. Gerd Jürgens  
 Betreuung PD Dr. Martin Hülskamp

4/01 – 4/04 Universität zu Köln  
 Fortsetzung der Promotionsarbeit  
 Institut für Botanik III, Prof. Dr. Martin Hülskamp